Spectral and Energy Efficiency in 5G Wireless Networks

Iyad Lahsen-Cherif

NNT : 2016SACLS506

Thèse de doctorat
de l'Université Paris-Saclay
préparée à l'Université Paris-Sud

Ecole doctorale n°580

Sciences et Technologies de l'Information et de la Communication

Spécialité : **Réseaux, Information et Communications**

par

M. LAHSEN-CHERIF Iyad

Spectral and Energy Efficiency in 5G Wireless Networks

Efficacité Spectrale et Energétique dans les réseaux 5G

Thèse présentée et soutenue à CentraleSupélec, Gif-sur-Yvette, le 02 décembre 2016.

Composition du Jury :

M. André-Luc Beylot	Professeur à l'ENSEEIHT, Toulouse	Rapporteur
M. Anthony Busson	Professeur à l'Université de Lyon	Examinateur
M. Bernard Cousin	Professeur à l'Université de Rennes 1	Examinateur
M. Steven Martin	Professeur à l'Université Paris 11	Président
Mme Lynda Mokdad	Professeur à l'Université Paris 12	Rapporteur
Mme Véronique Vèque	Professeur à l'Université Paris 11	Directrice de thèse
Mme Lynda Zitoune	Maître de Conférence à l'ESIEE, Paris	Co-Encadrante

Contents

List of Figures

List of Tables

To my parents,

Fatiha and Mohammed.

To my brothers,

Ayoub and Amine.

0.1 Résumé

La pénurie d'énergie et le manque d'infrastructures dans les régions rurales représentent une barrière pour le déploiement et l'extension des réseaux cellulaires. Les approches et techniques pour relier les stations de base (BSs) entre elles à faible coût et d'une manière fiable et efficace énergiquement sont l'une des priorités des opérateurs. Ces réseaux peu denses actuellement, peuvent évoluer rapidement et affronter une croissance exponentielle due principalement à l'utilisation des téléphones mobiles, tablettes et applications gourmandes en bande passante. La densification des réseaux est l'une des solutions efficaces pour répondre à ce besoin en débit élevé. Certes, l'introduction de petites BSs apporte de nombreux avantages tels que l'amélioration du débit et de la qualité du signal, mais entraîne des contraintes opérationnelles telles que le choix de l'emplacement des noeuds dans ces réseaux de plus en plus denses ainsi que leur alimentation. Les problèmes où la contrainte spatiale est prépondérante sont bien appropriés à la modélisation par la géométrie stochastique qui permet une modélisation réaliste de distribution des BSs. Ainsi, l'enjeu est de trouver de nouvelles approches de gestions d'interférence et de réductions de consommation énergétique dans les réseaux sans fil.

Le premier axe de cette thèse s'intéresse aux méthodes de gestion d'interférence dans les réseaux cellulaires se basant sur la coordination entre les BSs, plus précisément, la technique Coordinated MultiPoint Joint Transmission (CoMP-JT). En CoMP-JT, les utilisateurs en bordure de cellules qui subissent un niveau très élevé d'interférences reçoivent plusieurs copies du signal utile de la part des BSs qui forment l'ensemble de coordination. Ainsi, nous utilisons le modèle r-l Square Point Process (PP) à fin de modéliser la distribution des BSs dans le plan. Le processus r-l Square PP est le plus adapté pour modéliser le déploiement réel des BSs d'un réseaux sans fil, en assurant une distance minimale, (r - l), entre les points du processus. Nous discutons l'impact de la taille de l'ensemble de coordination sur les performances évaluées. Ce travail est étendu pour les réseaux denses WiFi IEEE 802.11, où les contraintes de portées de transmission et de détection de porteuse ont été prises en compte.

Dans le deuxième axe du travail, nous nous intéressons à l'efficacité énergétique des réseaux mesh. Nous proposons l'utilisation des antennes directionnelles (DAs) pour réduire la consommation énergétique et améliorer le débit de ces réseaux mesh. Les DAs ont la capacité de focaliser la transmission dans la direction du récepteur, assurant une portée plus importante et moins d'énergie dissipée dans toutes les directions. Pour différentes topologies, nous dérivons le nombre de liens et montrons que ce nombre dépend du nombre de secteurs de l'antenne. Ainsi, en utilisant les simulations, nous montrons que le gain, en énergie et en débit, apporté par les DAs peut atteindre 70% dans certains cas. De plus, on propose un modèle d'optimisation conjointe d'énergie et du débit adapté aux réseaux WMNs équipés de DAs. La résolution numérique de ce modèle conforte les résultats de simulation obtenus dans la première partie de cette étude sur l'impact des DAs sur

les performances du réseau en termes de débit et d'énergie consommée.

Ces travaux de thèse s'inscrivent dans le cadre du projet collaboratif (FUI16 LCI4D), qui consiste à concevoir et à valider une architecture radio ouverte pour renforcer l'accès aux services broadband dans des lieux ne disposant que d'une couverture minimale assurée par un réseau macro-cellulaire traditionnel. Le projet s'intéresse à accélérer l'extension de couverture cellulaire dans les pays émergents en concevant une architecture de réseau à faible coût qui s'appuie sur de nouvelles technologies backhaul apportant de la capacité et réduisant la consommation énergétique dans des zones non couvertes, ainsi sur la baisse des coûts de déploiement de l'architecture.

Chapter 1

General Introduction

Nowadays, 4.2 billion of people around the world, mainly in developing countries, are outside the digital revolution and do not have neither cellular networks nor Internet access [126]. This is due to many blocking factors such as: poor communication infrastructure, which is a major barrier of Internet penetration in rural areas. The lack of infrastructure requires higher costs (Opex & Capex) to the operators for network deployment, high costly cell towers, wired lines to connect BSs, default electrical grids, etc.

In this direction, the LCI4D project [4] aims at providing low cost infrastructure to connect isolated rural and sub-urban areas to the Internet. In order to reduce the installation and maintenance costs, LCI4D proposes the usage of self-configured Wireless Mesh Networks (WMNs) to connect outdoor femtocells to the remote Marco cell (gateway). These femtocells are multimode embedding both cellular and mesh WiFi technologies. The mesh WiFi part is used to form a mesh backhaul to relay cellular data of cellular devices to the gateway.

In one hand, it is important to note that today's networks continue to evolve and grow resulting more dense, complex and heterogeneous networks. This leads to new challenges such as finding new models to characterize the nodes distribution in the wireless network and approaches to mitigate interference. On the other hand, the energy consumption of WMNs is a challenging issue mainly in rural areas lacking of default electrical grids. Finding alternative technologies and approaches to reduce the consumed energy of these networks is a interesting task.

This thesis focus on proposing and evaluating interference management models for next generation wireless networks (5G and Very Dense High WLANs), and providing tools and technologies to reduce energy consumption of Wireless Mesh Networks (WMNs).

Two different problems are thus studied, naturally the thesis is divided into two parts along the following chapters.

Part I: Wireless Network Interference Management

The contribution of this part of the thesis is threefold. Firstly, we propose a new model for interference management in wireless networks based on coordination, mainly Joint Transmission (CoMP-JT). We extend this work to a WLANs scenario taking into account the constraints of this type of networks such as the carrier sensing range. Then, we study the resource allocation in LTE networks, by proposing new and realistic allocation strategies while considering a Poisson point distribution of eNodeBs.

We start the Chapter 2 by recalling the cellular network concept and detail the wireless network evolution by outlining requirements and techniques used in each cellular network generation. Then, from the large set of candidates techniques to satisfy the network performance for 5G such as using high frequency spectrum, densification, network virtualization and using new modulation and coding schemes (MCS), we choose the network densification direction. We present the network densification and the composition of these dense (heterogeneous) networks. Then, we outline the main problem of densification, *interference*. We introduce some techniques to manage interference. We detail the inter-cell interference coordination techniques and the two schemes of Coordination MultiPoint (CoMP): Joint Transmission and Coordinated Scheduling/Beamforming.

We provide stochastic geometry tools allowing us to characterize the interference and analyze network performance in Chapter 3. We introduce different types of point processes used in wireless networks. We present important performance metrics which will be used later in this dissertation, such as the coverage probability and the throughput. Then, we present some related work using point processes and evaluating the performance of both ICIC and CoMP interference management techniques.

We develop our interference management coordination (CoMP-JT) model in Chapter 4. The main idea of CoMP-JT is to turn signals generating harmful interference into useful signals. We develop a new model where BSs inside the coordinated set send a copy of data to border's users experiencing high interference. We consider the r-l Square point process to model the BSs distribution in the network. We derive network performance in terms of coverage probability and throughput. Additionally, we study the impact of the size of coordination set on the network performance. Results regarding this work were presented in

- I. Lahsen Cherif, L. Zitoune, V. Veque, "The r-l square point process: The effect of Coordinated-MultiPoint Joint Transmission," IEEE IWCMC 2015, Dubrovnik, Croatia.

In Chapter 5, we extend the results of the previous chapter and provide a new model adopted for Dense Very high throughput WLANs. We take into consideration constraints of WLANs in our model such as carrier sensing range. This subject is studied in

- I. Lahsen Cherif, L. Zitoune, V. Veque, "Performance Evaluation of Joint Transmission

Coordinated-MultiPoint in Dense Very High Throughput WLANs Scenario," IEEE LCN 2015, ClearWater Beach, Florida, USA.

In Chapter 6, we tackle resource allocation strategies to limit the interference in LTE networks. We study three cyclic allocation strategies: (i) the independent allocation, (ii) the static allocation and (iii) the load-dependent strategy. We derive tractable analytical expression of the first and second mean of interference. We validate the model using extensive simulations. Results regarding this work were submitted for a possible publication

- I. Lahsen Cherif, A. Busson, "Impact of Resource Blocks Allocation strategies on Downlink Interference distribution in LTE Networks," submitted for a journal publication.

Part II: Directional Antennas Wireless Mesh Networks

Reducing the energy consumption and improving the energy efficiency of WMNs is our concern at this part. Indeed, we aim at studying the impact of directional antennas technology on the performance of WMNs, using both analysis and simulations.

In Chapter 7, we present the important and necessary notions for this part. We start by defining the backhaul before, focusing on the wireless backhaul. We outline the problem of energy consumption in WMNs. Then, we motivate the scenario and the problem statement.

We start Chapter 8 by introducing notions of DAs necessary to the understanding of this chapter such as antenna gain and we outline a general optimization model. We present the main parameters impacting the network performance. Then, we discuss related works at different network layer and using different tools.

The contribution of Chapter 9 is twofold. We derive the Number of Links (NLs) for the chain and grid topologies for different antennas beams. These results are based on the routing tables of nodes in the network. We consider different scenarios such as *1Source-NDestinations* to model the downlink communications, *NSources-1Destination* to model the uplink communications and the *1Source-1Destination* as a baseline scenario. Using ns-3 simulator, we simulate network performance in terms of Mean Loss Ratio, throughput, energy consumption and energy efficiency. Then, we study the impact of number of beams, network topology and size, the placement of the gateway on the network performance. The results of this work can be found in:

- I. Lahsen Cherif, L. Zitoune, V. Veque, "Throughput and Energy Consumption Evaluation in Directional Antennas Mesh Networks," IEEE WiMob 2016, New York, USA.

In Chapter 10, we go beyond simulations and propose an optimization framework minimizing the consumed energy while maximizing the network throughput for DAs WMNs. We consider a weighted objective function combining the energy consumption and the throughput. We use *discrete*

power control to adapt transmission power depending on the location of the next hop. This model is a first step to approve simulation results obtained in Chapter 9. We use ILOG Cplex solver to find the optimal solution. Results show that DAs improves the network throughput while reduce the energy consumption and that power control allows to save more energy.

Part I

Wireless Network Interference Management and Performance Evaluation using Stochastic Geometry

Chapter 2

Introduction

Contents

2.1 Chapter Summary

The shift from data centric traffic to video centric traffic and the explosion of connected devices are the origin of the exponential growth in data traffic. Moreover, the scarcity of the frequency spectrum used for wireless communications becomes a challenging problem in order to maintain a good Quality of Service (QoS) for mobile users. Therefore, we need more spectral efficient techniques to support the intensive bandwidth applications such as multimedia applications.

In this chapter, we outline the mobile date growth. Then, we present the evolution of mobile wireless networks in terms of requirements and technologies behind each generation, and discuss

solutions to face with this exponential growth.

2.2 Mobile Data Tsunami

For the next five years, Cisco [10] is expecting that the mobile data traffic increases of nearly eightfold and reaches 30.6 exabytes (10^{18}) by 2020. This exponential increase in throughput demand must be accompanied with an increase, at the same speed, in network capacity. Cooper's law [36] states that wireless networks capacity double in every 30 months and highlight means (tools) increasing the network capacity: (i) Advanced Modulation and Coding schemes, (ii) More spectrum, and (iii) Increase of the number of cells. The two former improvements are in terms of (licensed) spectrum and physical layer improvements but are not efficient compared to their cost since it is expensive from the operators point of view. Moreover, the physical layer limits are already or near to be reached. Hence, the network densification, consisting in deploying small BSs to offload the Macro BS, is the key solution to meet the capacity requirements of the mobile data tsunami. In subsection 2.5, we will discuss features and composition of heterogenous networks.

2.3 Cellular Netoworks Planning

The transmission power of user equipments (UEs) is 0.2 Watt (200 mWatt), allowing the transmitted radio signals to propagate in the space for several kilometers. To enable communications and network connection for a given UE, at least one BS should be in its transmission range. To satisfy this condition, the operators must deploy regularly BSs to serve their users. Depending on the area, BSs deployment can be more or less dense. In fact, in rural areas, the operators seek to provide *coverage* for their users, while in urban areas, they look to provide *high network capacity*. Densification of some regions leads to severe problems such as high *interference* scenarios. The notion of interference will be explained in detail in Section 2.6.

It is important to note that before reaching the stage of spatial domain densification, the time, the frequency and the joint time-frequency domains have been passed through densification processes.

Additionally, the shift from Frequency Division Multiplexing (FDM) to Orthogonal Frequency Division Multiplexing (OFDM) used in 4G systems (and detailed in the next section) is considered as a frequency domain densification. Indeed, for the former, carriers are spaced and are far apart with respect to each other, while for the later, carriers are densely packed and are orthogonal to each other. Frequency densification leads to a efficient bandwidth usage since, due to the carriers orthogonality, no need of separate guard bands of each carrier. Figure 2.1 shows comparison between OFDM and FDM[1].

[1] hubpages.com/technology/Wireless-Communication-Systems-OFDM-OFDMA

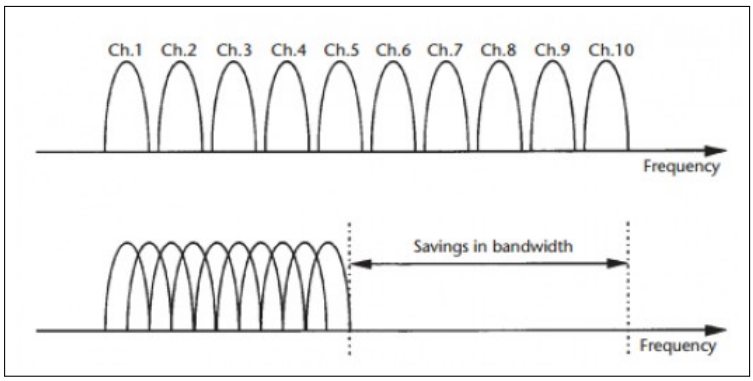

Figure 2.1: Comparison between FDM and OFDM [1].

In the next section, we outline the evolution of cellular networks.

2.4 Wireless Networks Evolution

Before wireless networks get to the stage that they reached today, they went through several specification phases and standardization processes. In this section, we survey the mobile networks evolution.

In the 1970s, first generation (1G) networks, consisting of *Analog Radio Systems*, was designed for *voice communications*. It was based on Frequency Division Multiple Access (FDMA) channel access method, where channels are frequency bands that users occupy during their communications. With the increase in number of users, each user requests a frequency band for communication. Following this, analog systems showed their limitations. The transition from analog to *digital systems* was crucial to solve such issue.

Global System Mobile (GSM) or the second generation (2G) mobile network is a digital system based on narrow band Time and Frequency division multiple accesses (TDMA & FDMA), designed to provide *voice with user mobility*. It uses three frequency bands: 900Mhz, 1800Mhz, and 1900Mhz and its transmission rate is up to 13 Kbps.

General Packet Radio System (GPRS) is an extension of GSM which consists in providing data services for 2G users over the mobile circuit switched systems. Unlike GSM, which dedicates resources to a user for a given (fixed) period of time, in GPRS, radio resources are allocated only if the user is active. Hence, many users can be scheduled to share the radio resource. This leads to an increase of GPRS transmission rate, which can reach 172Kbps.

Enhanced Data rates for Global Evolution (EDGE) speeds up data transmission up to 3 times compared to GSM/GPRS. The main differences between the GSM and GPRS are: (i) The former generations use GMSK as a modulation technique, while EDGE uses 8-PSK, (ii) The usage of more Modulation and Coding schemes (MCS): 9 MCSs instead of 4 MCSs in GPRS.

IMT-2000 specifications are a set of requirements for the third generation (3G), which focus on providing users *video telephony services* and *mobile Internet access*. 3G uses Wideband Code Division Multiple Access (W-CDMA) radio access technology to offer greater spectral efficiency and bandwidth to mobile network operators. The expected transmission rate is up to 384 kbit/s for 3G users. High Speed Packet Access (HSPA) (3.5G) is an extension of 3G systems which offers speed of 14.4 Mbit/s in downlink and 5.76 Mbit/s for uplink.

In 2008, ITU specified requirements of the fourth generation (4G) standards by defining IMT-A specifications. These requirements mainly consist of:

- *all-IP* packet switched networks.
- *Peak data rate* of 100Mbps for high mobility and 1Gbps for low mobility.
- *Link spectral efficiency* of 15-bit/s/Hz in the downlink, and 6.75-bit/s/Hz in the uplink.

4G [38] is based on many technologies such as: Orthogonal Frequency Division Multiplexing (OFDM), Multi-user Multiple Input Multiple Output (MIMO) which increases the spatial diversity, and Carrier Aggregation consisting on using multiple frequency bands for transmission.

In the following, we explain the technologies behind the 4G in detail:

- *Orthogonal Frequency Division Multiplexing (OFDM) [99]*: is a frequency-division multiplexing (FDM) scheme used as a digital multi-carrier modulation method. It consists in transmitting data over many narrow band careers of 180kHz each instead of spreading one signal over the complete bandwidth. In other words, OFDM uses a large number of narrow sub-carriers for multi-carrier transmission to carry data. Note that OFDM symbols form Resource Blocks (RBs), where each RB has a size of 180kHz in the frequency domain and 0.5ms in the time domain.

  OFDM has many advantages such as:

  - Dealing with severe channel conditions without complex equalization filters.
  - Simplifying channel equalization.
  - Eliminating inter symbol interference (ISI) using cyclic prefix.

  OFDM has also some drawbacks such as high peak-to-average ratio [46] and sensitive to frequency offset [107].

- *Multiple Input Multiple Output (MIMO) [52]* is a technology allowing BSs to transmit several data streams over the same carrier simultaneously. MIMO's advantages are:

  - Sensitivity to fading is reduced by the spatial diversity provided by multiple spatial paths.

– Power requirements associated with high spectral-efficiency communication can be significantly reduced.

Awaiting standardization of new wireless generations, 4G continues to evolve and yields LTE-A pro (4.5G). This progression provides 8× more peak rate and 6× more capacity compared to 4G. Aggregating 5 bands, the usage of 4×4 MIMO and a 256 QAM modulation are technology features behind 4.5G.

The fifth generation (5G) [18] will be a consolidation of existing wireless communication technologies and will deliver the capacity, connectivity and low latency to enable advanced applications. So far, only challenges and targets are fixed for 5G networks. Researchers are looking for technologies and tools to address these shift paradigms. In the following, we present 5G requirements:

- *Multi-Gbps Rates.*
- *Spectrum & Bandwidth flexibility.*
- *Network & Device Energy Efficiency.*
- *Massive Number of Devices*: Highly dense networks.
- *Latency and access delay* should be less than 1ms end-to-end round trip delay is fixed as a requirement.

This leads to a new network topology which is dense, heterogeneous, dynamic and complex. Hence, new tools are required to model and analyze these networks.

In section 2.5, we outline and discuss features of heterogeneous networks.

2.5 Heterogeneous Networks

Today cellular networks are evolving from an homogenous architecture to a composition of heterogeneous networks [53,85], composed of various sizes of base stations (BSs): Macro, Pico, Femto BSs and relays. Each of them having different capabilities, constraints, and operating functionalities. Tiers coexist, share the same spectrum and communicate with each other.

Pico and Femto BSs are small BSs generally deployed within an existing Macro network to offload the cellular traffic. Femto BSs have a small range compared to pico cells and can be deployed in a building or an enterprise setting by the end user and both operate in licensed bands.

The deployment of this type of infrastructure improves the coverage and throughput. Indeed, bringing the network (BSs) near to the end users improves the user-BS link quality. Furthermore, short transmission ranges of Femto BSs increase the *spatial reuse* by allowing concurrent transmission to use same resources while reducing interference.

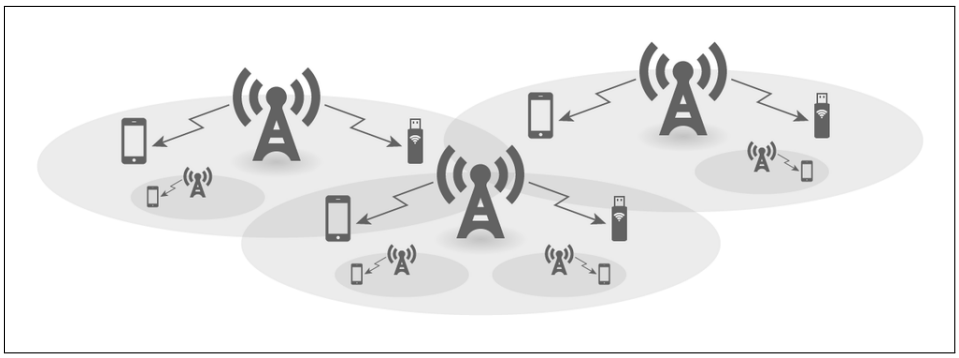

Figure 2.2: Illustration of an heterogeneous network composed of Macro and Femto BSs [2].

Femto BSs can operate in either open or closed access modes. Generally, Femto BSs deployed by the end users in residential setting usually operate in closed access mode, where a set of predefined users can connect to the network via this Femto cell. On the other hand, outdoor Femto BSs deployed by the operator are operating in the open access mode, that is, users in the coverage area of the open access Femto BS can use it to connect to the network.

In the next section, we introduce the wireless interference problem.

2.6 Interference Problem

Interference is the primary cause impacting the network performance. The interference problem in wireless communication is similar to collision phenomena in random access networks. A collision occurs when at least, two nodes, use a common resource or a shared medium to communicate. In wireless scenario, nodes represent BSs and resources can be frequency bands, time slots or resource blocks. The coexistence of several BSs all operating in the same frequency band, since the frequency reuse factor in LTE networks is 1, generates harmful inter-cell interference and directly affects performance of cell edge users. Generally, this problem occurs because BSs have a knowledge only of resources allocated to their attached users and do not have any knowledge about resources allocated to users attached to neighbor BSs. Hence, an independent resource allocation is performed at each BS and cell edge users of adjacent BSs may use the same radio resources resulting high interference and a degradation in network performance.

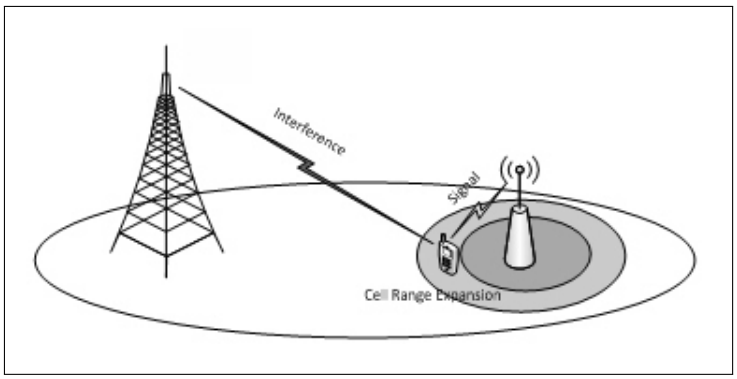

Figure 2.3: Interference in wireless networks [3].

Pico, femto and macro BSs overlap in many networks architecture resulting new interference scenarios in heterogeneous networks. In the following, we present notions of aggressor and victim cells occurring in the heterogeneous scenario.

As stated before, heterogeneous networks are composed of many tiers. Femto BSs are deployed by end users can operate in either closed or open access modes. In case of closed access Femto BSs, Macro users (MUE) in the coverage area of the femto cell can not be offloaded to the Femto cell. As a consequence, they suffer from strong interference from the Femto cell. In this case, the Femto cell is the aggressor and the macro cell is the victim cell. On the other hand, when Femto cell operates in open access mode, in some cases even if users are in the coverage area of femto cell the received signal from macro BS is strong compared to the signal received from Femto cell due to the low transmission power of Femto BSs. In this case, Femto BSs are the victim cells and the macro cell is the aggressor cell.

Figure 2.3 illustrates a wireless interference scenario, where the user receives a desired signal (solid line) from its serving BS, and experiences interference form neighboring BSs using the same recourses (dashed lines).

Many techniques can be used to mitigate interference. Interference management can be performed in the time, frequency or spatial domaine. Figure 2.4 illustrates a taxonomy of interference management schemes. These schemes can be performed in wireless network either using cooperation or without cooperation between network nodes. Two types of coordination based interference managements are considered: either ICIC (section 3.9) or Coordination multipoint (3.10).

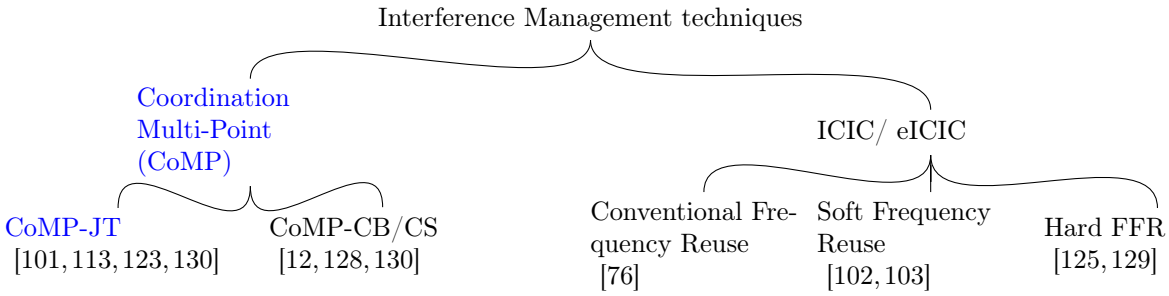

Figure 2.4: Interference Management Taxonomy.

2.7 Frequency Reuse

Frequency Reuse (FR) [76, 103, 129] is an inter-cell interference management technique used in OFDMA cellular networks (LTE). The available frequency band is divided into many sub-bands, depending on the used FR scheme and the FR factor. Three types of FR have been developed:

2.7.1 Conventional Frequency Reuse

Conventional frequency reuse [76] is the classical FR scheme where the frequency band is divided into Δ sub-bands. Each cell in the network is allocated one of the sub-bands to transmit to its mobile users. The sub-band is selected in such a way that the adjacent cells do not use the same sub-band. Hence, the interference experienced at the mobile users side is reduced by a factor of Δ.

2.7.2 Hard Fractional Frequency reuse (Hard FFR)

The total frequency band is divided into (Δ+1) sub-bands [103]. Each cell use the same sub-band for its inner region corresponding to the center region. The remaining Δ sub-bands are used for outer region corresponding to the border region.

2.7.3 Soft Frequency reuse (SFR)

The transmission band is divided into (Δ) sub-bands [129]. The outer region uses one frequency sub-band and the inner region uses the remaining (Δ-1) frequency sub-bands. The outer region sub-band of each cell is selected in such a way that the adjacent cells use different sub-bands for the edge users.

The definitions of the inner (cell center) and the outer (cell edge) regions of the hexagonal grid and the Voronoï cell model are different. In fact, for the hexagonal grid model, where the size and the shape of cell have an exact form, the inner region is defined by the inscribed circle. However,

when nodes are randomly distributed, the cell region is defined by the Voronoï tessellation. Hence, cell regions are defined as: if the SINR of a mobile user is greater than a pre-defined threshold γ then this user is in the cell center, otherwise the SINR is less than γ, then it is in the cell edge area.

2.8 Coordinated Multi-Point (CoMP)

CoMP is a coordination/cooperation technique used to reduce the interference and hence increases the network throughput. It improves the cell edge users throughput and decreases the outage probability. This coordination/cooperation is performed between BSs by exchanging either *data*: Joint Transmission (JT) or *channel state information*: Coordination Beamforming/Scheduling (CB/CS).

In JT, users receive multiple copies of the same data from different BSs in the coordinated set, and the signal received from BSs outside the coordinated set is seen as interference. In CB/CS, only beamforming vectors are shared between coordinated BSs. It is proved in [130], that the CoMP-JT strategy offers better performance than CB/CS.

The improvement in the network performance are approved in [22] using a realistic urban scenario.

2.9 Conclusion

In this chapter, we presented general definitions and notions of cellular wireless networks. We outlined the exponential data increase problem and discussed solutions such as network densification. Then, we presented interference problem and investigate Coordinated Multi-Point scheme used to combat interference.

In the next chapter, we present some useful point processes (p.p.) and works using these models to analyze network performance. Following that, we present some interference management technique by focusing on *coordination-based* schemes.

Chapter 3

Interference Characterization and Management Techniques

Contents

3.1 Chapter Summary

In this chapter we investigate analytical tools to model wireless networks. We provide and discuss stochastic geometry distributions used in literature to model positions of BSs in the plan. Then, we present a new powerful point process (p.p.) called *r-l* Square p.p. that alleviate problems of p.p. used in related works. Next, we discuss stochastic geometry models analyzing interference management schemes by focusing on coordination-based ones.

3.2 Introduction

Stochastic geometry was firstly introduced by Krickeberg in 1960s [78] to model positions of particles in a given area. Based on sophisticated models and random geometrical patterns, stochastic geometry provides suitable mathematical tools allowing to study the average behavior over many spatial realizations of a process whose points are generated according to given probability distribution.

Recently, stochastic geometry [59] has been applied to wireless networking concepts and design. Wireless networks can be seen as a collection of nodes placed in a given area. This allows to extract key parameters and gives an insight to the Signal To Noise Ratio (SINR) and other network performance metrics at the receiver, which closely depend on the BSs spatial distribution. Indeed, the received useful signal power and interference depend critically on the path-losses, namely, distances between numerous transmitters and receivers.

3.3 Stochastic Geometry

Network design and planning are important tasks for operators in the deployment of the conventional cellular network. Distribution of nodes in the space has an important impact on the network performance. Nodes should be placed in locations where they optimize the covered area and reduce the intercell interference. The grid lattice model is used in research to describe the position of BSs in cellular networks. However, small scale networks (Femto-, Pico- BSs) networks are deployed by the end users and lead to randomness in the network. To address this issue, tools to characterize random distribution of nodes in the network are needed. Stochastic geometry is a powerful tool to describe the network architecture. Point processes (p.p.) are widely used in wireless communications community to model BSs positions.

P.p. can be classified into different types reflecting: attraction, repulsion, and independence between points of the process. Many types of p.p. are considered in the related work as Poisson p.p., Ginibre p.p., Matérn p.p., the *r-l* square p.p., etc. Attraction occurs when points of a p.p. are more likely to be separated by a given distance, and repulsion when less likely.

Figure 3.1 illustrates a p.p. taxonomy. PPP is the p.p. with zero attraction between points.

More regular p.p. result when points repel each other (left). Clustered p.p. appear when points attract each other (right).

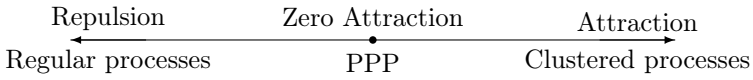

Figure 3.1: Point Processes Taxonomy.

In this section, we define the performance metrics and present relevant p.p. used in wireless communication to model nodes and users position in the network. First, we define the Poisson p.p. [20, 25, 51, 55] known by its irregularity and outline its properties. Then, we present two more regular PPs: Matérn p.p. [67, 89, 120] and Ginibre p.p. [43, 96, 117]. We conclude the section by presenting the r-l Square p.p. [28, 81, 82].

3.4 Performance Metrics

In this section, we define metrics for the network performance evaluation. These metrics are specially used to characterize the interference. We first define the coverage probability which is the probability that user SINR is greater than a given threshold. Then, we express the Shannon ergodic capacity in function of the coverage probability.

3.4.1 Coverage probability

The SINR reflects the quality of wireless connections. The SINR at the a given receiver is defined as:

$$\text{SINR} = \frac{\text{Useful signal}}{\text{Interference + Noise}} \tag{3.0}$$

where the useful signal is the signal that the UE receives from its serving BS, interference represents the summation of all signals received from BSs other than it serving one, and noise is for background noise. The coverage probability is defined as:

$$\Pr\{\text{SINR} \geq \theta\} = 1 - F_{\text{SINR}}(\theta) \tag{3.0}$$

where F_{SINR} is the cumulative distributed function (cdf) of the SINR and θ is the SINR threshold in dB. In general, θ variates in the range [-20 ,20dB]. For example,

- $\Pr\{\text{SINR} \geq -20dB\} = \Pr\{\text{Useful signal} \geq 0.01 \times (\text{Interference + Noise})\}$
- $\Pr\{\text{SINR} \geq 0dB\} = \Pr\{\text{Useful signal} \geq (\text{Interference + Noise})\}$
- $\Pr\{\text{SINR} \geq 20dB\} = \Pr\{\text{Useful signal} \geq 100 \times (\text{Interference + Noise})\}$

This metric reflects the probability that a user is served by a given BS. By served, we mean that it is able to decode the received signals from the BS. Note that if the SINR is bellow a given value (0dB), the user fails to decode signals so that it is not covered.

Note that in some cases noise limited or interference limited scenarios are considered in order to make performance analysis tractable. In the former, the interference is ignored and only the noise affects the signal. In the later, noise is ignored and signal degradation are caused by interference.

3.4.2 Throughput

In the following, we use a *modified Shannon capacity* to model the throughput or rate. It can be derived from the coverage probability by the following formula:

$$\begin{aligned} R &= \mathbb{E}(\log_2(1+\text{SINR})) \\ &= \int_0^\infty \Pr\{\log_2(1+\text{SINR} > t)\}dt \\ &= \int_0^\infty \frac{\Pr\{\text{SINR} > e^t - 1\}}{\log(2)}dt \\ &\overset{(a)}{=} \frac{1}{\log(2)}\int_0^\infty \frac{\Pr\{\text{SINR} > x\}}{(x+1)}dx \\ &= \frac{1}{\log(2)}\int_0^\infty \frac{p_c(x)}{(x+1)}dx \end{aligned}$$

Where (a) follows from a variable change ($x = e^t - 1$).

Hence, the throughput is derived by replacing $p_c(T)$ expression.

3.4.3 k-coverage probability

The k-coverage probability is derived from the SINR experienced by a typical user in the downlink channel from the k-th strongest base stations of a cellular network. It can be expressed as:

$$\begin{aligned} P_c^{(k)}(\theta) &= \Pr\{\mathcal{N}(\theta) > k\} \\ &= \Pr\{\sum_{\Phi} \mathbb{1}_{\text{SINR}>\theta} > k\} \end{aligned}$$

In the next section, we present and classify stochastic geometry models. Then, we discuss related work focusing on interference characterization using stochastic geometry tools.

3.5 Stochastic Geometry Models

3.5.1 Poisson Point Process (PPP)

Poisson p.p. is the most used example of irregular p.p. [12, 20, 25, 44, 45, 61] to describe spatial randomness of nodes in wireless networks.

3.5.1.1 Model

PPP is the point process with zero attraction, where points are distributed independently with no relationship between each other. It is characterized by two properties: the number of points in disjoint bounded sets are independent and have a Poisson distribution ([58]), that is:

- For every compact set $B \in \mathbb{R}^d$, $N(B)$ (the number of point of the process in B) has a Poisson distribution with mean $M(B)$. The probability that the number of points in B is k is given by
$$\mathbb{P}(N(B) = k) = \exp\left(\int_B \lambda(x)dx\right).\frac{\left(\int_B \lambda(x)dx\right)^k}{k!} \tag{3.-2}$$
- If $B_1, B_2, ..., B_m$ are disjoint compact sets, then $N(B_1), N(B_2), ..., N(B_k)$ are independent random variables.

For the two dimension case, $d = 2$, and an homogeneous PPP ($\lambda(x) = \lambda$), the first property can be written as:
$$\mathbb{P}(N(B) = k) = \exp\left(\lambda \mid B \mid\right).\frac{\left(\lambda \mid B \mid\right)^k}{k!} \tag{3.-2}$$

The independency of points generated in a PPP makes the process analytically *tractable*. More precisely, the useful properties of PPP help to derive closed forms of performance metrics.

Although its tractability, PPP does not model correctly nodes deployment in real scenarios. For example, as shown in figure 3.2, PPP can generate points close to each other, that is, two BSs covering roughly the same network area. This would generate very harmful interference if nodes use the same radio resources. This fact motivates the need of more regular and repulsive p.p. insuring a minimum distance between points to model nodes distribution.

Figure 3.2 illustrates an homogeneous PPP.

In the next subsection (Sec. 3.5.1.2), we present some related work using PPP to model and derive performance of wireless networks.

3.5.1.2 Related work based on PPP

A comparison is carried out between perfectly regular topology and a random PPP topology in [30]. As expected, a SINR degradation is observed for the random topology compared to the regular

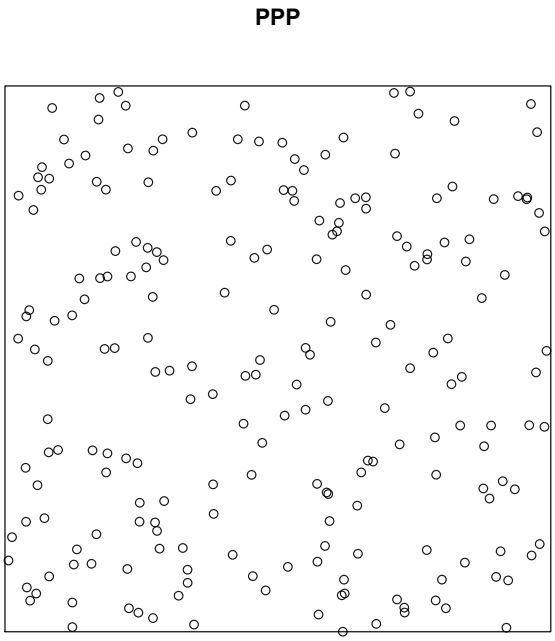

Figure 3.2: Homogeneous Poisson Point Process of intensity λ=200 (km^{-2}).

one. In fact, PPP is the worst network deployment case and gives the lower bound of network performance. Furthermore, this gap gets smaller for dense networks.

Network performance, in terms of coverage probability and rate, are derived for a K-tiers PPP network in [61, 62]. The notion of guard band region of a BS, aiming to classify interference and consisting of a ball of radius R_c centered at the BS, is presented. Two types of interference are considered: (i) dominant interferers and, (ii) interferers outside the guard region. Interference is characterized using Laplace Transform, and analytical expressions of the coverage probability and the average rate are derived using the Gamma approximation. Furthermore, the results show that Gamma distribution provides a good approximation of interference.

In those works, analysis is performed using the *Laplace Transform (LT)* and was limited to a Rayleigh fading channel. However, alternative tools can be used to simplify calculations and obtain more general results, considering a more general fading distribution. In this context, we can cite *Factorial Moment Measure* [25], *Moment Generating Function* [45], *Plancherel-Parseval theorem* [20].

The Moment Generation Function (MGF)-based approach is used to derive the PPP network performance in term of rate [45]. General fading distributions, Rayleigh, LogNormal and Nakagami-m channels, are considered. The MGF-based approach reduces the rate expression complexity from four to two integrals. Furthermore, the rate is independent of the BSs density and transmit powers.

The k-coverage probability, the probability that a user is covered by at least k BSs, of a K-tiers PPP network is investigated in [25], using Factorial Moment measures. Signal to Total Interference and Noise ratio (STINR) line ($\mathbb{R}^+$) p.p. is considered for analysis simplification. Note that STINR is expressed in function of SINR.

Even if PPP is recognized as a tractable modelling tool, it does not match to the realistic cellular deployment and a lot of works were interested in regular p.p.. In this p.p. type, there is neither attraction nor repulsion between points of the process.

3.5.2 Matérn Hard Core Process (MHCPP)

Martérn Point Processess are Hard Core p.p. firstly introduced by Matérn in [89]. They are models where points repel each other ([64, 67, 89, 120]). Matérn p.p. are not analytically tractable due to the non-independent nature of points.

Two types of Martérn Hard Core p.p. have been considered, Matérn I and Matérn II depending on the selection criterion of the points.

3.5.2.1 Type I

The Matérn I is derived from a stationary homogeneous PPP Φ_p of intensity λ_p by removing all points having neighbors within a distance δ. Points not satisfying the Matérn I condition are removed *simultaneously*. The intensity of the Matérn I, for the two dimension case, is

$$\lambda_m^{(I)} = \lambda_p \exp(-\lambda_p \pi \delta^2) \tag{3.-2}$$

3.5.2.2 Type II

The Matérn II is generated from a stationary homogeneous PPP as follows:

- Generate a parent PPP Φ_p with intensity λ_p.
- Associate each point $x \in \Phi_p$ to an independent uniform mark ($u_x \sim [0, 1]$).
- Retain a point in the daughter process Φ_m if it has the lowest mark in $B(x, \delta)$, the circle centered at x and with radius δ.

Analytically, the Matérn p.p. can be expressed as:

$$\Phi_m = \{x \in \Phi_p \ : \ m_x < m_y \ \forall y \in \Phi_p \cap B(x, \delta) \backslash \{x\}\} \tag{3.-2}$$

The intensity of Matérn II is given by

$$\lambda_m^{(II)} = \frac{1 - \exp(\lambda_p \pi \delta^2)}{\pi \delta^2} \tag{3.-2}$$

As in Matérn I, Matérn II points removal process is performed simultaneously. As a consequence, points eliminate each others. Matérn II keeps more points in the process than Matérn I. However, removing point by point may keep more points in the p.p.. Obviously, Matérn I is less denser than Matérn II, and both are less denser than PPP.

Matérn II p.p. is used to model nodes position in [67]. Using polar coordinates, a lower bound of the coverage probability (p_c) is derived. Then, based on a conjecture, a tighter lower bound is expressed. The proposed model is compared with a PPP, a square grid and a real BSs deployment. Results show that the (p_c) of the Matérn II is bounded between PPP as a lower bound (the worst case) and the grid square as an upper bound. Also, it is shown that the actual data fit the Matérn II p.p. for specific values of λ_m and δ.

In figure 3.3, we plot the parent PPP and the two daughter p.p.: Matérn I and Matér II. All the p.p. have the same intensity and the same distance threshold (for Matérn I and II)

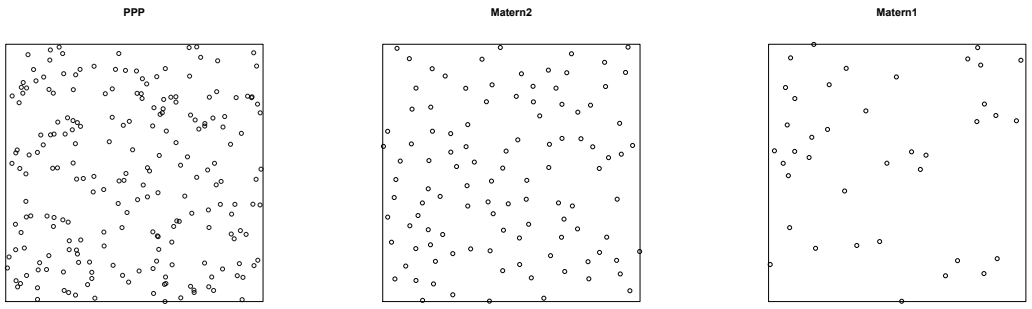

(a) PPP (b) MaternII (c) MaternI

Figure 3.3: Illustration of PPP, Matérn I and Matérn II all with the same intensity λ=200 and $\delta = 0.05$.

3.5.3 Ginibre Point Process (GPP)

The Ginibre point process [43, 96, 117] is a determinantal point process which induces a repulsion between points. This repulsion is interpreted by the probability density to place points. In fact, the probability to draw a point at the same position of an already drawn point is zero. This probability increases by increasing the distance from every existing points.

Analytical expression of the coverage probability (p_c) and its asymptotic property of a 1-tier GPP network is derived in [117]. It shows that in free noise regime (interference limited) the coverage probability is independent of intensity, transmit power, and path loss coefficient. This work was extended in [92] to a K-tier heterogeneous α-GPP network. The α-GPP is constructed from a parent GPP, where with probability α, a node in the parent GPP is selected to be in the α-GPP, and removed with probability $1-\alpha$.

A β-GPP homogeneous network is considered in [43], where $0 < \beta \leq 1$. β-GPP is constructed from a GPP by retaining, independently and with probability β, each point of the GPP and then applies an homothety of ratio $\sqrt{\beta}$ to the remaining points. Two approaches are used: Palm distribution and the reduced second moment to characterize the mean and variance of interference. Then the coverage probability is derived. A simplified expression of the mean interference is given for a given path loss function and a fixed path loss exponent. Extension of this work to an heterogenous network can analyze the impact of an non ideal backhaul and the effect of coordination/cooperation in the network performances.

All these p.p. either do not model the real deployment of nodes appropriately or are difficult to analyze. In the following, we present the r-l Square Point Process.

3.6 r-l Square Point Process

The r-l square p.p. ([28,81,82]) is a point process constructed to fit the real deployment of nodes. In this p.p., a minimum distance between processes is ensured.

PPP generates nodes independently in the plane, which leads to many problems such as uncovered regions or nodes very close to each other strongly interfering between each other. To overcome those problems, a new point process, called r-l square point process has been proposed in [28]. It is built as follows: the plane ($\mathbb{R}^2$) is divided into squares of the sizes $r \times r$. In each $r \times r$ square, a new sub-square of size $l \times l$ (with $0 \leq l \leq r$) is placed. A point is uniformly distributed in each sub-square. Those points represent the nodes. When $l < r$, this process is a Hard Core point process, as the points can not lie at a distance less than r-l. Hence, this model imposes that two points in adjacent squares can not be too close to each other (which reflects the real deployment of nodes and overcomes problems of the PPP). Mobile users are set according to a PPP in the plane. Illustration of this point process is given in figure 3.4.

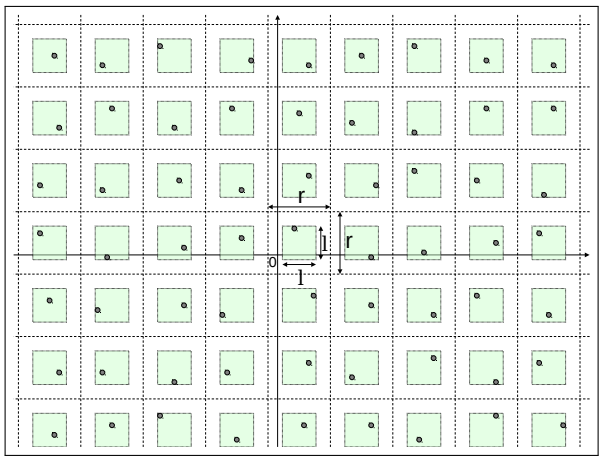

Figure 3.4: Construction of the *r-l* square point process [28].

3.7 Useful results of point processes

In this subsection, we present useful definitions and properties of p.p..

Theorem 3.7.1 (Campbell's theorem) *Let Φ be a point process and $f : \mathbb{R}^d \to \mathbb{R}$ be a measurable function. Then,*

$$\mathbb{E}\left[\sum_{x\in\Phi} f(x)\right] = \int_{\mathbb{R}^d} f(x)\Lambda(dx). \tag{3.-2}$$

This theorem, helps to compute the expected sum of a function over points of the process Φ.

Definition 3.7.2 (Moment generating functional (MGFL)) *Let Φ be a point process and $v : \mathbb{R}^d \to [0,1]$ be a measurable function such that $1 - v$ has a bounded support. Then, the probability generating functional of Φ is*

$$G[v] = \mathbb{E}\left(\prod_{x\in\Phi} v(x)\right). \tag{3.-2}$$

Definition 3.7.3 (Laplace transform) *Let Φ be a point process and $f : \mathbb{R}^d \to [0,1]$ be a measurable function. Then, the probability generating functional of Φ is*

$$\mathcal{L}_\Phi(f) = \mathbb{E}\left[\exp\left(-\int_{\mathbb{R}^d} f\Phi(dx)\right)\right]. \tag{3.-2}$$

Proposition 1 (relation between the Laplace transform and the PGFL) *The Laplace transform and the PGFL are linked by the following equation:*

$$\mathcal{L}[f] = G[\exp(-u)]. \tag{3.-2}$$

3.8 Taxonomy

In table 3.1 , we summarize the discussed works depending on the used p.p. to model BSs position and the used analytical tools.

	Laplace Transform (LT)	Moment Generating Function (MGF)	Factorial Moment Measure
Poison p.p.	Coverage [61, 62], Coordination [101, 123]	Rate [45]	Coverage [25]
Matérn p.p.	Coverage [64,67,89, 120]	-	-
Ginibre p.p.	Coverage [43,96,117]	-	-

Table 3.1: Classification of works with the corresponding PPs and tools.

In the next section, we outline some interference management schemes, then in section 3.10 we focus on *coordination-based* ones.

3.9 Inter Cell Interference Coordination (ICIC)/ enhanced ICIC (eICIC)

Inter Cell Interference Coordination (ICIC) is standardized in 3GPP release 8 ([63]). It aims at reducing interference for cell edge users experiencing low SINR. The main idea of ICIC is to use different radio resources for cell edge users than these used for cell center users. Coordination is performed as follows: BSs generate interference information (Relative Narrowband Tx Power (RNTP), High-Interference Indicator (HII), and Overload Indicator (OI)) for each radio resource (RB) and share them through X2 interface with adjacent BSs. Based on the shared information, neighbor BSs allocate radio resources in order to minimize the interference. Although ICIC reduces interference, ICIC reduces the network throughput since the full radio resources are not used in each cell.

Dynamic Fractional Frequency Reuse is investigated in [125]. The sub-band to be allocated to a cell edge region is dynamically chosen and it is proportional to the ratio of the area of the cell edge-region and the area of the cell. Results show that the dynamic planning enhances the performance compared to the classical planning. However, the performance analysis is based on Monte-Carlo simulations and the paper does not provide any analytical expression of the rate or the coverage probability even if the nodes are Poisson distributed which makes the analysis more tractable.

Random frequency sub-bands allocation for a PPP network is considered in [17]. The coverage probability and the throughput of an interference limited scenario are derived. It shows that increasing Δ, the frequency reuse factor, increases the coverage but reduces the throughput. This is explained by the fact that, the available bandwidth is divided by Δ. Furthermore, the average throughput is maximized for Δ=1.

In [102], authors analyze performance of Strict FFR and SFR using stochastic geometry tools. The coverage probability (p_c) is derived for both, users in the cell edge and in the cell center regions. The analytical expressions of p_c are simplified to a closed form expression for some special cases ($\alpha = 4$ and neglecting the noise, $\sigma^2 = 0$). It concludes that Hard FFR reduce interference more than SFR when no power control is performed and conversely when the transmission power to the cell edge user is adjusted (increased). However, the frequency sub-bands are allocated *randomly* to the cell edge regions. [103, 135] generalize the work in [102] to an heterogeneous network. [135] analyses the coverage probability p_c of a K-tiers network for both closed (CA) and open (OA) access modes. It concludes that, p_c of an edge user under OA mode can be *decomposed* to the sum of $(p_{c_i})_{1\leq i\leq K}$ of each tier under CA mode. Furthermore, for an interference limited scenario, p_c is independent from the channel parameter (mean). [115] proposes a distributed algorithm for frequency allocation in heterogeneous (2-tier) networks. Each femtocell runs the algorithm locally, and selects 3 frequency sub-bands (from 7) to use for transmitting to its attached users. The sub-bands are selected depending on the location of the femtocell, either in the center or the edge of the macro and on the received signal strength indication (RSSI) of frequency sub-bands. [79] analyses the impact of the power control on the overall throughput of the system. It concludes that the power level does not affect the rate of the inner region. However, it has an impact on the outer region rate.

To the best of our knowledge, all of these works either (i) consider a fixed network topology, the hexagonal grid topology, hence, the network performances are evaluated basing on numerical simulations or, (ii) are based on a random sub-band selection strategies. As a consequence, two adjacent cells may use the same sub-band for their outer region, which limit the effect of frequency reuse.

An enhanced version of ICIC (eICIC) is standardized in 3GPP release 10. It uses power, frequency and time domains to mitigate interference. Almost Blank Sub-Frames (ABSF) is the key feature of eICIC which allows time sharing of radio resources between different BSs. ABSF are sub-frames leaved empty (blank) by a BS (Macro BSs), so adjacent BSs (Pico, Femto BSs) can schedule these sub-frames to serve cell edge users experiencing low SINR.

ICIC and eICIC help reducing the interference of cell edge users. However, they do not improve the network performance, in terms of coverage probability and throughput. In fact, radio resources usage is restricted into the frequency domain for ICIC and into the time domain for eICIC. Furthermore, interference information are shared between adjacent BSs on a relatively long term basis,

resulting to an *outdated* information and, hence, fast changing channel conditions are not taken into account in the inter-cell coordination procedure. All of this motivate the need of a new powerful interference management schemes that overcome the listed problem.

In the next subsection, we present Coordination MultiPoint, a new powerful interference management scheme standardized in releases 11 and 12.

3.10 Coordination MultiPoint (CoMP) Models

In order to improve the overall quality (received SINR) of the edge users, Coordinated MultiPoint (CoMP) provides enables dynamic coordination over a variety of different BSs. Mainly, CoMP turns the inter-cell interference into useful signals. In this section, we outline and discuss works analyzing CoMP using stochastic geometry tools.

3.10.1 Joint Transmission (CoMP-JT)

In [101] *CoMP-JT* is studied. A K-tier heterogenous network is considered, where each tier is characterized by its own density, transmission power and path loss exponent. The position of nodes is modeled by a homogeneous PPP. Due to the stationary nature of PPP, only one user placed at the center is considered. A Rayleigh fading channel is assumed. All of nodes inside the cooperating set act as a serving node. As a consequence, the remaining nodes, outside the cooperating set, act as interferers. Two connectivity models (association rules) are considered in this contribution: (i) the user is connected to the strongest average received power among all nodes in the k tier network, and (ii) the user is connected to the nearest node from each tier. Analytical expression of coverage probability (p_c) is derived for the two cases and it is expressed as function of the Laplace transform of the interference and its depend on the transmit power, SINR threshold, and on the intensity. Two tiers are considered: a Macro and Pico networks, each having its specific node intensity and transmit power. For a SINR threshold of 0dB, it is shown that the cooperation scheme case 1 is better than the case 2 and its provides a gain of 20% in the coverage probability. Moreover, it outperform the non-cooperation scheme by a gain of 30%. It can be concluded that the cooperation improves the performance metrics and it is better to associate users the the strongest nodes instead of the nearest ones.

Location-Aware Cross-tier Cooperation (LA-CTC), a modified version of CoMP-JT, is proposed in [114]. A two tiers network of Macro and Pico cells is studied, and two independent homogeneous PPPs modeling nodes positions are considered. In LA-CTC, a user can operate in three modes: either in (i) non-CoMP Macro, or (ii) non-CoMP Pico, or (iii) CoMP user, depending on its location. In fact, users experiencing good SINR, from one tier are served only by one node and are not involved in CoMP procedure. They operate on either non-CoMP Macro or non-CoMP Pico mode depending

on from which tier they receive the strongest signal. Only users suffering from harmful interference and experiencing low SINR are involved in CoMP procedure and are served by the two tiers (Pico and Macro). Hence, the data exchange through the backhaul is reduced. Explicit forms of the outage probability and the ergodic rate are derived. Simulations show that the proposed scheme outperform the range expansion, fully cooperation approaches.

Based on user centric clustering and channel-dependent cooperation activation, *Non-Coherent Joint-Transmission (NC-JT)* is tackled in [123]. A K-tiers heterogeneous PPP network is considered. Notions of cooperative set and active cooperative set are introduced. The cooperative set of each tier is defined as: If the RSS of a BS at the user is greater than a threshold (Δ_k), then this BS belong to the cluster (user-centric cluster). The threshold depend on the allowable overhead on each tier. While, the active cooperative set is defined as follows: If the signal received at the typical user is greater than the cooperation activation threshold (T_k), then this BS joint the cooperative transmission. Note that each tier has a specific threshold that models the complexity and overhead allowed in each tier. Semi closed form of the coverage probability is derived for general fading distributions. Results shows that NC-JT can be used for load balancing between different tiers of the network by varying the thresholds (Δ_k and T_k).

3.10.2 Coordinated Beamforming/Scheduling (CoMP-CB/CS)

CoMP-CB/CS is addressed in [128], where a K-tiers PPP network is considered, each characterized by its transmit power p_k, number of antenna in each BS N_k, path loss exponent α_k and intensity λ_k (k is the index of the tier). The block fading is divided into two phases: (i) overhead messaging phase and, (ii) cooperation phase. In the overhead messaging phase: Using training sequences, users estimate the downlink channel at the beginning of each time slot. The estimated channel is compared to codewords $(c_i)_{i\in\mathbb{N}}$ of the codebook $C_{i,k}$ available at both sides (users and BSs). Then, the codeword maximizing $\mid h_i c_i \mid^2$ is selected and feedbacked to the serving BS. The serving BS transmits overhead information (consisting of $c_{i,k}$) via backhaul to other BSs in the coordination set. These BSs perform a zero forcing beamforming by selecting a preceding vector $f_{i,k}$ such that $\mid f_{i,k} c_{i,k} \mid = 0$. Analytical expression of throughput and bounds of the coverage probability are derived. Results show that CoMP-CB is not beneficial if the overhead messaging is larger than 60% of the block fading size, and 45% for the coverage. Furthermore, the larger the overhead messaging phase is, the worse the network performance are. Additionally, the impact of the coordination set size on performance is analyzed. It can be observed that coordinating with one and only one BS is the optimal solution taken into account the overhead delay constraints for heterogeneous networks (coordinating with more BSs leads to network performance degradation).

The impact of imperfect feedback (imperfect CSI) of a PPP network under *CoMP-CB/CS* scheme is investigated in [12]. Two bit allocation schemes are considered: (i) *Equal bit allocation*

Band: divide B_{total} equally between the N interfering channels and the useful channel $B_{0,l} = [B_{total}/N]$ and $B_0 = B_{total} - NB_{0,l}$, and (ii) *Adaptive bit allocation*: optimize the bit allocation strategy to optimize the loss in rate

$$B_{0,l} = \frac{B_i}{\mid \mathcal{K} \mid} + (N_t - 1)\log_2\left(\frac{(1+r_{0,l})^{-\alpha}}{\prod_{l\in\mathcal{K}}(1+r_{0,l})^{-\alpha/|\mathcal{K}|)}}\right). \tag{3.-2}$$

$$\begin{cases} min_{B_{0,1},\ldots,B_{0,N}} & \sum_{l=1}^{N}(1+r_{0,l})^{-\alpha}\Gamma\left(\frac{2N_t-1}{N_t-1}\right)2^{-\frac{B_{0,l}}{N_t-1}} \\ & \text{s.t}\sum_{l=1}^{N}B_{0,l} = B_i \text{ , and } B_{0,l} > 0 \end{cases}. \tag{3.-2}$$

An upper bound of mean loss in rate due to limited feedback $\Delta\tau$ is derived.

Figure 3.2 shows a taxonomy of the discussed works.

CoMP schemes	Papers	Techniques
CoMP-JT	[101]	*CoMP-JT* for a PPP K-tier heterogenous
	[114]	*Location-Aware Cross-tier Cooperation (LA-CTC)*
	[123]	*Non-Coherent Joint-Transmission (NC-JT)* for a K-tiers PPP network
CoMP-CB/CS	[128]	*CoMP-CB/CS* for a PPP K-tier heterogenous
	[12]	Imperfect feedback of a PPP network under *CoMP-CB/CS*

Table 3.2: Taxonomy of CoMP schemes.

3.11 Conclusion

In this chapter, we mentioned the advantages of using p.p. in wireless communication to model the spatial distribution of nodes. Furthermore, we presented related work dealing with interference management schemes by focusing on coordination-based schemes.

In the next chapter, we present a new interference management model based on CoMP-JT, while using tools from stochastic geometry to model nodes positions in the network. Furthermore, we derive performance metrics in terms of coverage probability and throughput. Then, we investigate the impact of the coordination set size on these metrics.

Chapter 4

The r-l square point process: The effect of coordinated multipoint joint transmission

Contents

4.1 Chapter Summary

A 1-tier network composed by multimode low power nodes (LTE/Wifi) is considered as a cost-efficient solution for operators to improve services in poorly or uncovered rural areas. Using an interference coordination technique, network performance can be further improved. Stochastic geometry gives a set of tools to model the location of base stations and user equipments in such wireless networks. Using a spatial model we analyse the network performance in terms of coverage probability and data rate. To realistically model multimode node locations, a new point process model, called the r-l square point process (p.p.), is developed. The model of downlink communication including the coordination technique is developed and it allows to evaluate the system performances in term of coverage probability and throughput. Results show that cooperation

among nodes improves the network performance.

This chapter is structured as follows. We give a general introduction in the next section. In section 4.3 we detail our new analytical model of coordination based on $r - l$ square p.p.. We will evaluate the resulting model by simulation and discuss the results in section 4.4. We will conclude the chapter in section 4.5 and give some remarks to improve the model in the future works.

4.2 Introduction

According to ITU statistics, there are over 6.8 billion active subscribers of cellular networks [126]. However, nowadays many rural areas all over the world are still lacking of the connectivity service. This is due to two main factors : the installation cost of macro base stations (BS) and the non existence of any kind of wired infrastructure in such areas. An innovative and a cost-efficient solution for operators to provide services to poorly-covered or uncovered areas is the deployment of outdoor multimode femtocells. A multimode femtocell is a low power node (LPN) operating on both cellular (4G/LTE) and Wi-Fi technologies. This new generation of femtocells are expected to offload the cellular network traffic on Wi-Fi bands to improve the capacity in case of dense networks [21].

As the position of nodes plays an important role in wireless communications, the multimode femtocell location should be defined carefully. LPNs must not be lied too close together to reduce the interference mainly at the cell edge. But at the same time, they should not be further apart than Wi-Fi transmission range. The aim is to form a Wi-Fi mesh network using the Wi-Fi interfaces of these nodes, and to use it as an access network to the macro base station. As a consequence, the underlying Wi-Fi mesh network extends the coverage of the macro BS to consider far mobiles users, as shown in figure 1.

To deploy such a network in rural zone, it is expected that multimode base stations are outsourced or managed by some Virtual Operators (VOP) such as city hall, schools or compagnies. So that, the scenario of figure 1 considered here is completely different from classical deployment of femtocells which intends to increase the capacity of macro cellular network in urban regions. In such cases, the position of the femtocell BS is user-dependent leading to dense network. In stochastic geometry, Poisson point process is intensively used to study the performance of such deployment in terms of coverage/outage probability, and bit rate [12, 20, 25, 43–45, 61, 96, 117]. The Poisson Point Process model is used as it is more trackable than others point processes of stochastic geometry.

To the opposite to PPP model, and to consider the scenario of the figure 4.1, [28] proposed a new point process called *r-l* square process to model the position of the multimode femtocell BSs and to evaluate the coverage probability depending on the distance that separates the nodes. *r-l* square process allows a correlation between nodes defined by Wi-Fi communication ranges and deployment policies specified by the Virtual Operators responsible of the deployment of these base

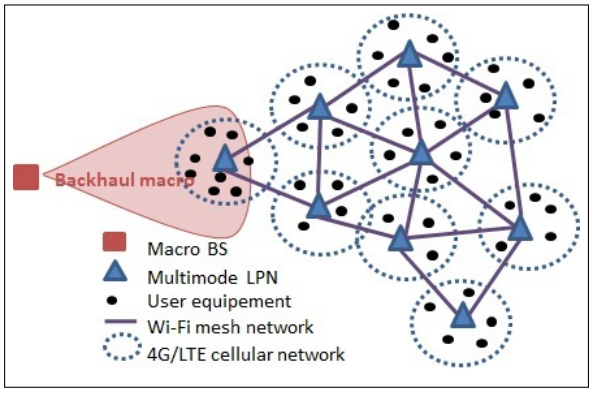

Figure 4.1: Femtocell and Wi-Fi mesh network architecture.

stations in the rural region.

However, like femtocell networks in rural region used to increase the capacity, our scenario suffers from interference. This is mainly due to the difference between the coverage of both cellular (4G/LTE) and WiFi technologies. For example, commercial outdoor femtocell base stations ensures a coverage about 750m with a transmission power of 5watts, whereas outdoor WiFi access points cover only 250m. Consequently, when many multimode LPNs are used to cover a region, a severe interference can be generated between LTE femtocells.

Hence, interference is one of the challenges facing the femtocells deployment which affect considerably the network performance. Recently, the Coordinated Multi-Point techniques (CoMP) has been attracting more attention, as stated in Chapter 3. This coordination technique intends to reduce interference and improve throughput of cell edge users. Joint Transmission (JT) and Coordinated Beamforming/Scheduling (CB/CS) are two ways to perform CoMP.

The aim of this work is to improve the coverage probability of a 1-tier network composed of low power nodes (scenario in fig 4.1) using a coordination technique. To realistically model femtocell locations the $r - l$ square process is used. The model of downlink communication including the coordination technique is developed and allows us to evaluate the system performance in terms of coverage probability and throughput.

In the following, we focus on the downlink and we evaluate the performance in terms of coverage probability, under the r-l square model described above when coordination in particular CoMP-JT is applied between nodes to mitigate the interference. We assume an ideal Wi-Fi mesh network to transmit all duplicated signals without overloading links.

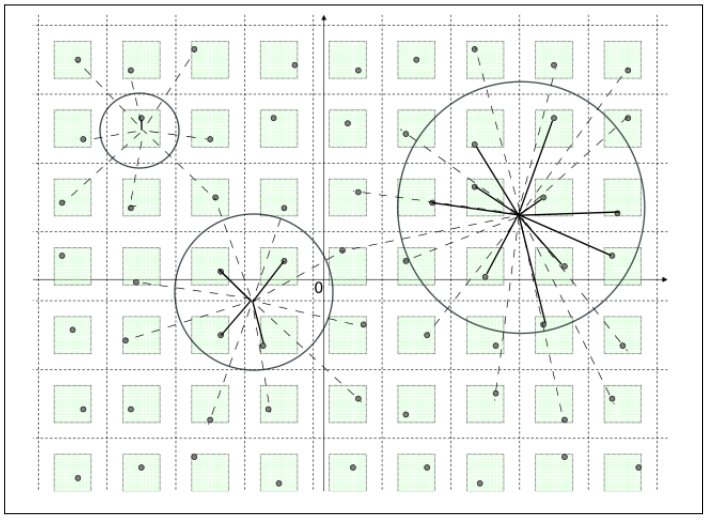

Figure 4.2: Illustration of the coordinated set $B_u(d)$: The solid lines represent the useful signal received by a mobile user from the BSs inside $B_u(d)$ and the dashed lines represent the interference.

4.3 Coordinated-MultiPoint Joint Transmission model

CoMP-JT is a cooperation technique used to reduce interference. User equipment receives data not only from its serving BS but also from all BSs in the coordinated set. Signals received from nodes outside the coordinated set are seen as interference. This is illustrated by the following equation 5.3.

The received signal at the typical user equipment u is:

$$y = \underbrace{\sum_{X_i \in \mathcal{C}} \sqrt{p_t}\xi_i \sqrt{l(||X_i - u||)}}_{\text{Useful signal}} + \underbrace{\sum_{X_j \in \Phi \setminus \mathcal{C}} \sqrt{p_t}\xi_j \sqrt{l(||X_j - u||)}}_{\text{Interference}} + \underbrace{N}_{\text{Noise}} \tag{4.0}$$

where Φ is the r-l square p.p., p_t is the transmission power of nodes (it is assumed to be the same for all nodes), $(\xi_i)_i$ are i.i.d $\sim \mathcal{CN}(0,1)$ Gaussian random variables with mean 1 modeling fading, $l(.)$ is the path loss function and $N \sim \mathcal{CN}(0, \sigma^2)$ is an additive white Gaussian noise (AWGN). $\mathcal{C}$ is the coordinated set and is defined as follows:

$$\mathcal{C} = \{X_i \in \Phi \text{ s.t.} X_i \in B_u(d)\} \tag{4.0}$$

Nodes not in the coordinated set ($\Phi \setminus \mathcal{C}$) act as interferers. In other words, the coordinating BSs are the BSs inside the ball $B_u(d)$ centered at u and radius d. All BSs outside the ball act as interferers. Figure 4.2 illustrates examples of two coordinated sets with different sizes. Solid lines indicate the useful or duplicated signals received by the mobile user u located at the center of the circle.

Thus, the SINR is given by

$$\text{SINR} = \frac{\mid \sum_{X_i \in \mathcal{C}} \sqrt{p_t}\xi_i \sqrt{l(||X_i - u||)} \mid^2}{\sum_{X_j \in \Phi \setminus \mathcal{C}} p_t \mid \xi_j \mid^2 l(||X_j - u||) + \sigma^2} \tag{4.0}$$

Proposition 2 *The coverage probability under CoMP-JT is given by:*

$$\begin{aligned} p_c(T) &= \Pr(SINR > T) \\ &= \prod_j \mathbb{E}\left[\left(\frac{1}{1 + T\frac{l(||X_j - u||)\mathbb{1}_{\{X_j \notin B_u(d)\}}}{\sum_i l(||X_i - u||)\mathbb{1}_{\{X_i \in B_u(d)\}}}}\right)\right] \\ &\times \mathbb{E}\left[\exp\left(-T\frac{\sigma^2}{\sum_{X_i \in \mathcal{C}} p_t l(||X_i - u||)}\right)\right] \end{aligned}$$

Proof 1

$$\begin{aligned} p_c(T) &= \Pr(SINR > T) \\ &= \Pr\left\{\frac{\mid \sum_{X_i \in \mathcal{C}} \sqrt{p_t}\xi_i \sqrt{l(||X_i - u||)} \mid^2}{\sum_{X_j \in \Phi \setminus \mathcal{C}} p_t \mid \xi_j \mid^2 l(||X_j - u||) + \sigma^2} > T\right\} \\ &= \Pr\left\{\mid \sum_{X_i \in \mathcal{C}} \sqrt{p_t}\xi_i \sqrt{l(||X_i - u||)} \mid^2 \right. \\ &\left. > T\left(\sum_{X_j \in \Phi \setminus \mathcal{C}} p_t \mid \xi_j \mid^2 l(||X_j - u||) + \sigma^2\right)\right\} \\ &\overset{(a)}{=} \mathbb{E}\left[\exp\left(-T\frac{\sum_{X_j \in \Phi \setminus \mathcal{C}} p_t \mid \xi_j \mid^2 l(||X_j - u||) + \sigma^2}{\sum_{X_i \in \mathcal{C}} p_t l(||X_i - u||)}\right)\right] \\ &= \mathbb{E}\left[\exp\left(-T\frac{\sum_{X_j \in \Phi \setminus \mathcal{C}} p_t \mid \xi_j \mid^2 l(||X_j - u||)}{\sum_{X_i \in \mathcal{C}} p_t l(||X_i - u||)}\right)\right] \\ &\times \mathbb{E}\left[\exp\left(-T\frac{\sigma^2}{\sum_{X_i \in \mathcal{C}} p_t l(||X_i - u||)}\right)\right] \end{aligned}$$

where (a) follows the hyper exponential property. The first term is as follows:

$$\begin{aligned}
&\mathbb{E}\left[\exp\left(-T\frac{\sum_{X_j\in\Phi\setminus\mathcal{C}} P_t \mid \xi_j \mid^2 l(||X_j-u||)}{\sum_{X_i\in\mathcal{C}} P_t l(||X_i-u||)}\right)\right]\\
&= \mathbb{E}\left[\exp\left(-T\frac{\sum_j \mid \xi_j \mid^2 l(||X_j-u||)\mathbb{1}_{\{X_j\notin B_u(d)\}}}{\sum_{X_i\in\mathcal{C}} l(||X_i-u||)}\right)\right]\\
&= \mathbb{E}\left[\prod_j \exp\left(-T\frac{\mid \xi_j \mid^2 l(||X_j-u||)\mathbb{1}_{\{X_j\notin B_u(d)\}}}{\sum_{X_i\in\mathcal{C}} l(||X_i-u||)}\right)\right]\\
&\overset{(b)}{=} \mathbb{E}\left[\prod_j \left(\frac{1}{1+T\frac{l(||X_j-u||)\mathbb{1}_{\{X_j\notin B_u(d)\}}}{\sum_{X_i\in\mathcal{C}} l(||X_i-u||)}}\right)\right]\\
&= \mathbb{E}\left[\prod_j \left(\frac{1}{1+T\frac{l(||X_j-u||)\mathbb{1}_{\{X_j\notin B_u(d)\}}}{\sum_i l(||X_i-u||)\mathbb{1}_{\{X_i\in B_u(d)\}}}}\right)\right]\\
&= \prod_j \mathbb{E}\left[\left(\frac{1}{1+T\frac{l(||X_j-u||)\mathbb{1}_{\{X_j\notin B_u(d)\}}}{\sum_i l(||X_i-u||)\mathbb{1}_{\{X_i\in B_u(d)\}}}}\right)\right]
\end{aligned}$$

where (b) from the fact that $(\mid \xi_i \mid^2)_i$ *are exponentially distributed.*

Remark 1 *In the Interference limited (free noise) regime, the coverage probability is independent from the transmit power of the LPNs.*

The rate can be derived from the coverage probability by the following formula:

$$\begin{aligned}
R &= \mathbb{E}(\log_2(1+\mathrm{SINR}))\\
&= \int_0^\infty \Pr\{\log_2(1+\mathrm{SINR}>t)\}dt\\
&= \int_0^\infty \frac{\Pr\{\mathrm{SINR}>e^t-1\}}{\log(2)}dt\\
&\overset{(a)}{=} \frac{1}{\log(2)}\int_0^\infty \frac{\Pr\{\mathrm{SINR}>x\}}{(x+1)}dx\\
&= \frac{1}{\log(2)}\int_0^\infty \frac{p_c(x)}{(x+1)}dx
\end{aligned}$$

Where (a) follows from a variable change ($x = e^t - 1$).

Hence, the throughput is derived by replacing $p_c(T)$ (Eq. 2) in equation (4.3).

Remark 2 *The expectation in eq. 4 is over the p.p. and it is difficult to compute because the*

Parameters	Values
r	50 m
l	30 m
Path-loss function	$l(r) = r^{-\alpha}$
α	3.0
p_t	250 mW
Bandwidth	10 MHz
Noise	Normal ($1.0e^{-11}$, $3.76e^{-11}$)

Table 4.1: Parameters for the numerical evaluation.

probability density function (pdf) of the r-l square p.p. is unknown. Hence, Monte Carlo simulation is used to validate results.

4.4 Simulation and results

We consider a 1-tier network composed by LPNs connected by a mesh network. According to [124] which gives guidelines of picocells characteristics, we set $p_t = 250mW(24dBm)$, r = 50m, the sides of squares, and l= 30m, the sides of sub-squares. By this configuration, the distance between two nodes can not be less than $r - l$ = 20m. The path loss model considered is given by: $l(r) = r^{-\alpha}$, where α is the path loss exponent. Furthermore, we use a bandwidth of 10 MHz. We consider a network composed of 25 squares and a typical user placed in the center of the grid. We take, for analysis, the mean over 1000 realizations of the spatial process. Simulation parameters are summarized in table I.

Figure 4 shows the coverage probability p_c of a user placed at the cell edge versus d, the radius of the coordinated set. It reflects the impact of the coordinated set size on this performance metric. We plot p_c for three values of the SINR threshold, -2 dB, 0 dB and 2 dB. We observe that the coverage probability increases with the radius of the coordinated set and it is too close to 1 when the radius of the coordinated set exceeds 70m (equivalent to 5-6 LPNs in $\mathcal{C}$). Obviously, the smaller the SINR threshold T is, the better the coverage is ($p_c(-2dB) > p_c(0dB) > p_c(2dB)$).

In figure 4.4, we show the coverage probability of the CoMP-JT versus the SINR threshold. Simulations are performed for six values of d, the ball radius: 30, 50, 75, 100, 150 and 200m. Figure 4.4 shows the effect of coordination for these values of d on the coverage. In fact, when d becomes larger, the coordinated set size is increased, the coverage probability is enhanced. This gain can be characterized as follows:

$$G(p_t) = \frac{(P_c^{\text{Coordinated set radius}})^{-1}(p_c)}{(P_c^{\text{Baseline radius}})^{-1}(p_c)} \tag{4.-6}$$

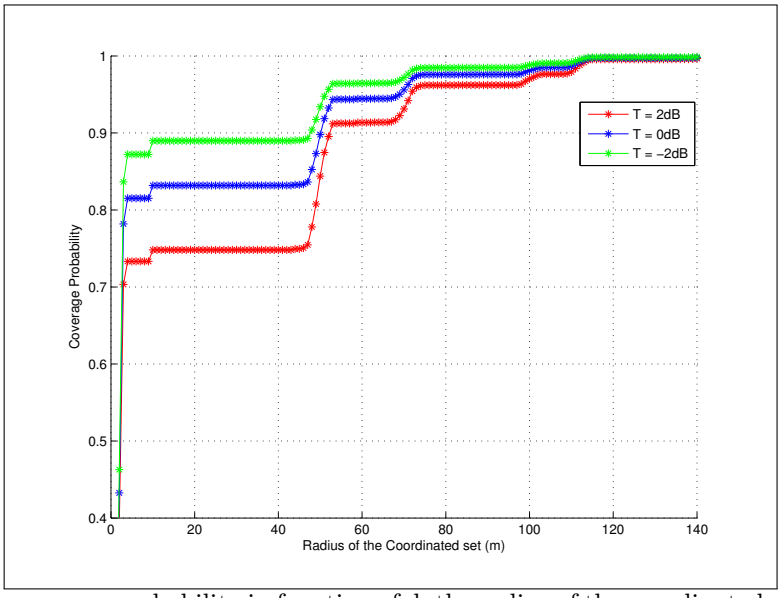

Figure 4.3: The coverage probability in function of d, the radius of the coordinated set $\mathcal{C}$ for different values of the SINR threshold T.

where $P_c^{\text{Baseline radius}}$ and $P_c^{\text{Coordinated set radius}}$ are the coverage probabilities of the r-l square when the user equipment is served by its serving BS and when the radius of B_u is d, respectively. The case d = 30m represents the baseline radius because only the serving BS is inside the coordinated set. $(.)^{-1}(p_c)$ is the SINR threshold value where the coverage probability is set to p_c. This definition is similar to the coding gain in the coding theory. Table (table II) gives some examples of the gain that we can get from cooperation.

Figure 4.5 shows the average rate versus the radius of the coordination set for different values of the path loss exponent. The average data rate is an increasing function of number of BSs in $\mathcal{C}$. We can also see that the curves have a step function form. This can be explained by the fact that

Baseline radius	**Coordinated set radius**	Gain
30 m	50 m	2 dB
30 m	75 m	2.5 dB
30 m	100 m	2.7 dB
30 m	150 m	2.9 dB
30 m	200 m	3 dB

Table 4.2: The cooperation gain.

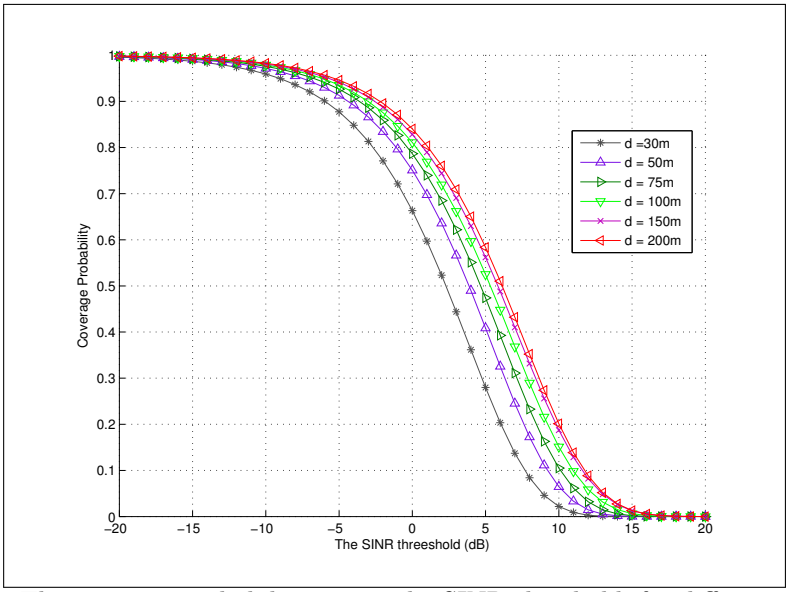

Figure 4.4: The coverage probability versus the SINR threshold, for different values of d.

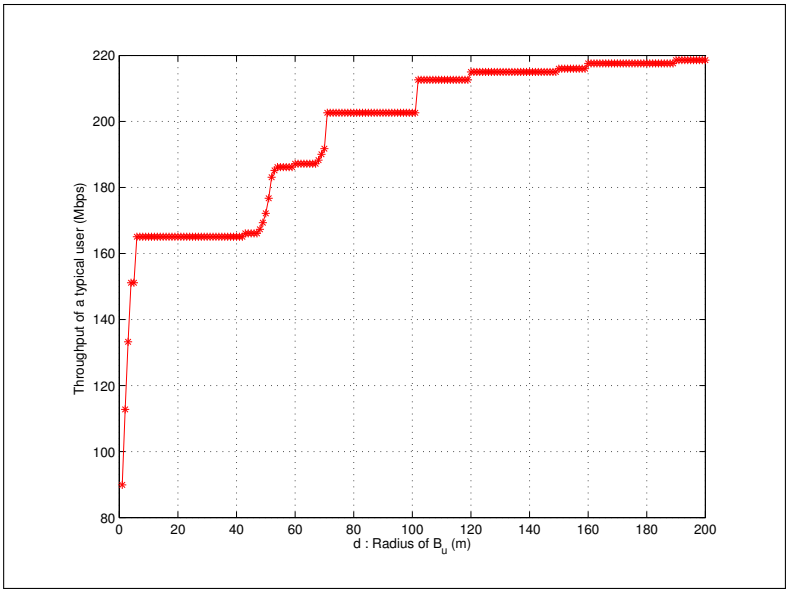

Figure 4.5: Throughput of a typical user in function of the coordination set size.

the rate remains constant until a new BS joint the coordinated set. The transition from one stair to the upper one is done when a new BS joint the coordinated BSs.

For the coverage and the throughput, it is clear from fig. 4.4 and fig. 4.5, that after a certain radius of the coordination set, those performance metrics remain constant or slightly improve. This can be explained by the fact that the interference is mainly generated by the neighbor BSs (the 8 squares) surrounding the serving BS.

In a configuration of 5×5 squares, we have shown for different CoMP sizes that this technique effectively improves the performance in terms of coverage probability and throughput.

4.5 Conclusion

In this chapter, we consider a 1-tier network composed of multimode femtocells (LTE/Wi-Fi) linked by a mesh network. It is a cost-efficient solution proposed by cellular operators to offer connectivity service to mobile users in uncovered or poorly covered rural areas. In such deployment, mobile users communications are carried in through the Wi-Fi mesh network to access the macro base station.

We focus our work on the evaluation of the gain that can provide the coordination multipoint joint transmission approach (CoMP-JT) when used to mitigate interference between multimode femtocells. CoMP-JT is a cooperation method where a mobile user receives duplicated signals from a coordinated set of femtocells, in order to limit interference and enhance network performance mainly the coverage probability and the throughput. We use the $r-l$ square point process proposed earlier to model the multimode femtocells position. We derive the expressions of the coverage probability p_c and the rate R of a typical user on the downlink. By simulation, we showed that increasing the coordination set size improves the performance of our system. Furthermore, we conclude that after a certain coordination set radius (d) threshold it is inefficient to add more BSs to the coordination set $\mathcal{C}$.

In the next chapter, we present a new model, based on Joint Transmission Coordinated-MultiPoint (CoMP-JT) in order to evaluate the performance of dense very high throughput WLANs.

Chapter 5

Performance Evaluation of Joint Transmission Coordinated-MultiPoint in Dense Very High Throughput WLANs Scenario

Contents

5.1 Chapter Summary

In this chapter, we propose to use the Joint Transmission approach of Coordinated Multipoint (CoMP-JT) of cellular networks to reduce the interference in dense Very High Throughput (VHT) wireless LANs. VHT WLANs are based on wider channel bandwidth, efficient modulation techniques and support for spatial streams using MIMO schemes. However, the interference problem

persists despite these approaches, and thereby prevents mobile stations from fully reaping the capacity improvement of such networks. In order to optimize the coverage and minimize the cell overlap in dense environment like stadium scenario, AP locations must be planned carefully. To this end, we model the positions of nodes using a spatial stochastic model called the $r - l$ square point process introduced in [28]. Then, we derive the coverage probability and throughput expressions and investigate the benefit of Joint Transmission coordination technique. Using simulation, we characterize the performance metrics for different sizes of coordinated set and carrier sensing domain of access points. Our results show that CoMP-JT is a promising scheme for dense WLANs.

The chapter is structured as follows. In section 5.3, we recall the $r - l$ square p.p. and derive the analytical model of CoMP-JT. Simulation results are discussed in section 5.4. We conclude the chapter in section 6.7 and give some perspectives to this work.

5.2 Introduction

In the last Wi-Fi standards and amendments, Task Groups of IEEE 802.11 are seeking to provide very high throughput (VHT) and low latency services over wireless local area networks (WLANs). The aim is to fulfill the increasing demand of end users and the exponential growth of wireless data traffic. New standards like 802.11ac, also called Gigabit Wi-Fi, are expected to provide up to 7 Gbps in 5GHz band [34]. These improvements are based on three factors: wider channel bandwidth, efficient modulation techniques and support for spatial streams using MIMO scheme and its variations. However, even using this new generation of wireless access points (APs), the interference problem cannot be totally avoided in dense networks. As a consequence, critical applications such as high definition video streaming (HDTV) cannot fully benefit from this new generation of WLANs.

High density WLANs, like multi-apartment building [11] and stadiums [110], face significant challenges due to the very high number of APs in closed proximity. It results in a significant increase of interference level for co-channel APs due to the limited number of non-overlapping channels, the unplanned selection of primary channels and channel widths, and the unplanned deployment of APs with factory default parameters. Authors of [11, 48] show that the number of interfering access points highly affect the throughput and they propose power control and rate regulation algorithms to reduce the interference among neighboring APs. From a systems modelling approach, authors of [100] use a modified Matérn point process (p.p.) to consider the impact of CSMA/CA and address planning problems to provide a certain QoS with a reduced deployment cost. In [70], the required APs density to meet an average traffic demand is estimated.

Coordinated Multipoint in cellular networks (CoMP) Taking advantage of multiple antenna in MIMO systems, CoMP is a cooperation technique with the objective of reducing the

interference and hence increasing the cellular network throughput. In a cellular network, Base Stations (BSs) communicate with each other over a backhaul network and exchange data in Joint Transmission mode (CoMP-JT). Users receive multiple copies of the same data from different BSs in the coordinated set, and the signal received from BSs outside of the coordinated set is seen as interference. Several works investigate the modeling and evaluation of CoMP approaches using stochastic geometry as discussed in Chapter 3.

However, only a few works have considered the CoMP approach in WLANs. For example, [84] deals with the feasibility of CoMP in IEEE 802.11 High Efficiency WLAN (HEW) and gives directives to integrate coordination in such networks. It proposes a centralized architecture where an AP is chosen as a controller to coordinate transmissions.

In this chapter, we aim at analyzing the interference in dense Wi-Fi networks. Three main contributions are presented in this chapter:

- Utilization of Joint Transmission Coordination Multipoint approach, usually used in cellular networks, to manage the interference and hence improve the received signal quality.

- Mathematical framework to model the coordination in Wi-Fi networks using a realistic p.p.. We use a spatial stochastic model, the $r-l$ square p.p., which is more appropriate to model dense WLANs, where positions of APs are correlated like in stadium deployment in order to ensure high capacity. We derive the coverage probability and the throughput expressions when CoMP-JT is performed.

- Evaluation of the analytical model performed using Monte Carlo simulation in MATLAB.

5.3 Joint Transmission Coordination Model

To represent the APs locations we use the two dimensional r-l square point process model described in 3.6. It allows us to characterize the interference resulting from the close proximity of co-channel APs in high-density WLANs.

We focus on the downlink and we evaluate the performance in terms of coverage probability and throughput, under the $r-l$ square model described above when coordination in particular CoMP-JT is applied between APs to mitigate the interference. We assume an ideal backhaul network connecting APs to transmit duplicated data or to share data used for cooperation without collisions and retransmissions.

CoMP-JT is a cooperation technique used to reduce the interference. In the classical CoMP-JT a mobile user receives data not only from the serving AP, but also from APs in its coordinated set. Signals received from APs outside the coordinated set are seen as interference. This is illustrated

by equation (5.3). First, we define the coordinated set as follows:

$$\mathcal{C} = \{X_i \in \Phi \text{ s.t.} X_i \in B_u(d)\} \tag{5.0}$$

where Φ is the $r - l$ square p.p., X_i is the AP i and $B_u(d)$ is the ball of radius d centered at u, the typical user. Here d is the radius of the coordinated set.

The received signal at a typical user station u is:

$$y = \underbrace{\sum_{X_i \in \mathcal{A}} \sqrt{p_t}\xi_i \sqrt{l(||X_i - u||)}}_{\text{Useful signal}} + \underbrace{\sum_{X_j \in \mathcal{B}} \sqrt{p_t}\xi_j \sqrt{l(||X_j - u||)}}_{\text{Interference}} + \underbrace{N}_{\text{Noise}} \tag{5.0}$$

where p_t is the transmission power of nodes (APs), which is assumed to be the same for all APs, $(\xi_i)_i$ are i.i.d $\sim \mathcal{CN}(0, 1)$ Gaussian random variables modeling fading, $l(.)$ is the path loss function and $N \sim \mathcal{CN}(0, \sigma^2)$ is an additive white Gaussian noise (AWGN). $\mathcal{A}$ and $\mathcal{B}$ represent the set of APs sending useful signals and the set of interferers, respectively.

The Distributed Contention Function (DCF) is a contention-based decentralized approach which uses Carrier Sense Multiple Access with Collision Avoidance (CSMA/CA). It allows to reduce collisions and enhance the network data rate.

Remark 3 *In this chapter, we are interested in one typical user located at the edge of the cell, which represents all the remaining users in the same case. Therefore, we derive the analytical expressions considering that only the serving AP (nearest to the mobile user) will perform the CSMA/CA procedure.*

Let CS_{thr} be the carrier sensing threshold.

An AP can transmit if it satisfies the following carrier sensing condition:

$$\mathbb{E}_\xi \left[\xi_i \mid\mid X_i \mid\mid^{-\alpha} p_t\right] \leq CS_{th} \tag{5.0}$$

Hence, an AP located at distance $\mid\mid X_i \mid\mid$ is allowed to transmit if and only if $\mid\mid X_i \mid\mid \geq \left(\frac{p_t}{CS_{th}}\right)^{1/\alpha}$. Let define the radius of carrier sensing domain as: $d_{CS} = \left(\frac{p_t}{CS_{th}}\right)^{1/\alpha}$.

We define the useful APs and interferers sets as follows:

- $\mathcal{A}$: is the set of APs in the coordination set $\mathcal{C}$ *and* outside the contention domain of the serving AP. It can be expressed as:

$$\mathcal{A} = \left\{X_i \in \phi \text{ s.t. } X_i \in B_u(d) \cap \bar{B}_{X^*}(d_{CS})\right\} \tag{5.0}$$

  Where X^* is the serving AP and $\bar{A}$ represents $\Phi \backslash A$.

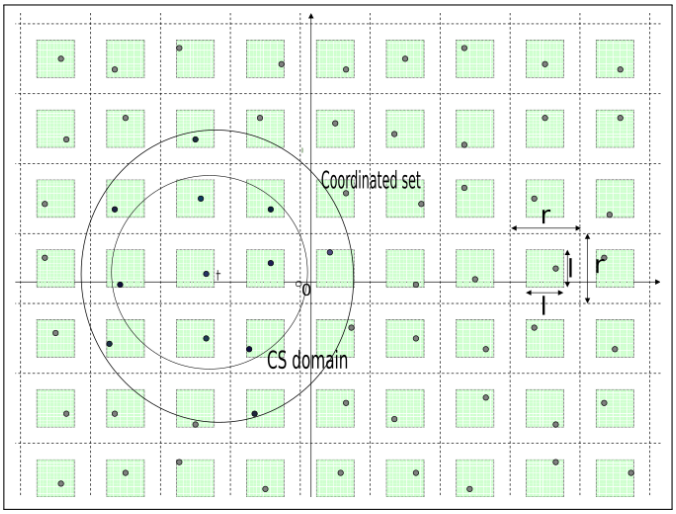

Figure 5.1: The $r - l$ square p.p., the serving AP is the nearest one to the typical user.

- $\mathcal{B}$: represents the set of interferers,

$$\mathcal{B} = \left\{ X_i \in \phi \text{ s.t. } X_i \in \bar{B}_u(d) \cap \bar{B}_{X^*}(d_{CS}) \right\} \tag{5.0}$$

Figure 5.1 illustrates the carrier sensing (CS) domain and the coordinated set $\mathcal{C}$.

In the following, we derive the analytical expression of the coverage probability of a typical user.

Proposition 3 *The coverage probability under CoMP-JT is given by:*

$$\begin{aligned} p_c(T) &= \Pr(SINR > T) \\ &= \prod_j \mathbb{E}\left[\left(\frac{1}{1 + T \frac{l(||X_j - u||)\mathbb{1}_{\{X_j \in \bar{B}_u(d) \cap \bar{B}_{X^*}(d_{CS})\}}}{\sum_i l(||X_i - u||)\mathbb{1}_{\{X_i \in B_u(d) \cap \bar{B}_{X^*}(d_{CS})\}}}} \right) \right] \\ &\times \mathbb{E}\left[\exp\left(-T \frac{\sigma^2}{\sum_{X_i \in \mathcal{A}} p_t l(||X_i - u||)} \right) \right] \end{aligned}$$

Proof 2

$$
\begin{aligned}
p_c(T) &= \Pr(SINR > T) \\
&= \Pr\left\{ \frac{\mid \sum_{X_i \in \mathcal{A}} \sqrt{p_t}\xi_i \sqrt{l(||X_i - u||)} \mid^2}{\sum_{X_j \in \mathcal{B}} p_t \mid \xi_j \mid^2 l(||X_j - u||) + \sigma^2} > T \right\} \\
&= \Pr\left\{ \mid \sum_{X_i \in \mathcal{A}} \sqrt{p_t}\xi_i \sqrt{l(||X_i - u||)} \mid^2 \right. \\
&\left. > T \left(\sum_{X_j \in \mathcal{B}} p_t \mid \xi_j \mid^2 l(||X_j - u||) + \sigma^2 \right) \right\} \\
&\overset{(a)}{=} \mathbb{E}\left[\exp\left(-T \frac{\sum_{X_j \in \mathcal{B}} p_t \mid \xi_j \mid^2 l(||X_j - u||) + \sigma^2}{\sum_{X_i \in \mathcal{A}} p_t l(||X_i - u||)} \right) \right] \\
&= \mathbb{E}\left[\exp\left(-T \frac{\sum_{X_j \in \mathcal{B}} p_t \mid \xi_j \mid^2 l(||X_j - u||)}{\sum_{X_i \in \mathcal{A}} p_t l(||X_i - u||)} \right) \right] \\
&\times \mathbb{E}\left[\exp\left(-T \frac{\sigma^2}{\sum_{X_i \in \mathcal{A}} p_t l(||X_i - u||)} \right) \right]
\end{aligned}
$$

where (a) follows the hyper exponential property. The first term is as follows:

$$
\begin{aligned}
&\mathbb{E}\left[\exp\left(-T \frac{\sum_{X_j \in \mathcal{B}} P_t \mid \xi_j \mid^2 l(||X_j - u||)}{\sum_{X_i \in \mathcal{A}} P_t l(||X_i - u||)} \right) \right] \\
&= \mathbb{E}\left[\exp\left(-T \frac{\sum_j \mid \xi_j \mid^2 l(||X_j - u||) \mathbb{1}_{\{X_j \in \bar{B}_u(d) \cap \bar{B}_{X^*}(d_{CS})\}}}{\sum_{X_i \in \mathcal{A}} l(||X_i - u||)} \right) \right] \\
&= \mathbb{E}\left[\prod_j \exp\left(-T \frac{\mid \xi_j \mid^2 l(||X_j - u||) \mathbb{1}_{\{X_j \in \bar{B}_u(d) \cap \bar{B}_{X^*}(d_{CS})\}}}{\sum_{X_i \in \mathcal{A}} l(||X_i - u||)} \right) \right] \\
&\overset{(b)}{=} \mathbb{E}\left[\prod_j \left(\frac{1}{1 + T \frac{l(||X_j - u||) \mathbb{1}_{\{X_j \in \bar{B}_u(d) \cap \bar{B}_{X^*}(d_{CS})\}}}{\sum_{X_i \in \mathcal{A}} l(||X_i - u||)}} \right) \right] \\
&= \mathbb{E}\left[\prod_j \left(\frac{1}{1 + T \frac{l(||X_j - u||) \mathbb{1}_{\{X_j \in \bar{B}_u(d) \cap \bar{B}_{X^*}(d_{CS})\}}}{\sum_i l(||X_i - u||) \mathbb{1}_{\{X_i \in B_u(d) \cap \bar{B}_{X^*}(d_{CS})\}}}} \right) \right] \\
&= \prod_j \mathbb{E}\left[\left(\frac{1}{1 + T \frac{l(||X_j - u||) \mathbb{1}_{\{X_j \in \bar{B}_u(d) \cap \bar{B}_{X^*}(d_{CS})\}}}{\sum_i l(||X_i - u||) \mathbb{1}_{\{X_i \in B_u(d) \cap \bar{B}_{X^*}(d_{CS})\}}}} \right) \right]
\end{aligned}
$$

where (b) from the fact that $(\mid \xi_i \mid^2)_i$ *are exponentially distributed.*

Remark 4 *In the Interference limited (free noise) regime, the coverage probability is independent from transmit powers of APs.*

The rate can be derived from the coverage probability by the following formula:

$$\begin{aligned} R &= \mathbb{E}(\log_2(1+\text{SINR})) \\ &= \int_0^\infty \Pr\{\log_2(1+\text{SINR} > t)\}dt \\ &= \int_0^\infty \frac{\Pr\{\text{SINR} > e^t - 1\}}{\log(2)}dt \\ &\overset{(a)}{=} \frac{1}{\log(2)}\int_0^\infty \frac{\Pr\{\text{SINR} > x\}}{(x+1)}dx \\ &= \frac{1}{\log(2)}\int_0^\infty \frac{p_c(x)}{(x+1)}dx \end{aligned}$$

Where (a) follows from a variable change ($x = e^t - 1$).

Hence, the throughput is derived by replacing $p_c(T)$ (Eq. 3) in Eq. (5.3).

Remark 5 *The expectation in Eq. (3) is over the p.p. and it is difficult to compute it because the probability density function (pdf) of the $r - l$ square p.p. is unknown. Hence, Monte Carlo simulation is used in order to validate results.*

5.4 Performance evaluation: simulation and results

We consider a network composed of 7×7 (49) APs distributed in the plan according to the $r - l$ square p.p., all transmitting with the same power p_t. As we said, a typical user will have the same performance as other users, so we do not derive results for all users. We consider one typical user placed uniformly at the edge of a big square ($r \times r$) in the grid. According to [70] which gives guidelines of APs characteristics, we set the transmission power to $p_t = 100$mW (20dBm), $r = 50m$ (sides of squares) and $l = 30$m (sides of sub-squares). By this configuration, the distance between two nodes can not be less than $r - l = 20$m. The path loss model considered is given by: $l(r) = r^{-\alpha}$, where α is the path-loss exponent. Furthermore, we use a bandwidth of 10MHz. We take the mean over 1000 realizations of the spatial process.

Remark 6 *As explained before, the carrier sensing domain and the cooperation domain are illustrated by balls of radius d centered at u, and d_{CS} centered at X^*, respectively. To make the analysis of the result more clear and easier, and since the distance $\|u - X^*\|$ is not significant, we use the following nomenclature:*

- *$d \leq d_{CS}$: the coordinated set $\mathcal{C}$ is inside the carrier sensing domain, $B_{X^*}(d_{CS})$.*
- *$d \geq d_{CS}$: the coordinated set includes the carrier sensing domain.*

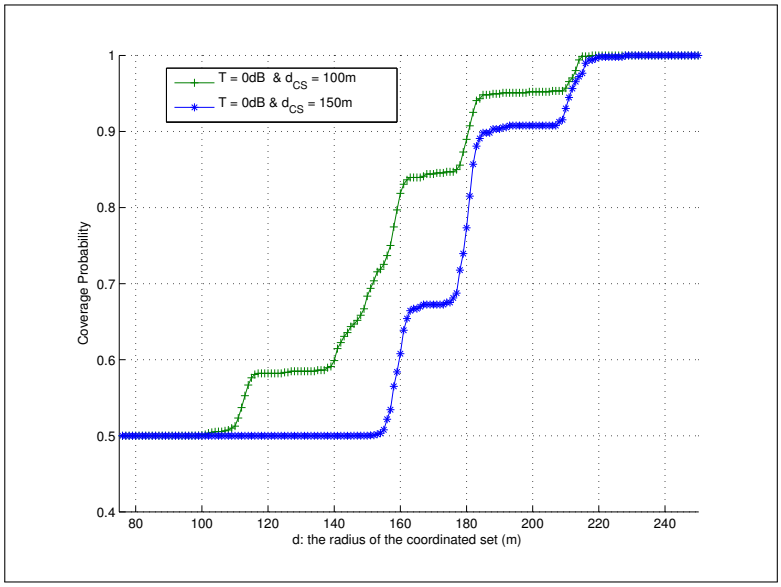

Figure 5.2: p_c vs d for two values of d_{CS} (the carrier sensing radius).

In Figure 5.2, we plot the coverage probability versus the coordinated set radius for two values of the radius of the carrier sensing domain, d_{CS} = 100m and 150m. It can be seen that the coverage probability remains constant ($p_c = 0.5$) for values of d less than d_{CS} (d $\leq d_{CS}$) *and* increases when $d \geq d_{CS}$. This can be explained by the fact that when increasing d, more APs will join the coordinated set. However, since the serving AP performs the CSMA/CA procedure, APs inside the ball of radius d_{CS} are silent. Namely, an AP sends a useful signal if it is in the coordinated set, and not in the coordination carrier sensing domain. The step function form of the increasing part of the coverage probability is explained as: p_c remains constant until a new AP joins $\mathcal{A}$, then it moves to the next step.

In contrast, we keep the carrier sensing radius threshold fixed and we vary d. Figure 5.3 shows the coverage probability depending on the radius of the carrier sensing domain. It can be seen that the coverage probability decreases for values of d_{CS} less than d, the coordinated set $\mathcal{C}$ threshold, and increases for values greater that d. Actually, the number of potential coordinated APs which are muted (silent) grows when increasing d_{CS} until it reaches d. Therefore, the coverage probability starts to increase, because interfering APs outside the coordination set and inside the carrier sensing domain, are silent.

Figure 5.4 shows the impact of the cooperation on the user rate. The radius of the carrier sensing domain is fixed to d_{CS}= 150m. Remember that the maximal rate is about 195 Mbps. The rate remains constant for values of d less than d_{CS}. In fact, when increasing the radius of the coordination set, the APs in $\mathcal{C}$ become silent due to the CSMA/CA procedure. Starting from values

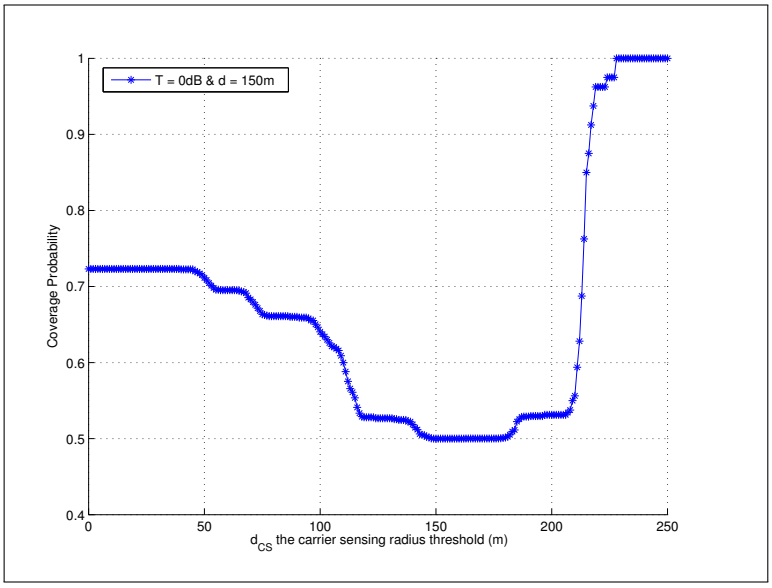

Figure 5.3: p_c vs d_{CS}, for d = 150m, radius of the coordinated set.

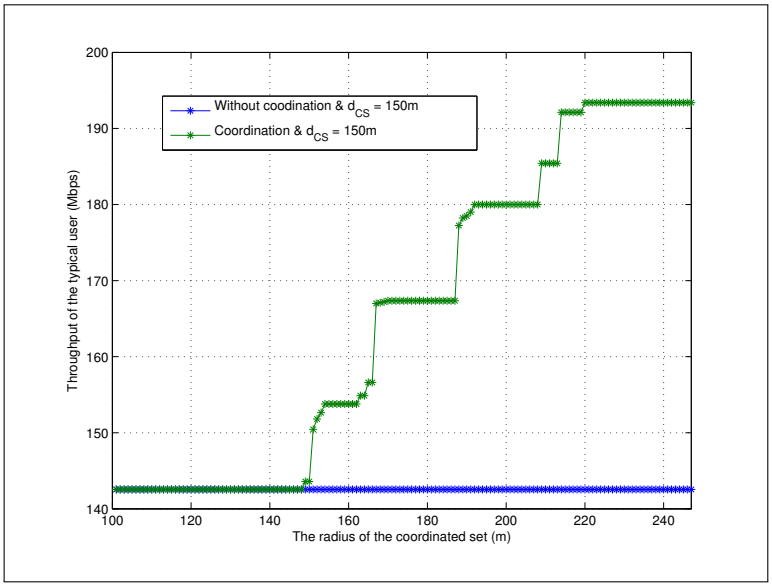

Figure 5.4: Throughput vs d_{CS}, for d = 150m, radius of the coordinated set.

of d around d_{CS}, the rate is improved because the APs joining $\mathcal{C}$ are outside the carrier sensing domain. Hence, they send an effective signal which improves this performance metric.

5.5 Conclusion

In this chapter, we use Coordinated Multipoint Joint Transmission to mitigate the interference problem in dense VHT WLANs. We use the $r - l$ square p.p. to model APs positions and derive the coverage probability and the throughput. Using simulation experiments, we evaluate the gain of this technique considering different values of SINR, the carrier sensing threshold of CSMA/CA access control and different sizes of the coordinated set. Our results show that CoMP-JT is a promising approach in dense mesh networks.

The main challenges of using CoMP-JT approaches in WLAN are related to the CSMA/CA protocol which does not provide any synchronization between APs. In a future work, we will interest in integrating the coordination in WLANs [84], mainly by modifying the control plan of Wi-Fi networks. Moreover, considering CoMP in dense WLANs with another access protocol like TDMA is an interesting perspective.

Chapter 6

Impact of Resource Blocks Allocation strategies on Downlink Interference distribution in LTE Networks

Contents

6.1 Chapter Summary

The wireless interference occurs when two or more eNodeBs use the same resource blocks. This problem becomes more severe when these eNodeBs are adjacent. In this work, we propose a model based on stochastic geometry to assess downlink interference in LTE networks. The originality of this work lies in the proposition of resource blocks assignment strategies and realistic traffic patterns included in the model. We derive tractable formula for the first two moments of interference. Simulations that cover a large set of scenarios show the accuracy of our proposals and allow us to compare these strategies with more complex ones that rely on global interference minimization. Numerical evaluations highlight the behavior of the LTE network for different traffic patterns/load, eNodeB density, amount of resource blocks, and offer insights about possible parameterization of the LTE network with regard to the spatial reuse.

The remainder of this work is organized as follows: In the next section we introduce the chapter. In section 6.3 we present the system model. We develop the three proposed assignment strategies in section 6.4. In section 6.5, we derive the first and second moments of each allocation strategy. Then, in section 6.6 we present numerical results and conclude the chapter in section 6.7.

6.2 Introduction

Capacity of cellular networks is still an important issue and must continuously increase to satisfy the growing demand of traffic from users and applications. Long Term Evolution, and Long Term Evolution-Advanced [5] (LTE-A) have been recently standardized to improve the network capacity and support this traffic growth. One of the solutions brought by LTE is the enhancement of the frequency reuse of the radio spectrum. Usage of these resources is performed by a scheduler that assign resource units, named *resource blocks* (RB), to the users. A RB is a channel (an OFDMA channel composed of a set of OFDM subcarriers) for the duration of one time slot. Inter-cell interference is generated when users located in different cells use the same RB. A static RB assignment, where disjoint resources are distributed to each cell, may lead to an inefficient resource usage. Instead, assignments can be centralized for a certain number of neighborhood cells to enhance the spatial reuse of the resources to adapt RB assignments to the load in each cell while ensuring a low level of interference. In order to increase the capacity, the scheduler that manages RB assignments increases the frequency reuse by assigning more times the same RB to different users. In this context, interference becomes the key factor that limits the global performance of

the system. Several studies have proposed assignment strategies performed at the scheduler aiming to minimize global interference [60, 86]. These strategies are evaluated through simulations for different scenarios. However, the state of the arts lack of general models that allow to understand the impact and the performances of the different assignment strategies at a larger scale and for more general scenarios. Nevertheless, some models based on Stochastic geometry have been proposed. [24, 131, 133] propose spatial and tractable models that take into account the traffic demand in the interference computation, but they do not consider concrete assignment RB algorithms. Moreover, these models assume that users are modeled through a homogeneous point process and consequently the load associated to a cell depends on its size (the greatest cell having the highest load). Instead, cellular networks are generally designed to keep an equivalent level of load in each cell.

In this work, we propose to integrate in a stochastic geometry model assignment strategies and realistic traffic demands. The number of allocated resources for an eNodeB (evolved Node B) at a given time follows the distribution of the number of clients in a M/M/C/C queue. It models the number of communications in progress when both communications inter-arrival and their duration follow an exponential distribution. Such assumptions are still pertinent in cellular networks as it has been recently shown [83]. We focus mainly on assignment algorithms, named *cyclic assignment*, that depend only on distances between eNodeB. Beside, we consider an approach which consists in finding the RB assignment which minimizes the sum of interference at each user. This strategy is consequently referred as *Minimizing global Interference* hereafter. These algorithms are combined with a power allocation scheme that depends on the channel quality of each user. For the cyclic assignment, we propose an analytical estimation of the two first moments of interference. Also, we perform a large set of simulations to assess interference characteristics at a typical user for numerous different configurations.

6.3 System Model

Locations of eNodeB are modeled by an homogeneous Poisson point process $N_e = \{X_i\}_{i \in \mathbb{N}}$ distributed in $\mathbb{R}^2$ with intensity λ_e. Points X_i are indexed with regard to their distance to the origin. We consider a downlink system between a typical user and its nearest eNodeB. Without loss of generality, we assume that this user is located at the origin. Users are assumed to be associated with their closest eNodeB. Channels between eNodeB and the typical user are modeled through a sequence of i.i.d. random variables $(h_i)_{i \in \mathbb{N}}$. The transmission power between an eNodeB and one associated user at distance r is given by the function $T_x(r)$. This function models the power control algorithms implemented at the eNodeB. The scheduler manages a set of RB_{max} resource blocks that are common to all eNodeB. For each traffic demand, the scheduler assign one RB. Traffic demands exceeding RB_{max} at an eNodeB are not served. Note that the model can be easily extended with a random number of RB for each demand. The typical user uses a RB denoted res (it is the index

of the RB - it belongs to the set $\{0, 1, .., RB_{max} - 1\}$). An eNodeB interferes with the typical user if and only if it reuses the same RB res. The interference at the typical user can be expressed as:

$$I = \sum_{i=1}^{\infty} w_i \cdot h_i \cdot T_x \left(\|X_i - U_i\| \right) \cdot l(\|X_i\|) \tag{6.0}$$

where $l(.)$ is the path-loss. U_i is the random variable modeling location of a user attached to eNodeB at X_i. We assume that U_i is uniformly distributed in the Voronoï cell formed by the process N_e and with nucleus X_i. Note that when users are distributed according to a Poisson process, they are also uniformly distributed in their cell. The sequence of r.v. $(w_i)_{i \in \mathbb{N}}$ indicates which eNodeB interferes. That is

$$w_i = \begin{cases} 1, & \text{if eNodeB at } X_i \text{ uses RB } res \\ 0, & \text{otherwise.} \end{cases} \tag{6.0}$$

By convention, we set $w_0 = 0$. Obviously, $(w_i)_i$ depend on the RB allocation strategy.

6.3.1 Reuse Factor (Δ)

Reuse factor Δ has an important role in modeling the reuse of a given resource. We consider that the mean load for each eNodeB is $\frac{RB_{max}}{\Delta}$ in average (with $\Delta \geq 1$). A given RB is then reuse every Δ eNodeB in average. The reuse factor Δ depends on the traffic demand. If eNodeBs have a lot of traffic demand, high amount of RBs are needed to serve these requests, hence Δ must takes small values and resources are reused by near (adjacent) eNodeBs. On the other hand, if the network is not loaded, few RBs are needed to serve the traffic requests, hence Δ takes high values and the resources are reused by distant eNodeBs.

6.3.2 Number of RBs used at an eNodeB: the M/M/C/C queue

In the $M/M/C/C$ queueing model, customers arrive according to a Poisson distribution (in $\mathbb{R}$) and service times are exponentially distributed. M/M/C/C queue models a system with C resources and with no queuing capacity, i.e. a customer cannot enter in the system if all resources are busy. It is adapted to a phone network where a call is dropped if no resource are available. In this work, we consider the M/M/C/C to model the users demand in RBs. More precisely, we use a $M/M/RB_{max}/RB_{max}$ queue, where the process describing the time of the traffic demand from the users is a Poisson process and where the servers are the set of available RBs ($\{0, 1, .., RB_{max} - 1\}$). In order to have a mean reuse factor of Δ, the parameter of the queue (the load) is set in such a way that the mean number of customers in the system, or equivalently the mean number of busy resource blocks, is equal to $\frac{RB_{max}}{\Delta}$. The distribution of the number of busy resource blocks for a given eNodeB i denoted R_i, is then given by:

$$\mathbb{P}\left(Ri = k\right) = \pi_0 \frac{\rho^k}{k!} \tag{6.0}$$

where ρ is the load ($\rho = \frac{RB_{max}}{\Delta}$). As mentioned earlier, we assume that a user is uniformly distributed in the Voronoï cell of its eNodeB.

It is worth noting, that with this model, the users location does not follow Poisson point process. Indeed, we model only users which have a communication in progress and not all potential users. The number of users in a Voronoï cell follows the distribution given in Eq. (6.3.2) since it corresponds to the number of allocated RBs. The number of users is thus not dependent on the Voronoï cell size. It seems to be due to the fact that operators dimension their network according to the expected load, with "big cells" for regions with a small number of users, and "small cells" for dense regions.

6.4 Assignment strategies

In this work we consider different allocation strategies

- Cyclic Allocation:
  - Independent allocation: serves as a benchmark allocation to compare the performance of other allocation strategies.
  - $M/M/RB_{max}/RB_{max}$ allocation: models the *realistic* distribution of traffic demand that users request to their attached eNodeB.
  - Static allocation: reflects a fixed allocation where all eNodeBs have a fixed and equal traffic requests.
- Minimizing global interference allocation.

6.4.1 Cyclic assignment

We consider three different allocation strategies:

6.4.1.1 Independent allocation (Benchmark allocation)

with this strategy each eNodeB selects its resources independently of the other eNodeB. In this case, we assume that an eNodeB has a probability $\frac{1}{\Delta}$ to reuse the RB res. The point process describing the interfering eNodeB is then a thinned Poisson point process in $\mathbb{R}^2 \backslash B(O, \|X_0\|)$ with parameter $\frac{\lambda_e}{\Delta}$.

6.4.1.2 Static allocation

we assign a constant proportion $\frac{RB_{max}}{\Delta}$ of the available resources to each eNodeB. They are allocated in their index order: eNodeB 0 uses RB from 1 to $\frac{RB_{max}}{\Delta}$ (it includes the typical user), eNodeB 1 from $\frac{RB_{max}}{\Delta}+1$ to $2\frac{RB_{max}}{\Delta}$, etc. We loop when all resources have been used. Consequently, eNodeB that reuses the resource res have an index with the form $k \cdot \Delta$ with $k > 0$.

6.4.1.3 $M/M/RB_{max}/RB_{max}$ allocation

an eNodeB i ($i > 0$) has a traffic demand which is modeled by a random variable D_i. Therefore, we consider a sequence of i.i.d. r.v $(D_i)_{i \in I\!N}$ that follow the distribution of the number of customers in a $M/M/RB_{max}/RB_{max}$ queue. The load ρ in the $M/M/RB_{max}/RB_{max}$ is equal to $\frac{RB_{max}}{\Delta}$ ($\frac{1}{\Delta}$ per server). The number of RB used by eNodeB 0, denoted $\bar{D}_0$ is strictly positive since there is a communication in progress with the typical user. Its distribution is thus slightly different: $\mathbb{P}(\bar{D}_0 = k) = \mathbb{P}(D_0 = k | D_0 > 0)$. The RB used by the typical user, res, is uniformly distributed among D_0 (i.e. $\mathbb{P}(res = k | \bar{D}_0 = N) = \frac{1}{N}$ for $k < N$). Moreover, we need to evaluate the difference between res and D_0 to know when res will be reused. Consequently, we introduce the r.v. R_0 with distribution

$$\mathbb{P}(R_0 = k) = \mathbb{P}(\bar{D}_0 - res = k) = \frac{\pi_0}{1-\pi_0} \sum_{u=k+1}^{RB_{max}} \frac{\rho^u}{u!u} \tag{6.0}$$

π_0 is the probability to have 0 customer in the $M/M/RB_{max}/RB_{max}$ queue. As for the static allocation, we allocate the required resources to each eNodeB in their index order:

- eNodeB 0 uses RB from 0 to $min(\bar{D}_0, RB_{max} - 1)$, etc.
- An eNodeB k uses the RB indexed from $(\bar{D}_0 + \sum_{i=1}^{k-1} D_i + 1) mod(RB_{max})$ to $(\bar{D}_0 + \sum_{i=1}^{k} D_i) mod(RB_{max})$.

We illustrate this allocation strategy in Figure 6.1.

6.4.2 Minimizing global interference

We compare the previous strategies to a RB assignment where the sum of interference at each user is minimized. Our approach is similar to the one developed in [86]. The problem has been shown NP-hard, so we use a simple greedy algorithm to find the assignment that minimizes global interference (Algorithm 1). As traffic demands associated to users are ordered randomly (by nature with our simulations), we allocate a RB to each user/traffic demand in this order. At each step, we assign the resource block that minimizes the sum of interference for the current users. This algorithm mimics an assignment strategy where RB are assigned at the arrival of traffic demands without changing the already assigned RB. The number of users attached to each RB follows the same distribution as the $M/M/RB_{max}/RB_{max}$ allocation.

Algorithm 1: Minimizing global interference

Data: RB_{max}: Maximum available RBs.
cost: variable to store the sum of interference of the current allocation strategy.
bestCost: variable representing the sum of interference of the best allocation strategy, initiated to -1.
Result:

```
1  for each rb ∈ {0, 1, .., RB_max − 1} do
2      if rb is free then
3          if It is the last user to be allocated (all users have a RB), we proceed to evaluate this
           allocation scheme then
4              cost ← sum_Interference() ;
5              if bestCost <0 or cost<bestCost (Allocating this rb to this user generate low
               interference (cost) than allocation it to an other user (bestCost)) then
6                  Save this allocation strategy ;
7                  bestCost = cost ;
8              end
9          else
10             if bestCost <0 then
11                 Move to the next user ;
12             else
13                 costCost ← sum_Interference() ;
14                 if cost < bestCost then
15                     Move to the next user ;
16                 end
17             end
18         end
19         Desallocate rb ;
20     end
21 end
```

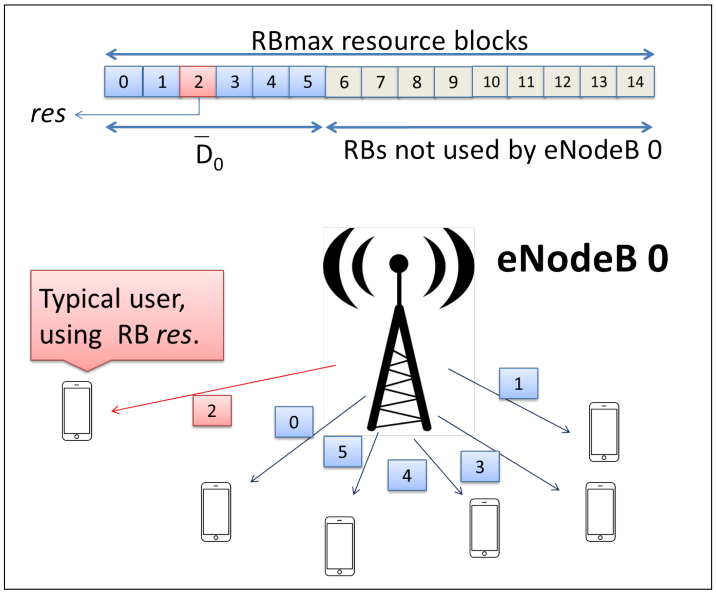

Figure 6.1: 5 users are attached to eNodeB 0. So, $\overline{D}_0 = 5$ RBs are used among $RB_{max} = 15$ available RBs. The typical user uses the RB *res* with index 2.

6.5 Interference characterization

We derive mean and variance of interference for the different cyclic assignment strategies.

6.5.1 Mean of interference

The mean is derived from Eq. 6.3:

$$\mathbb{E}[I] = \mathbb{E}[h_1] \sum_{i=1}^{+\infty} \mathbb{E}[w_i] \mathbb{E}\left[T_x(\|X_i - U_i\|) \cdot l(\|X_i\|)\right] \tag{6.0}$$

In this equation, w_i has been disjoin from the esperance as it is independent of the process N_e (according to the defined strategies). We evaluate $E\left[T_x(\|X_i - U_i\|)l(\|X_i\|)\right]$ as $E\left[T_x(\|X_i - U_i\|)\right]E[l(\|X_i\|)]$. This approximation does not introduce a bias as the first term depends mainly on the Voronoï size, whereas the second term depends on the distance between the nucleus and the origin.
$E\left[T_x(\|X_i - U_i\|)l(\|X_i\|)\right]$ can be rewritten under Palm expectation with regard to the process N_e:

$$\mathbb{E}\left[T_x(\|X_i - U_i\|)l(\|X_i\|)\right] = \mathbb{E}^0_{N_e}[T_x(\|U_0\|)] \tag{6.0}$$

The distribution of $\|U_0\|$ under this Palm expectation is not known but some approximation exists. We use the one proposed in [131], where the density of $\|U_0\|$ is approximated by $2\pi\lambda_e c r e^{-\lambda_e c \pi r^2}$ with $c = 1.25$. We performed a Monte-Carlo method to validate this assumptions with 2 millions of samples. The value that minimizes the error with regard to the L^1 norm is $c = 1.256$, but the dif-

ference between the empirical pdf and the extrapolated one still presents an error of approximately 10%. It will be the main cause of errors between our estimations and simulations. We obtain the following approximation for the mean interference:

$$\mathbb{E}[I] \approx \mathbb{E}[h_1]\mathbb{E}^0_{N_e}[T_x(\|U_0\|)] \sum_{i=1}^{+\infty} \mathbb{P}(w_i = 1)\mathbb{E}\left[l(\|X_i\|)\right] \tag{6.0}$$

The different allocation strategies lead to the following probabilities (for $i > 0$):

- *Static allocation*

$$\mathbb{P}(w_i = 1) = \mathbb{1}_{i \cdot mod(\Delta)=0} \tag{6.0}$$

- *$M/M/RB_{max}/RB_{max}$ allocation*

$$\mathbb{P}(w_i = 1) = \pi_0^i \sum_{u=0}^{RB_{max}-1} \mathbb{P}(R_0 = u)$$
$$\times \sum_{k=0}^{i \cdot RB_{max}-1-u} \frac{(\rho(i-1))^k}{k!} \sum_{l=\left\lfloor \frac{p+u}{RB_{max}}+1 \right\rfloor \cdot RB_{max}-(p+u)}^{RB_{max}} \frac{\rho^l}{l!}$$

- *Independent allocation* $\mathbb{P}(w_i = 1) = \frac{1}{\Delta}$.

Proof 3

$$
\begin{aligned}
&\mathbb{P}(w_i = 1) \\
&= \sum_{k=0}^{i} \mathbb{P}\left(R_0 + \sum_{j=1}^{i-1} D_j < k \cdot RB_{max}, R_0 + \sum_{j=1}^{i} D_j \geq k \cdot RB_{max} \right) \\
&= \sum_{k=0}^{i} \sum_{p=(k-1)\cdot RB_{max}}^{k\cdot RB_{max}-1} \mathbb{P}\left(R_0 + \sum_{j=1}^{i-1} D_j = p, R_0 + \sum_{j=1}^{i} D_j \geq k \cdot RB_{max} \right) \\
&= \sum_{k=0}^{i} \sum_{p=(k-1)\cdot RB_{max}}^{k\cdot RB_{max}-1} \mathbb{P}\left(R_0 + \sum_{j=1}^{i-1} D_j = p, D_i \geq k \cdot RB_{max} - p \right) \\
&= \sum_{k=0}^{i} \sum_{p=(k-1)\cdot RB_{max}}^{k\cdot RB_{max}-1} \sum_{u=0}^{RB_{max}-1} \mathbb{P}(R_0 = u) \\
&\quad \times \mathbb{P}\left(\sum_{j=1}^{i-1} D_j = p - u, D_i \geq k \cdot RB_{max} - p \right) \\
&= \sum_{k=0}^{i} \sum_{p=(k-1)\cdot RB_{max}}^{k\cdot RB_{max}-1} \sum_{u=0}^{RB_{max}-1} \mathbb{P}(R_0 = u) \\
&\quad \times \mathbb{P}\left(\sum_{j=1}^{i-1} D_j = p - u \right) \cdot \mathbb{P}\left(D_i \geq k \cdot RB_{max} - p \right) \\
&= \sum_{k=0}^{i} \sum_{p=(k-1)\cdot RB_{max}}^{k\cdot RB_{max}-1} \sum_{u=0}^{RB_{max}-1} \mathbb{P}(R_0 = u) \cdot \\
&\quad \times \mathbb{P}\left(\sum_{j=1}^{i-1} D_j = p - u \right) \cdot \pi_0 \sum_{l=k\cdot RB_{max}-p}^{RB_{max}} \frac{\rho^l}{l!} \\
&= \sum_{k=0}^{i} \sum_{p=(k-1)\cdot RB_{max}-u}^{k\cdot RB_{max}-1-u} \sum_{u=0}^{RB_{max}-1} \mathbb{P}(R_0 = u) \cdot \\
&\quad \times \mathbb{P}\left(\sum_{j=1}^{i-1} D_j = p \right) \cdot \pi_0 \sum_{l=k\cdot RB_{max}-(p+u)}^{RB_{max}} \frac{\rho^l}{l!} \\
&= \sum_{u=0}^{RB_{max}-1} \mathbb{P}(R_0 = u) \\
&\quad \cdot \sum_{k=0}^{i\cdot RB_{max}-1-u} \pi_0^{i-1} \frac{(\rho(i-1))^k}{k!} \cdot \pi_0 \sum_{l=k\cdot RB_{max}-(p+u)}^{RB_{max}} \frac{\rho^l}{l!} \\
&= \pi_0^i \sum_{u=0}^{RB_{max}-1} \mathbb{P}(R_0 = u) \\
&\quad \cdot \sum_{k=0}^{i\cdot RB_{max}-1-u} \frac{(\rho(i-1))^k}{k!} \sum_{l=\left\lfloor \frac{k+u}{RB_{max}}+1 \right\rfloor \cdot RB_{max}-(k+u)}^{RB_{max}} \frac{\rho^l}{l!}
\end{aligned}
$$

6.5.2 Variance of Interference

The variance can be expressed as

$$\mathbb{V}(I) = \mathbb{E}[I^2] - \mathbb{E}[I]^2 \tag{6.-1}$$

For the second moment, with the same assumption, we obtain

$$\mathbb{E}[I^2] \approx \mathbb{E}[h_1^2] E^0_{N_e}[T_x(\|U_0\|)^2] \sum_{i=1}^{+\infty} \mathbb{E}\left[l\left(\|X_i\|\right)^2\right] \mathbb{P}(w_i = 1)$$
$$+ 2E[h_1]^2 E^0_{N_e}[T_x(\|U_0\|)]^2 \sum_{1 \le i < j < +\infty}^{+\infty} \mathbb{E}\left[l\left(\|X_i\|\right) l\left(\|X_j\|\right)\right] \mathbb{E}[w_i w_j]$$

where $\mathbb{E}[T_x(\|X_i - U_i\|)T_x(\|X_j - U_j\|)]$ has been approximated as

$$\mathbb{E}[T_x(\|X_i - U_i\|)]\mathbb{E}[T_x(\|X_j - U_j\|)] = \mathbb{E}^0_{N_e}[T_x(\|U_0\|)]^2 \tag{6.-2}$$

It can be easily shown that the sequence $(w_i)_{i>0}$ is an homogeneous Markov chain for the three strategies:

- *Static allocation*

$$\mathbb{P}(w_i = w_j = 1) = \mathbb{1}_{i \cdot mod(\Delta)=0; j \cdot mod(\Delta)=0} \tag{6.-2}$$

- *$M/M/RB_{max}/RB_{max}$ allocation*

$$\mathbb{P}(w_i = w_j = 1) = \mathbb{P}(w_{j-i} = 1)\mathbb{P}(w_i = 1) \tag{6.-2}$$

- *Independent allocation*

$$\mathbb{P}(w_i = w_j = 1) = \frac{1}{\Delta^2} \tag{6.-2}$$

The other terms can be computed easily as the distribution of $\|X_i\|$, and the joint distribution of $(\|X_i\|, \|X_j\|)$ such as

$$f_{\|X_i\|}(r) = \frac{(\lambda_e \pi)^{i+1}}{i!} 2r^{2i+1} e^{-\lambda_e \pi r^2} \tag{6.-2}$$

and

$$f_{(\|X_i\|, \|X_j\|)}(r, u)$$
$$= \frac{(\lambda_e \pi)^{j+1}}{i!(j-i-1)!} 4ur^{2i+1}(u^2 - r^2)^{j-i-1} e^{-\lambda_e \pi u^2} \mathbb{1}_{u>r}$$

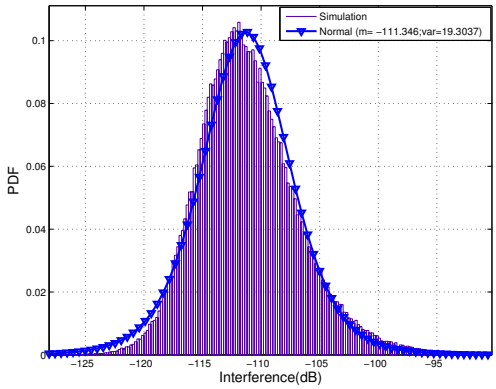

(a) $\Delta = 3$

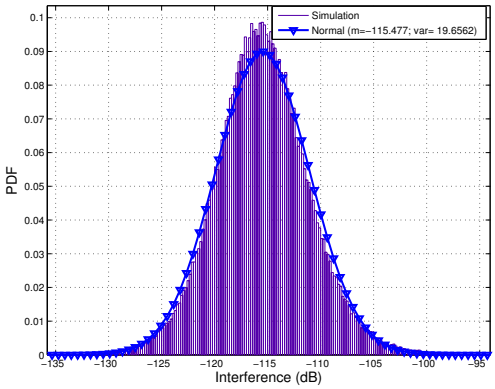

(b) [$\Delta = 5$

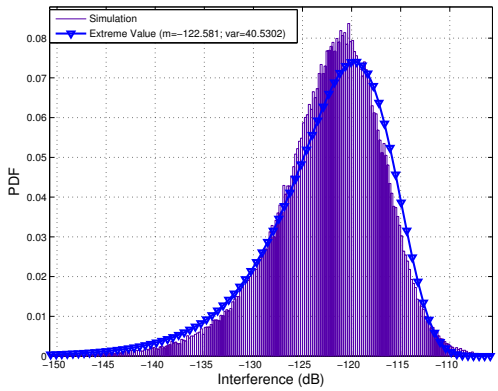

(c) $\Delta = 3$

Figure 6.2: Interference distribution for the $M/M/RB_{max}/RB_{max}$ allocation: empirical and extrapolation.

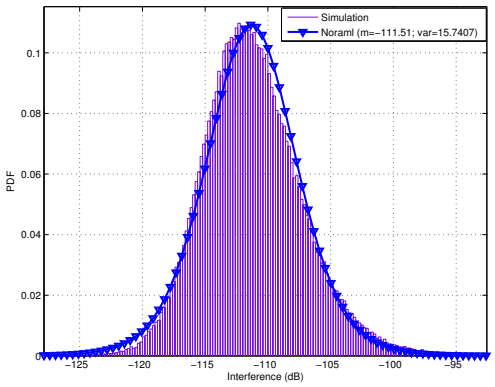

(a) $\Delta = 3$

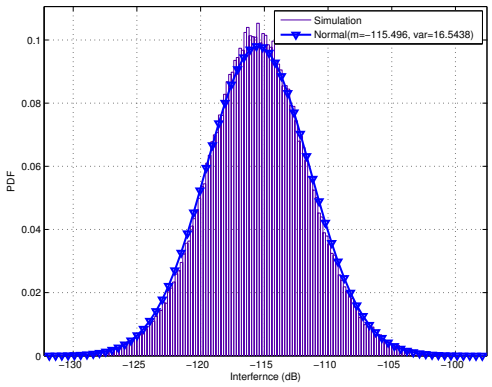

(b) $[\Delta = 5$

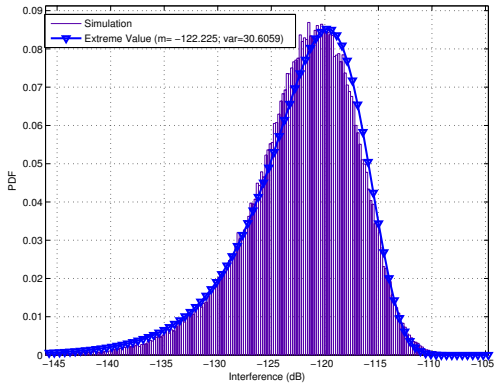

(c) $\Delta = 3$

Figure 6.3: Interference distribution for the static allocation : empirical and extrapolation.

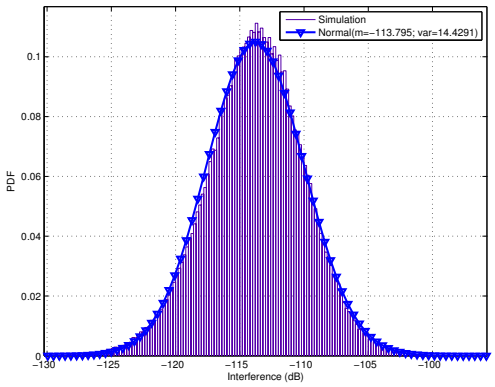

(a) $\Delta = 3$

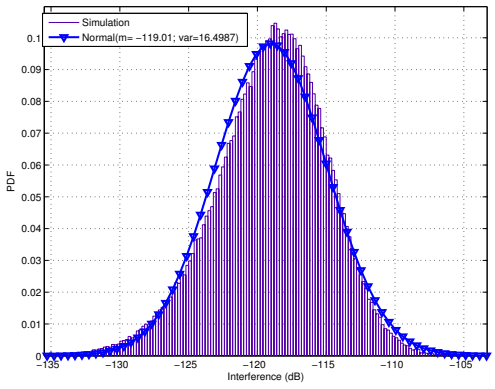

(b) $[\Delta = 5$

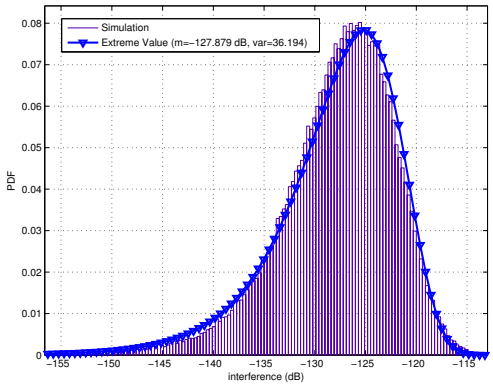

(c) $\Delta = 3$

Figure 6.4: Interference distribution for the heuristic allocation: empirical and extrapolation.

Assignment strategy	Δ	Mean		Variance	
		Theoretical	Simulation	Theoretical	Simulation
Static	3	$1.41e-11$	$1.29e-11$	$1.01e-21$	$1.09e-21$
allocation	5	$4.58e-12$	$4.45e-12$	$4.22e-23$	$4.64e-23$
	10	$9.74e-13$	$1.06e-12$	$1.19e-24$	$1.34e-24$
$M/M/RB_{max}/RB_{max}$	3	$1.72e-11$	$1.72e-11$	$1.17e-20$	$1.34e-20$
allocation	5	$5.39e-12$	$5.16e-12$	$2.98e-22$	$2.83e-22$
	10	$1.17e-12$	$1.15e-12$	$4.44e-24$	$3.85e-24$
Independent	3	$5.55e-11$	$4.98e-11$	$2.60e-19$	$2.29e-19$
	5	$3.33e-11$	$3.00e-11$	$1.57e-19$	$1.41e-19$
	10	$1.67e-11$	$1.47e-11$	$7.81e-20$	$7.47e-20$
Heuristic	3		$1.60e-11$		$9.02e-21$
cyclic	5		$4.23e-12$		$1.45e-22$
	10		$7.62e-13$		$3.94e-24$
Minimizing	3		$6.07e-12$		$4.31e-23$
global	5		$1.87e-12$		$3.59e-24$
interference	10		$3.79e-13$		$2.96e-25$

Table 6.1: Mean and Variance of Interference (in W) for the different assignment strategies and different reuse factor.

6.6 Numerical results

We consider the same path-loss function as [86] expressed in dB: $l(r) = -128.1 - 37.6 \cdot log_{10}(r)$ where r is the distance (in km). $T_x(.)$ is then set in such a way to guarantee to each user a minimum receiving power. We consider the case of an E-UTRA channel with a bandwidth of 5MHz with $RB_{max} = 15$ [6]. We set the transmission power function $T_x(.)$ to ensure a signal power greater or equal to $-72.4dBm$ at the reception as specified in [6]. For each 50 meters (from 50 to 500 meters), we compute the minimum transmitting power to reach this threshold ($Tx(r) \cdot l(r) \geq -72.4dBm$ for each interval of 50 meters leading to 10 possible transmission powers). This step function models the case where eNodeB has a set of predetermined power. The process intensity modeling eNodeB is equal to 2.25 per km^2. It corresponds to the intensity of base stations in Paris [1]. Random variables h_i are supposed constant equal to 1. This assumption facilitates interpretation of the results but a non zero variance can be considered as well. It simply adds a factor in terms of variance (cf. Eq. 6.5.2). We simulate the different strategies through a simulator coded in C available here [2]. The observation window is a square of 4×4 km^2. The typical user for which we study interference is the closest to the center of this square. For each set of parameters, simulations have be run

[1] https://www.antennesmobiles.fr/

[2] http://www.anthonybusson.fr/comLettersSimulation.zip

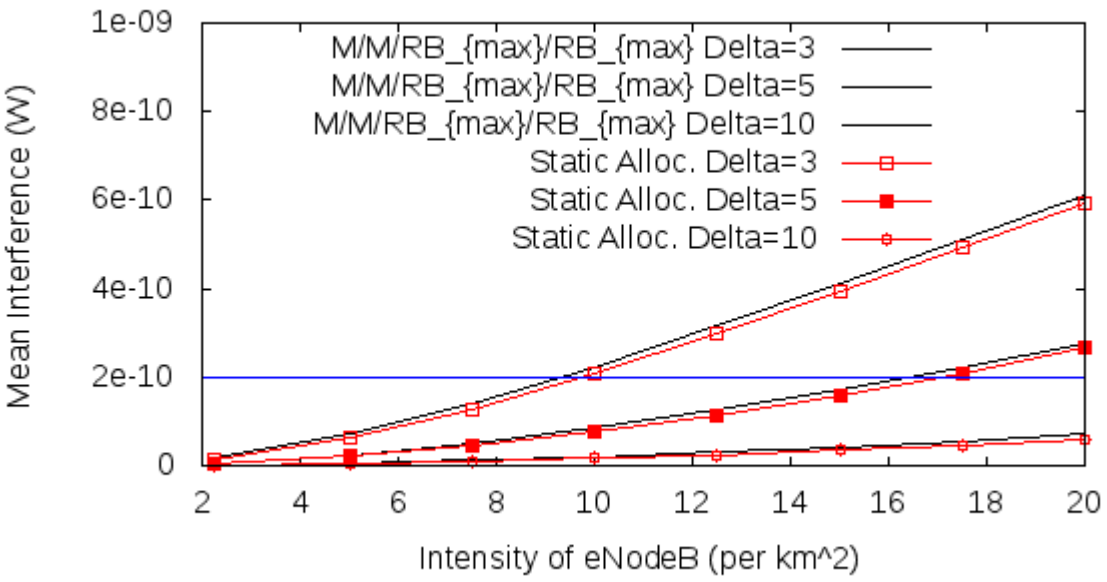

Figure 6.5: Mean interference when the density of eNodeB increases. Only theoretical results are shown - but the errors with simulations is of the same order than in Table 6.1 and varies between 2 and 12%. The horizontal line indicates that to ensure a mean interference less than $2e-10$, the possible couples of (intensity of eNodeB, Δ) are approximately (9.5,3), (17, 5) and (*,10).

$200,000$ times. The different mean, variance, empirical distributions are thus based on $200,000$ samples. With this number of samples, confidence intervals are negligible and are consequently not presented.

6.6.1 Mean and Variance of interference

In Table 6.1, we show the mean and variance of interference obtained from simulations and computed from formula (6.5.1) and (6.5.2). The difference varies from 2 to 11% between theoretical and simulation results for the mean, and from 7 to 13% for the variance. As expected, mean interference between the static and $M/M/RB_{max}/RB_{max}$ allocations are equivalent. They differ in variance with a maximum factor of 10. The independent allocation leads to a significant increase of interference which can reach a factor of 10^4 for the variance. It empirically proves that a thinned Poisson process cannot be used as approximation to model realistic assignment strategies.

6.6.2 Approximation of distribution of interference

The empirical interference distributions are shown in Figure 6.2 (in dB) for the $M/M/RB_{max}/RB_{max}$ allocation, in Figure 6.3 (in dB) for the static allocation and in Figure 6.4 (in dB) for the heuristic cyclic allocation. Parameters are set according to the maximum likelihood. The difference between the extrapolated and empirical curves are less than 9% w.r.t. the L^1 norm. We performed two hypothesis tests, T-test and Smirnov-Kolmogorov, for all scenarios. The alternative hypothesis is ruled out for all extrapolations. The most accurate distributions vary according to Δ: Normal and Extreme value (EV) distributions for $\Delta = 3$, 5 and 10 respectively. It can be seen that for small values of Δ, the interference distribution follows the normal distribution, while for high values of Δ its has a Extreme value distribution. Observe that the EV distribution has an exponential increase followed by a heavy upper tail. That is, values less than the interference mean occur more than ones greater than the mean.

We performed simulations and theoretical estimations of mean and variance for different values of RB_{max} (6, 15, 25, 50, 75 and 100 corresponding to different bandwidth of E-UTRA) and adapt the workload to have the same Δ reuse factor. It appears that interference moments are quite insensitive to this parameter. as we observe less than 20% of variation.

6.6.3 Network densification

In order to illustrate the behavior of the system when eNodeB becomes denser, we show in Fig. 6.5 mean interference when the intensity of eNodeB increases, from the actual intensity 2.25 to 20 eNodeB per km^2. This densification has an important impact on interference which increases with a factor up to 46 for the two strategies. This analysis can allow to determine the set of parameters that fulfill a constraint in terms of interference. An example is given in the caption of Fig. 6.5.

The proposed cyclic strategies are centered around the typical user. In order to show that our model is able to capture interference properties of a more global algorithm, we simulate an heuristic (Algorithm 2) analogous to the one which minimizes the global interference. Traffic demands from users are considered in their arrival order. For each demand the scheduler chooses a RB which is not used. If such RB is not available, it evaluates the distance at which each RB is used, and selects the farthest one. Results are shown in Table 6.1 ("Heuristic cyclic"). The traffic demand for each eNodeB follows the $M/M/RB_{max}/RB_{max}$ distribution. Mean interference values coincide with our model, and with only a factor 2 for the variance, validating our approach.

6.6.4 Minimizing global interference

It was not possible to derive a tractable model for this scenario. Simulations have shown that this allocation strategy correlates transmission powers, distance between eNodeB reusing the same resource, and the random variables w_i. These correlations are caused by the fact that a resource

Algorithm 2: Heuristic Minimizing global interference

```
   Data: RB_max, NumOfUsers, user, cost, bestCost
   condition =1
   Result:
 1 for i ∈ [0, NumOfUsers] do
 2     condition=1;
 3     user = i;
 4     while condition do
 5         if user=i-1 or (i=0 and user=NumOfUsers) then
 6             condition = 0 (go to line 12)
 7         end
 8         if rb is the best resource block to be allocated to the user then
 9             Allocate rb to the user;
10         end
11         if then
12         end
13     end
14     cost ← sum_Interference();
15     if i=0 or cost<bestCost then
16         bestCost = cost;
17         Save this allocation strategy;
18     end
19     Desallocate all;
20 end
```

block allocated to a user that requires a low transmission power can be reused at a short distance, and inversely. The transmission power is then correlated to w_i and to the distance of the eNodeB that reuses the same resource. A statistical study based on simulations shows that the empirical distributions of the distance from interferers to the typical user are close to a Normal distribution, with a mean which can be approximated by $\mathbb{E}[\|X_{k\cdot\Delta}\|]$. However, the correlation of these distances with the transmission powers impedes proposition of an approximation for Eq.6.5.1. In Table 6.1, we observe that mean interference is divided by a factor of 2 to 3 with regard to the 2 other strategies (Static and $M/M/RB_{max}/RB_{max}$). Extrapolations of the interference distributions are the same as for the other strategies except for $\Delta = 3$ where a Normal law offers a better fit than a t-Location scale. Even if interference is lower for this approach, its complexity in terms of feedback/measures from users and eNodeB is significantly greater than the other strategies. Indeed, it assumes that the scheduler knows, before an assignment, the interference contribution of each eNodeB on each user. Such complexity for a gain factor of only $2 - 3$ is questionable.

6.6.5 Comparing different allocation strategies

In Figure 6.6, we compare the interference PDF of different allocation strategies. It can be seen that the independent allocation is the worst allocation strategy since two adjacent BSs may use the same resources. The $M/M/RB_{max}/RB_{max}$ allocation handles more the interference since the resource blocks are not selected randomly as in the independent allocation. The $M/M/RB_{max}/RB_{max}$ allocation is followed by the static allocation. The heuristic cyclic allocation outperforms the three allocation strategies and manages better the interference since it allocates resources that minimize the interference for the current users.

6.6.6 Impact of Δ

Figure 6.7 shows the interference PDF (dB) for different values of Δ (3, 5 and 10) for the $M/M/RB_{max}/RB_{max}$ allocation strategy. It can be shown that increasing the reuse factor, reduce the interference. Small values of Δ mean that the system is fully loaded, therefore resources are busy and reused by closest eNodeBs, while high values of Δ mean low loaded network and hence resource are reused by farthest eNodeBs in the network.

6.7 Conclusion

In this chapter, we have proposed a spatial stochastic model that takes into account RB assignment strategies and realistic traffic demands. For cyclic assignment, where the scheduler assigns RB according to the eNode distances from the users, we derive simple and accurate estimations for the two first moments of interference. These moments can be used to determine parameters of known

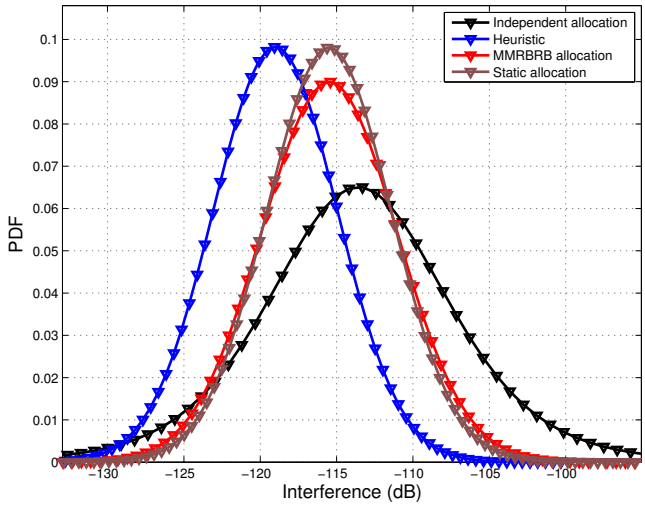

Figure 6.6: Interference PDF for the four allocation strategies and for Δ=5

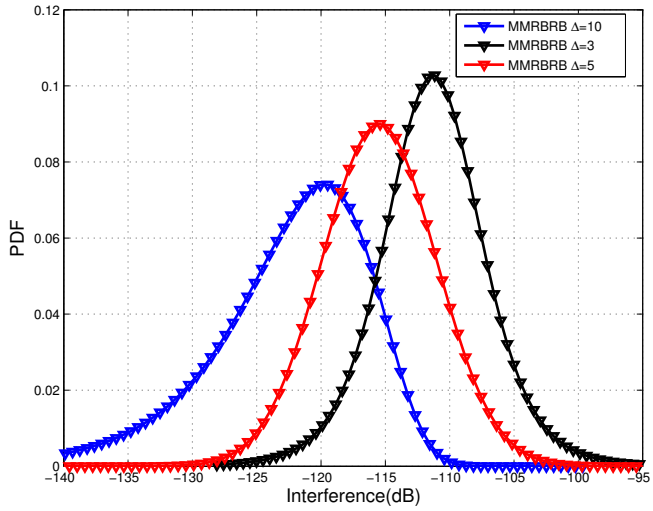

Figure 6.7: Interference PDF of the $M/M/RB_{max}/RB_{max}$ allocation strategy for different values of Δ

distribution. Interference distribution can then be used to compute more complex quantities as SINR, BER or throughput. Simulations that have been performed for this work run on several

days for each set of parameters [3] to obtain the required number of samples whereas theoretical evaluations took only a few minutes. The models are thus more tractable and allow the studying of the behavior of the LTE network through its main parameters and may give some insights on their design.

[3] with an ad hoc software developed in C running on a 4 x Quad-Core AMD Opteron(tm) Processor 8356.

Part II

Wireless Mesh Network: Directional Antennas approach

Chapter 7

Scenario and Motivations

Contents

7.1 Chapter Summary

This chapter provides an introduction to the second part of this thesis. Briefly, it aims at introducing definitions, basis and notions which are going to be used later in this part.

The main contribution of this part of the thesis is to propose energy efficient approaches for wireless mesh networks. In this chapter, we present generalities about backhaul and Wireless Mesh Networks (WMNs). Furthermore, we outline the importance of energy efficiency in these types of networks. Then, we motivate the network scenario used in this work.

7.2 Backhaul

Generally, the backhaul is the portion of network between core network and the fronthaul. The main role of a backhaul network is to carry packets from and to the core network. There are many varieties of scenarios where backhaul are used such as:

- *Cellular networks communications*: connecting base stations to the core network (controllers).
- *Satellite communications*: getting data to the point from which it can be broadcasted to end users.
- *Submarine communications*: connecting a landing point to the main terrestrial network of the region.
- *Mesh networks*: connecting wirelessly network nodes.

In a WMN, the mesh nodes jointly establish backhaul in order to enable mesh clients to forward their traffic to the Internet through gateways.

7.2.1 Mesh Networks Overview

Wired-based backhaul networks, such as wired LANs, provide a network throughput up to a dozen of Gigabits due to the huge available bandwidth. However, these networks face many difficulties such as the ones related to planning, deployment, flexibility, network extension and modularity.

WMNs [13] partially solve these constraints and propose a wireless connection between nodes in the networks. They are self-organizing, easy and fast to deploy with reduced costs compared to wired networks. WMNs have a wide range of applications such as sensor networks, military services and backhaul for cellular networks. In the last case, which was recently introduced in [21], a mesh network is expected to be used : (i) to offload the cellular traffic of macro base stations in urban areas [54] [21], and (ii) as a cost-efficient solution to offer the connectivity service in rural environment by extending the coverage of a macro base station [21], as proposed in the LCI4D project [4].

WMNs are generally composed of (i) *mesh routers* which are access points which form the network to connect (ii) *mobiles/end users* among each others, and finally (iii) *mesh gateways* in charge of routing the user traffic to/from the Internet.

WMNs have many characteristics :

- Multi-hop networks [27, 47]: Depending on the used routing protocol, traffic is forwarded, following a given path, through intermediate hops to reach the Internet gateways.
- Multi-channels [109]: Channel access is controlled by the Distributed Coordination Function (DCF) mechanism and nodes can transmit only if the channel is sensed free. The multichannel characteristic allows nodes to have simultaneous transmission on different frequency channels without generating interference. Note that nodes should be equipped by Network Interface Cards (NICs) which enable the multi-channels feature.

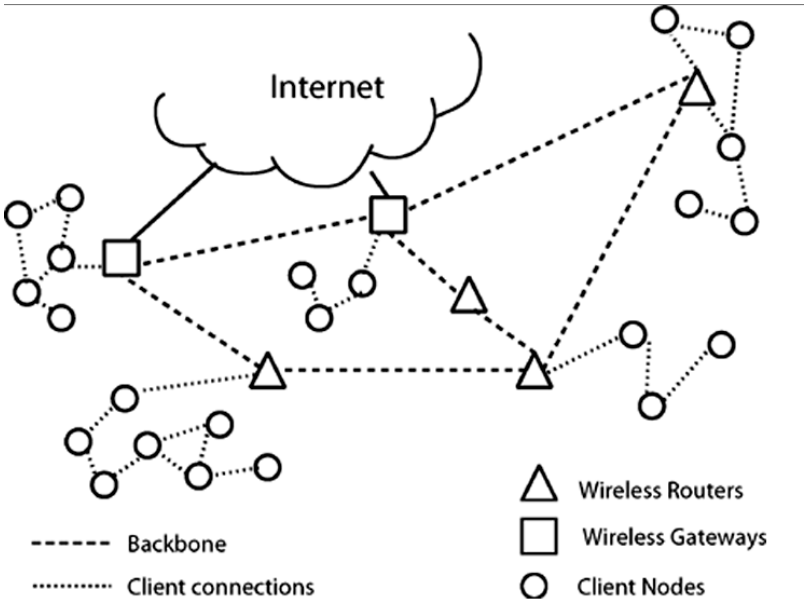

Figure 7.1: Wireless Mesh Network [50].

- Dynamicity [49]: Topology of WMNs can change over time by removing or adding nodes to the networks. In fact, the topology is easily reconstructed and established after the changings occur in the network, which is not the case in wired networks.

- Flexibility: Node placement is important in WMNs in order to ensure network connectivity and a minimum QoS. WMN nodes can be placed wherever they maximize the network performance and do not require any installed infrastructure to be deployed.

7.2.2 Wireless Backhaul

Operators must extend their infrastructure by deploying more nodes in the cellular network to deal with the increasing capacity demand. This task becomes impractical and inefficient for operators using wired/fiber links to connect nodes, since additional costs of deployment and maintenance are added. Wireless backhaul solves this paradigm. As stated in subsection 7.2.1, nodes cooperatively maintain network connectivity. In other words, each node in the network is reachable from any other node and that the user traffic can be successfully forwarded to/from the Internet gateway. Additionally, the most interesting characteristic of the wireless backhaul is its flexibility compared to wired backbones.

Usage of WMNs backhaul is widely tackled in the literature. More recent works show the

performance of wireless backhaul for cellular networks, such as indoor small cell networks [1] [104], heterogeneous cellular networks with densely underlaid small cells [2] [134], and LTE networks [21].

However, many difficulties still face wireless backhaul such as supporting the huge increase in data demand and satisfying the QoS constraints.

7.3 Energy Consumption

Power consumption is one of the important issues in WMNs since nodes are usually powered by battery with limited capacity [3] [4]. According to [19], 50-70% of the total power is consumed by power amplifiers, responsible of sending the signal through the antennas. Hence, finding approaches and schemes reducing/optimizing the amplifiers activity is an important task to increase the network lifetime and reduce the consumed energy.

The topic of reducing the consumed energy is widely addressed in literature, considering various tools and different scenarios. In chapter 8 we will discuss some of these works. Additionally, previous works show that using Directional Antennas (DAs) reduces the transmission power [97]. In this part of the thesis, we propose to use DAs to reduce the energy consumption and to improve the network energy efficiency. The energy efficiency metric reflects the amount of necessary energy to satisfy a given throughput.

7.4 Motivations

The lack of infrastructure is the main blocking factor of either cellular networks or Internet access extension to rural regions. This miss of infrastructure is justified by high costly wireless networks equipments such as cell towers and wired lines.

In this direction, many international companies around the world show there is growing interest in connecting the rural regions and work to improve the Internet accessibility. For instance, Facebook Inc. [91] proposes to use solar powered drones to provides Internet access to suburban areas, while Google Inc. [75] launched in 2013, its Loon project aiming to connect developing world to the Internet. Loon project is a network of balloons traveling on the edge of space. This is roughly the same objective of the LCI4D project [4], which is to provide low cost tools, technologies and features to connect isolated rural areas.

The common features of these solutions are: (i) not being hungry in energy consumption and, (ii) not requiring installed infrastructure. Thus, following these two guidelines is mandatory for the success of the project.

[1] www.interdigital.com/download/54313ecbe2622845250001bc
[2] lib.tkk.fi/Dipl/2012/urn100686.pdf
[3] *www.digi.com/pdf/wp_zigbeevsdigimesh.pdf*
[4] *www.linear.com/designtools/wireless_mesh_networks.php*

7.5 Scenario and Problem Statement

An alternative approach to reduce the high costly operator's activities related to planning, deployment and maintenance of the radio access network is the use of a self-configured WMN to connect outdoor multimode femtocells to a remote base station. A multimode femtocell is a low power node (LPN) embedding both cellular (4G/LTE) and mesh WiFi technologies. The mesh nodes form a local backhaul network to gather and relay cellular data of cellular devices on to the macro base station through an edge gateway as illustrated in Fig. 7.2. As a consequence, the underlying WiFi mesh network extends the coverage of the macro base station to consider remote mobile users. Therefore, the mesh backhaul network must be available and resilient. However, the shortage of energy in these settlements leads to optimize the energy consumption of the wireless backhaul network.

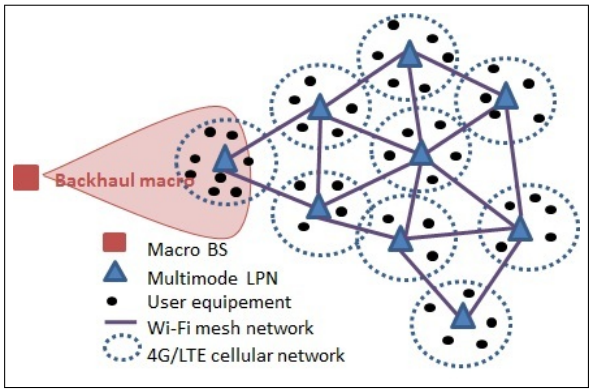

Figure 7.2: Low-cost infrastructure combining Femtocells and Wifi mesh APs [4].

In this part of the thesis, we aim at evaluating the performance using optimization and simulation tools, of a mesh backhaul network with DAs, considering the scenario of Fig. 7.2. Opposite to classical WMNs, in this scenario, the mesh backhaul network has only one gateway to relay data from/to the macro cellular network which should be an issue or a bottleneck in case of an overloaded network. Therefore, it is very important to evaluate the efficiency of this solution in terms of throughput and energy efficiency depending on the spatial nodes and flows distribution over the network.

Chapter 8

Directional Antennas & Mesh Networks: state of the art

Contents

8.1 Chapter Summary

Our work focus on using directional antennas (DAs) for wireless mesh networks (WMNs). In this chapter, we give a general presentation of directional antennas (DAs) and highlight the benefits that this type of antennas brings. Then we discuss optimization models, MAC layer modifications and routing algorithms dealing with omnidirectional antennas (OAs) and DAs to improve wireless mesh networks performance.

8.2 Directional Antennas (DAs) Generalities

8.2.1 Directional Antennas Gain

At the transmitter level, antennas send electromagnetic radiations in the form of radio waves. These waves are propagated in the space at the light speed, transporting useful information toward the receiver. On the other side, the receiver collects the electromagnetic waves and transforms them to electrical energy. Basically, antennas radiate in all directions of the space, hence all nodes in their sensing range hear the ongoing transmission. This type of antennas is known as omni-directional antennas (OAs).

Unlike OAs, *directional antennas (DAs)* have an increased range and allow to communicate with far nodes. DAs have the ability to focus their transmission energy toward the desired receiver, which increases the spatial reuse. This helps reducing interference and allows concurrent and parallel transmissions. Indeed, for a M-sectors DA, one of the M sectors can be selected to communicate with desired destination, by beamforming the antenna in the direction of this node. Nodes falling in the region of the remaining $M-1$ sectors sense the channel as free and can start parallel transmissions without overlapping with the main ongoing transmission. Additionally, due to the high DAs gain, far nodes can be reached with the same transmission power. Furthermore, according to related work, DAs reduce the end-to-end delay, network collisions and transmission power while increasing the network throughput.

Figure 8.1 shows the coverage range of an omni, a 2-beams and a 4-beams antenna, respectively. It can be seen that the higher the directional gain is the wider is the directional beam range and higher is the transmission power.

In the following, we show the importance of the transmission and reception gains on the received power at the receiver level. The transmission power is given by the *Friis free space* equation:

$$P_r = g_r g_t \frac{\lambda^2}{(2\pi d)^2} P_t. \tag{8.0}$$

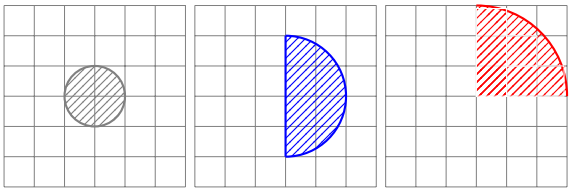

(a) Omni (b) 2-beams (c) 4-beams

Figure 8.1: The coverage area of the Omni-, 2-beams and 4-beams antenna.

where d is the distance between the transmitter and receiver, g_r and g_t represent the receiver and transmitter gains respectively, P_t is the transmission power and λ is the propagation wavelength. This shows the importance of the antenna gains at both sides, transmitter and receiver. It can be seen that in the linear domain the received power increases linearly with the antenna gains.

Eq. 8.2.1 illustrates the output power of a DA.

$$P_{out} = g_{DA}.P_t \qquad \text{(Watt)}. \tag{8.0}$$

where P_{out} is the output power (i.e the radiated power), g_{DA} is the antenna gain, and P_{in} is the input power.

The coverage ranges of an OA, R_{OA}, and a DA, R_{DA}, are related by the following equation [31]:

$$R_{\mathrm{DA}} = \frac{g_{\mathrm{DA}}}{g_{\mathrm{OA}}} R_{\mathrm{OA}}. \tag{8.0}$$

where, g_{DA} and g_{OA} are the DA and OA gains, respectively. Hence, the coverage range is improved, in a given direction, by:

$$\Delta R = (\frac{g_{\mathrm{DA}}}{g_{\mathrm{OA}}} - 1) R_{\mathrm{OA}}. \tag{8.0}$$

Furthermore, the transmission power is also improved by a factor of:

$$\Delta P = (1 - \frac{g_{\mathrm{OA}}^2}{g_{\mathrm{DA}}^2}) P_{\mathrm{OA}}. \tag{8.0}$$

8.2.2 Switched and Steerable beams DAs

Two types of directional antennas are considered: *(i)* switched beam antennas [23] where beams are fixed/predefined and *(ii)* steering beam antennas [98] where beamwidth depends on the location and the distance to the receiver. The switched beam antenna is more costly efficient than the steering beam one, since complex DSP operations are used to adapt the beamwidth [73].

8.2.3 Problems facing DAs networks

In the previous section, we presented DAs and the benefits they can bring to improve the network performance. However, the usage of DAs in a WMN is challenging and faces with many problems such as deafness and hidden node problems.

In the following, we outline these problems and present related work proposing solutions to alleviate these problems.

8.2.3.1 Deafness

When nodes are equipped with DAs capabilities, deafness problem may arise and cause communication failures. Figure 8.2 illustrates a scenario of deafness problem where node C tries unsuccessfully to communicate with node A, because node A points its beam toward node B and does not hear messages from node C even if it is in its communication range.

Solutions to this problem are proposed by modifying the MAC protocol. ToneDMAC [32] consists of using multiple tones to alleviate deafness. It is based on informing a node's neighborhood of its activity through omnidirectional tone-notification. DMAC/DA [122] (Directional MAC/Deafness Avoidance) is used to alleviate the deafness problem by sending "Wait To Send" frames transmitted by the transmitter and the receiver after the successful exchange of directional RTS and CTS to notify the on-going communication to potential transmitters.

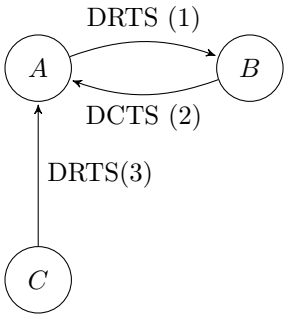

Figure 8.2: Deafness

8.2.3.2 Hidden Terminal

The hidden node problem arises when two or more nodes can not hear each other. The hidden terminal problem may occurs for many reasons:

- *Unequal gains in OAs and DAs* [69]: Figure 8.3 illustrates this problem where node A sends a Directional RTS (DRTS) to its intended receiver B which, in turn, replies with a Directional CTS. A and B beamform towards each other and start exchanging data. C is far enough

from B and did not receive its Directional CTS (B's DCTS). Hence, it is not aware of the transmission between A and B. Suppose at this stage C wants to communicate with D, then it sends a DRTS toward D. This leads to a collision at node B.

Figure 8.3: Hidden terminal (Case I).

- *Unheard RTS/CTS*: Figure 8.4 illustrates this case. Assume that node A is beam formed toward node B and are communicating after exchanging a Directional RTS (DRTS)/Directional CTS (DCTS). On the other hand, suppose that node D has some packets to send to node C and it sends a DRTS to node C, which replies with a DCTS. Once node C receives node's D DCTS it starts transmitting data. Node A does not able to hear and unaware of the exchange between nodes C and D since it is beamformed toward node B. If A finishes its communication with B and wants to communicate with node D, it will send a DRTS and a collision at node D will be occurred.

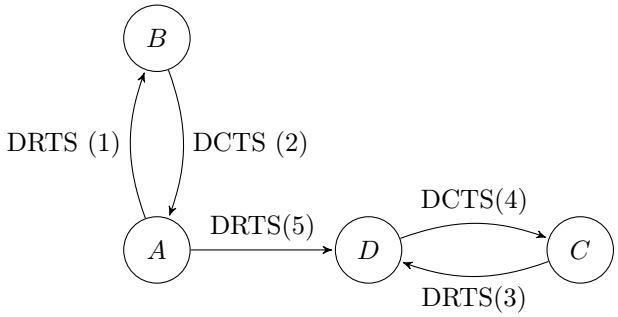

Figure 8.4: Hidden terminal (Case II).

Many solutions are discussed in the literature such as increasing the nodes transmitting power and using a wireless central coordinated protocol [72].

-

OAs and DAs have been widely studied in previous works. In the following we discuss works interested in physical layer for both DAs and OAs networks, such as power control, link adaptation or MCS [16, 26, 93, 94, 106, 111, 136]. Then, we outline works studying the impact of MAC protocols

and propose MAC layer modifications such as directional and multihop RTS/CTS to enhance both throughput and energy efficiency [33,41,77,97]. To conclude the section, we present works proposing routing protocols to improve throughput, delay and network energy efficiency [112, 116].

8.3 PHY layer Optimization

In literature, several works were interested in using optimization tools to improve performance of WMNs. These works use either linear solvers (as Cplex [37] which is based on branch-and-cut program) or/and propose heuristics to solve the NP-hard considered optimization problems.

8.3.1 General Optimization Model

Combinatorial optimization in WMNs was firstly introduced in [94]. In the following, we provide a *general* optimization model optimizing jointly the throughput, the energy consumption and the deployment costs (Capex and Opex) of WMNs as following:

$$\begin{cases} \text{Minimize} \quad \alpha.\mathcal{E} + \beta.\mathcal{IR} + \gamma.\mathcal{C} \\ \text{s.t} \\ \text{Link capacity constraints,} \\ \text{Flow conservation constraints,} \\ \text{QoS constraints} \end{cases} \tag{8.0}$$

where $\mathcal{E}$, $\mathcal{IR}$ and $\mathcal{C}$ represent the energy consumed, the inverse of throughput and the cost related to deployment, respectively. α, β and γ are real values $\in$ [0,1] representing weighting coefficients satisfying $\alpha + \beta + \gamma \leq 1$.

The energy consumed in a WMN depends on many factors such as:

- *The activity time*, in fact, if packets stay longer in a node, this node will consume higher energy. The packets awaiting time depends on many factors such as collisions and network congestion.
- *Attached users* or the traffic that each node needs to forward. In fact, users generate traffic which must be forwarded to intermediate nodes until reaching the gateway. Hence, high number of attached users cause high nodes activity, and hence lead to a high energy consumption.
- *Transmission power levels*: Transmission power highly affects the energy consumed. Hence, the need of power control approaches to control and optimizes the transmission power.

The constraints of the outlined optimization problem are:

- *Link capacity constraint* which ensures that the traffic transiting a link do not exceed the link capacity.
- *Flow conservation constraint*, which ensures that all flows that a node receives, either from its attached users or from neighbors nodes to relay, are forwarded.
- *QoS constraints* are to guarantee QoS requirements.

In the following, we discuss optimization-based works used to improve network performance for both OAs and DAs networks and highlight the impact and gain of DAs over OAs networks. Then, we present the proposed heuristics and resolution approaches. Generally, the network performance tackled in literature lies on throughput, end-to-end delay and energy consumption/efficiency.

8.3.2 OAs Networks Optimization

The deployment costs and the energy consumption of mesh networks are jointly minimized in [26,29], by considering a weighted objective function combining Capex and Opex. This is equivalent to $\beta = 0$ in the optimization problem (8.3.1). Three scenarios are considered: (i) the small, (ii) medium and (iii) large size networks, where each network is composed of clients generating traffic, mesh routers (responsible of traffic forwarding) and mesh APs (as gateway) to forward traffic to the Internet. Two types of traffic are considered such as the standard traffic and the busy traffic. Simulation results show that the optimal solution (obtained using Cplex) can save up to 30% of energy and that the standard traffic scenario consumes less energy.

The authors of [106] present an optimization framework and provide guidelines for network design based on the obtained results. They use continuous power control and multi-rate transmissions to optimize the energy-capacity tradeoff which corresponds to $\gamma = 0$ in the optimization problem (8.3.1). The physical link (e, P_t, r) used to model the radio transmission parameters is composed of the logical link (e), which is used to model the routing paths, the transmission power (P_t), the rate (r) and it is established only if the SINR satisfies the requirements of the corresponding transmission rate ($SINR > \beta(r)$). The considered energy consumption model from [68] is composed of (i) a fixed cost corresponding to the energy consumed in the idle state, and (ii) a linear variable cost which depends on the node which is either transmitting or receiving. The authors propose two Master optimization linear problems (LP), one to Maximize the Capacity (MPMC) and the other to Minimize the Energy Consumption (MPME). They use a column generation algorithm of linear programming to solve the optimization problem and they show that a solution can be obtained in a reasonable time for a network size of 30 nodes. For a fixed modulation and coding scheme (MCS), simulation results show that: (i) when increasing the maximum transmission power (P_{max}), higher capacities can be reached with the same energy consumption, (ii) compared to a fixed transmit power, power control reduces the consumed energy and improves the network capacity and (iii) the

uplink-only, downlink-only or mix traffics do not have an impact in the energy consumption nor in the capacity. Then, it studies the impact of using many MCSs (5) on the energy-capacity trade-off by investigating the impact of the topology and the weight distribution (Poisson, uniform random and homogeneous traffic demands). However, no multi-channel nor directional antennas scenarios are considered.

The work in [94] considers an omnidirectional multichannel wireless network. It formulates the congestion problem as an Integer linear programing problem (ILP) and proposes an Iterative Local Search (ILS) algorithm to solve the ILP problem. The objective function consists of minimizing network congestion, corresponding to α=0 and γ=0 in the optimization problem (8.3.1). Since the network complexity increases exponentially with a number of integer variables, it proposes an ILS by relaxing some conditions and fixing some variables. Different types of traffic are considered for simulations: UDP and TCP and internal and external traffics. Internal traffic consists of traffic from a mesh node inside the network to other non-gateway node in the network, while external traffic is from a node inside the network to a gateway node. Extensive ns-2 simulations show that increasing the number of flows improves the throughput and PDR, and reduces the Round-Trip time (for the TCP traffic) and the end-to-end delay. Furthermore, increasing the interfaces in each node and the number of channels increases the network throughput and reduce the round-trip time.

In [93], the authors propose jointly optimization of the energy consumption and the end-to-end delay using a Mixed Integer Linear Programing (MILP) approach. The cost function is a weighted sum of the delay and the energy consumption. That is, $\gamma = 0$ in the optimization problem (8.3.1). They proceed to a linearization process of the non linear constraints of the minimization problem by introducing new variables. The GLPK (GNU Linear Programming Kit) package [7] is used to solve the MILP problem. In their solution, each access point (AP) can adapt its transmit power by choosing a power level depending on the number and locations of the attached users and their distance to neighbor base stations. The output of the minimization problem is the set of active APs and the transmission power of each AP. Simulations results show a gain of 16% compared with a fixed transmission power strategy. However, this work uses only omni-directional antennas. Furthermore, the problem is solved using a solver and no heuristic or analytic solutions are proposed.

The topology control and the Routing assignment problems are jointly solved in [127]. It shows that the formulated problem can be reduced to the *NP-hard partition problem*. It proposes TORA (Topology and Routing Assignment) based on Ant Colony algorithm for the NP hard problem. Two types of traffic are considered for simulations: (i) Normal distributed UDP to analyze the end-to-end delay and loss ratio, and (ii) CBR TCP traffic to analyze the throughput. Compared to the Shortest path algorithm, TORA achieves lower packet loss ratio and higher TCP throughput.

In [16] a joint routing and scheduling optimization framework is considered where the energy consumption and throughput are optimized using a Mixed Integer Linear Program (MILP). Since the complexity of the optimization problem grows exponentially with the number of integer vari-

ables, the authors propose an heuristic based on Ant-Colony (AC) algorithm. Simulations are performed for different network loads: 5, 10 and 15 clients, and each client generates a CBR traffic. A multi channel network is considered where each node can choose one among many channels to communicate. Results show that AC algorithm and optimal solution fit and they outperform the shortest path routing algorithm. Then, authors show that the proposed algorithm improves performances in terms of average throughput, energy consumption and average path length. However, they do not differentiate a transmission activity from a reception activity and consider only two states of a node either active or not active. Nevertheless, this is not a strong assumption since the transmission energy is much higher than energy needed for reception [111].

In table 8.1 we summarize the previously discussed works.

Paper	Optimization Method	Metric	Gain
[16]	Mixed Integer Linear Program (MILP) using Cplex & Ant-Colony (Omni)	Energy and throughput optimization	-
[26, 29]	Joint design and management optimization (Omni)	Deployment cost and the energy consumption	30 %
[106]	Continuous power control and Muti-rate transmissions (omni)	Energy and Throughput Optimization	-
[94]	Integer linear programing problem & Iterative Local Search (Omni & multi-channel)	Energy and Throughput	-
[127]	Topology control and the Routing assignment (TORA)	Packet loss ratio and throughput	-
[93]	Mixed Integer Linear Programing (MILP) approach	Energy consumption and the end-to-end delay	16 %

Table 8.1: Classification of optimization-based approach in OAs WMNs.

8.3.3 DAs Networks Optimization

More recently, DAs technology was used in wireless mesh networks to improve their performance. Researchers tackled these problems using different tools such as optimization by considering different scenarios. In the following, we focus on optimization based work.

The work in [94] is extended in [111] by considering a directional antennas network. The authors propose an Iterative Local Search (ILS) to solve the considered MILP. The MILP investigates the network congestion minimization. The considered optimization problem is equivalent to the problem in (8.3.1) with α=0 and γ=0. Compared to the OAs model ([94]), the proposed DAs scheme reduces the end to end delay and improves the packet delivery ratio. However, the impact of the directional antenna on the energy consumption is not considered.

The authors of [136] consider a DAs network and study its reliability. They consider two MILP problems to model the reliability of DA-WMNs. The first problem is Max-Min optimization problem

and aims to maximize the minimum flow. The minimum flow corresponds to the difference between the link capacity and the amount of traffic transiting that link at a given time. While the second aims to minimize the number of directional antennas. This is due to the fact that DAs are more expansive than OAs and those DAs limit the robustness of the network by decreasing its reliability. The optimal value of the first problem (the maximum flow) is used in the second problem. Then, an algorithm verification is proposed, to test the feasibility of the obtained solutions. Optimal solutions obtained using Cplex and different random topologies size are considered. The number of directional antennas beams is provided for each scenario and for different values of α ($\in [0, 1]$ to indicate the expected service quality after a failure).

In order to improve the network throughput in a DAs WMN, [108] optimizes the link scheduling and power control. It uses an "exact cone-plus-ball" antenna model. It develops an interference model dedicated to DAs by considering two interference types: (i) primary interference caused by the node itself (Self-interference) due to collision and multicast, and (ii) secondary interference due to simultaneous transmissions of different pairs of nodes. Then, it proposes the Generalized Physical Interference Model (GPIM) as an interference model of DAs which is similar to OA Physical interference model (OPIM) adopted for OAs. It considers that a transmission is successful only if the SINR is greater than a given threshold. Simulation results of a network composed of 40 mesh routers and 3 gateways show that increasing the beamwidth implies a throughput decrease for different transmit power levels. Furthermore, it shows that the throughput increases while increasing the maximum transmit power.

The authors of [42] tackle the performances of DAs in a multichannel scenario. To improve the throughput, it combines the spatial separation from using DAs and frequency separation using the orthogonal channels. At first, it proposes and evaluates a WMN architecture. Then, it proposes a distributed routing protocol for directional channel assignment. It evaluates the packet delivery ratio, the average delay and the throughput by varying the sending traffic per nodes and for different number of available channels. Simulation results show that the proposed architecture and routing algorithm provide gain compared to an OAs network. In fact, while the number of available physical channels is decreasing (from 12 for 802.11a to 3 for 802.11b) the performance experiences a degradation. It concludes that the less are the available channels are the more the contention is and the performance is worst. Furthermore these results are validated by using a testbed composed by 16 nodes.

In [69], exhaustive simulations are used to compare the performance of using directional antennas over omnidirectional antennas in terms of mean throughput, delay and fairness. The network is composed of 9 nodes (3×3 grid topology), each equipped with a 4-beams antenna. Three simulation scenarios are considered where only one source transmits data to the other nodes in the network. The source location changes in each scenario. Depending on the considered scenario, the mean distance to the source node, in number of hops, changes and it directly affects the throughput and

delay: the lesser the number of hops, the better the network performance is. Furthermore, this study concludes that for low load traffic, there is no advantage of using directional antennas and that the gain is important for high load traffic. However, only static routes are used to carry data from the source node to the destinations since no routing algorithm is used.

In table 8.2 we summarize the previously discussed works.

Paper	Scheme	Metric
[111]	Integer linear programing problem & Iterative Local Search (Directional & multi-channel)	E2E delay and Throughput
[136]	Max-Min flow problem & Minimizing the number of directional antennas	Network reliability
[108]	Link scheduling and power control	Network throughput
[42]	Multichannel DAs network	Packet Delivery Ratio, Average Delay and Throughput
[69]	Exhaustive simulations	Throughput, Delay and Fairness

Table 8.2: Classification of optimization-based approach in DAs WMNs.

8.3.4 Beyond optimization

In addition, many works go beyond optimization and use various tools to evaluate performance of DAs networks.

In [118], the authors extend the asymptotic analysis for an omnidirectional network introduced in [57] by considering the nodes equipped by directional and smart antennas. Thus, they compute an upper bound of the average transmission rate of each node. The asymptotic rate depends on the number of elements (beams), the antenna gain, the beamwidth, and the number of nodes in the network.

In [74, 95], the throughput of a grid network with one gateway is evaluated using techniques from information theory. It shows that the throughput is upper bounded by $\frac{C}{n}$, where C is the maximum capacity of any link in the network and n is the number of nodes.

The authors in [39] analytically derive the benefits of directional antennas compared with omni-directional antennas in terms of delay and throughput. The analysis are in three steps: *(i)* Network establishment *(ii)* Routing: nodes choose the shortest distance to forward packets, *(iii)* Transmission Scheduling: where a TDMA scheme is considered. The paper shows that directional antennas increase the transmission range and reduce the interference.

Using stochastic geometry, the authors in [66] consider a network composed of nodes equipped with sectorial antennas where each node has M sectors. They derive analytically the optimal contention density (i.e the maximum density of concurrent transmissions) which is related directly

to the transmission capacity. It shows that the transmission capacity can be increased by M^2.

[40] shows the impact of multi-channel technology on directional antennas by deriving the capacity bounds (the lower and the upper bound). Results show that combining these two technologies reduce the interference and enhance the network connectivity.

8.4 Medium Access Control (MAC)

As stated before Medium Access Control protocols (MAC) such as DCF require that nodes in the vicinity of an ongoing transmission stay silent in OAs network. In DAs networks, nodes in the vicinity of an ongoing transmission can initiate and engage a communication simultaneously without generating interference. Hence, the need of new MAC protocols exploiting DAs features. In this section, we present works dealing with DAs at MAC layer. We first discuss works proposing schemes to improve the network throughput, then we tackle the ones interested in reducing the energy consumption.

8.4.1 Throughput

Two schemes of directional MAC protocol are discussed in [77], namely DMAC1 and DMAC2, to reduce collisions in Ad-Hoc networks. They assume that (i) each node is equipped with a GPS to know its position and positions of its neighbors, (ii) a node can not transmit simultaneously into different directions, (iii) if a node receives an RTS or CTS from a given direction, and it is not involved in this communication, it blocks this (and only this) direction until the end of the transmission. In this way, unlike OAs, it can use other unblocked directions to communicate. The main difference between the two schemes is that DMAC1 uses DRTS while DMAC2 combines ORTS and DRTS.

- In DMAC1, RTS is sent directionally (DRTS) with the position of the transmitting node and CTS is sent omni-directionally (OCTS) with the positions of the receiving and the transmitting nodes while Data exchange and acknowledgement are directional. When neighbor's nodes of the receiving node (in its communication range) receive the OCTS with its geographic position, they block this direction during the communication time and they are free to use other unblocked directions for transmission. However, DMAC1 have some limitations. In fact, since the DRTS is sent directionally toward the desired receiving node, neighbors of the sending node are not aware of this communication and this may lead to network collisions.

- In DMAC2, two approaches are considered: ORTS and DRTS. The former, ORTS, is sent if the node is allowed to transmit in all direction, where it means that, no direction is blocked due to simultaneous transmissions. While the later , DRTS, is sent when there is a blocked

direction due to a concurrent transmission. The node transmits DRTS toward the desired destination.

In Multi-hop MAC (MMAC) [33] two types of neighbors are considered: (i) Directional - Omni directional (DO) and (ii) Directional - Directional (DD) ones. Communications for the former type are possible when the transmitting node is operating on Directional mode and the receiving node in omnidirectional one. While for the later transmitting and receiving nodes can communicate only when both are pointing to each other using directional antennas. MMAC introduces forwarding-RTS which is a RTS used when the desired receiving node is not a DD neighbor. Then, the sending node sends a forwarding-RTS to DO intermediate nodes which will be forwarded to the receiving node. Once the forwarding-RTS received, the receiving node points it directional antenna toward the sending nodes and sends a directional CTS before the directional data exchange starts.

Directional version of the Virtual Carrier Sensing (DVCS) is discussed in [121]. It has three main phases (i) AoA (Angle of Arrival): each time a node receives a packet from other nodes and it records it in its table (ii) locking and unlocking destination, and (iii) DNAV which is the directional version of Network Allocation Vector.

The authors in [97] introduce the notion of Angle-of-Arrival (AOA) table which records the neighboring/receiving nodes and their corresponding beams/direction, so that the RTS/CTS can be sent directionally toward the desired receiving node. The work considers four MAC schemes:

1. The basic IEEE 802.11 scheme which sends the RTS and CTS omni-directionally.

2. The RTS is sent omni-directionally on the free sectors which are not in an ongoing transmission, and the CTS is sent omni-directionally.

3. RTS is sent as in (2) but the CTS is sent directionally towards the direction of the node sending the RTS.

4. The RTS and CTS are both sent directionally.

For the four schemes data is exchanged directionally. Simulation results show that directional RTS/CTS exchanges offer better performance in terms of throughput and energy saving. Next, they propose the new Directional MAC protocol based on Power Control, DMACP protocol. The RTS/CTS exchange phase is similar to scheme *(4)*, and the data packets are sent with reduced power (-6dB compared to the transmission power of RTS/CTS messages) to reduce the interference.

The problem of optimal node placement in DAs networks is tackled in [132] in order to ensure a full coverage and global network connectivity. Two antennas models are considered: the sectored model and the knob model. The former is the simplest and the common way to model the coverage range of a DA. The later takes consideration of the side lobes and models more realistically a DA.

8.4.2 Energy consumption

The IEEE 802.11 [9] standard has considered the energy efficiency in WMNs in its first releases. It presents the power saving mode (PSM) where time is divided into beacon periods, and each beacon period is divided into ATIM (Announcement Traffic Indication Message) window and a data window. During the ATIM window source and destination perform a handshake. During the data window, they exchange Data/ACK while other nodes which do not have data to send go to "Doze" state to save energy. However, PSM introduces latency for incoming packets.

[41] combines the benefits of the power saving mode (PSM), multi-channel MAC protocol and directional antennas to propose MMAC-DA protocol. During the ATIM window nodes proceed to channel selection and transmission direction. The source node initiates the 3-way handshake by sending an omni directional ATIM message containing its available channel list. Once received by the destination node, it records the direction of the source and chooses a channel to use for transmission depending on both its and source available channel lists, then replies omni directionally to the source node using a A-ACK (ATIM-ACK). The handshake is ended by the A-Res source reply. Note that nodes which overhear the control messages exchange during the ATIM window must update their available channel lists. If the ATIM period ends successfully, source and destination exchange data during the data period, otherwise node are turned to the doze state to save energy. MMAC and classical IEEE 802.11 are used as benchmark schemes. Simulation results show that MMAC-DA improves network performance in terms of throughput, packet delivery and energy efficiency when network goes near to saturation (i.e. high network arrival rate). The gap between the energy consumed in the doze state (0.045W) and energy consumed in idle state (1.15W) explain the fact that MMAC and MMAC-DA, implementing PSM, are energy efficient compared to classical IEEE 802.11.

The authors of [119] use electrically steerable beams and propose an algorithm aiming to find a energy efficient routes ensuring network connectivity in a DAs network. The proposed algorithm consists of three steps:

1. Shortest Cost Routing: Considering all possible paths for all possible nodes. Djikstra is used to find the shortest path. Furthermore, it uses two metrics to model the energy efficiency of a given path : (a) minimize the energy consumed per packet (b) maximize the network lifetime. It assumes that traffic from a given source to a given destination follows the same path.

2. Link flow matrix calculation: Computing the links flow between each pair of nodes.

3. Topology update (taking into account information of the two firsts steps and that a DA can Transmit to only one node at a time) and scheduling.

Simulation results show that increasing the average vertex degree increases the network lifetime by 4 times and that DAs network have a better lifetime than OAs network.

The authors of [14, 15] consider a directional antenna network and derive the throughput and energy consumption expressions in honey grid topology. Then, they show that directional antennas help to reduce the energy consumed by network and the more the antennas are directive the better is the performance. This work can be extended using a random distribution of nodes (PPP or a general PP).

In table 8.3 we summarize the discussed works.

Paper	Scheme	Idea	Enhancements
[9]	PSM	ATIM & Data windows	Energy consumption
[41]	PSM-DA	Mutli-channel MAC & Power Saving Mode (PSM) & DA	Throughput, PDR and energy efficiency
[77]	DMAC1	DRTS (Directional RTS)	Throughput
[77]	DMAC2	ORTS and DRTS	Throughput & Reduce network collision
[33]	MMAC	Multi-hop MAC (forwarding-RTS)	Throughput
[121]	DVCS	Directional VCS version	Throughput
[97]		Directional RTS/CTS	Throughput and energy consumption
[31]		Friis Propagation Model	Communication range, reception and transmission powers

Table 8.3: Classification of DA-MAC protocols.

All the cited works consider most of the time several gateways. However, when only one gateway exists in the mesh network, several issues can appear due to the congestion/collision near to this gateway which affects the network performance like energy consumption and energy efficiency. We claim that it is important at the first step of the study to evaluate by simulation the benefits of DAs in such case considering both uplink and downlink transmissions with a weak and heavy traffic load.

8.5 Routing

Routing in OAs WMNs has been an active area of research for many years. Routing protocols are responsible of establishing links and finding routes from a given source to a given destination. Many types of routing protocols are considered in OAs such as: (i) reactive (AODV [1] and DSR [2]) and (ii) proactive (as OLSR[3]) protocols. These protocols are not suited for DAs networks since DAs

[1] Ad-hoc On-demand Distance Vector protocol
[2] Dynamic Source Routing protocol
[3] Optimized Link State Routing protocol

have different functionally and features than OAs. Hence, the need of new routing protocols are adapted to DAs networks. In the following, we present DAs routing protocols proposed in related work.

8.5.1 Energy Consumption

Energy Efficient Directional Routing (EEDR) is proposed in [116]. EEDR is a routing algorithm between actor nodes in a Wireless Sensor and Actor Network (WSAN) characterized by its robustness, energy awareness and fairness. It proposes an algorithm to determine the Maximum Capacity Path between two nodes of the network (i.e. two edges of the graph) and a second algorithm for route scheduling. Two types of routing are considered: (i) Intra-Partition Routing and (ii) Inter-Partition Routing. For the former, a leader node is elected to coordinate the communication between actor nodes inside the partition for the route discovery phase. The later is used when a node is needed to send data to an other actor node. Firstly, it checks if the route to this destination is available in its route-cache. If so, this route is used for data transmission. Otherwise, it performs a route discovery process which is composed of three main steps: (a) Route Discovery (b) Directional broadcast, and (c) Sensor-to-Actor routing. (a) The actor node initiates the process by sending a route request packet to the partition leader node. If the destination belongs to the same partition the packet is forwarded directly to the destination actor nodes. If not, the route request packet is forwarded to all actor nodes in the partition and directional broadcast is started. (b) All actor nodes in the partition directionally broadcast the route request packet (received form leader node). The actor nodes are aware of the position of neighbor nodes. By this way, each actor node uses sectors (for the directional broadcast) which do not overlap with directional broadcast of its neighbors. (c) In face of Sensor-to-Actor routing: Sensors in the directional range of each actor node will receive the broadcasted route-discovery packet after the directional broadcast. Then, it checks in its routing table if it has actor nodes of other partitions and forwards the packet. Once the actor nodes of other partitions receive the route discovery packet, they forward it to the leader actor which has a global knowledge of the partition until the actor destination is founded. Simulations are performed for static and mobiles topologies and show that EEDR improves the network lifetime by 80 % compared to AODV routing protocol. Furthermore, using 6-sectors actor nodes improves the lifetime by 10% compared to 4-sector actors.

[112] considers a mobile ad hoc scenario and proposes modifications of DSR protocol [87] which is a simple and efficient on-demand routing protocol designed specifically for use in multi-hop wireless ad hoc networks of mobile nodes. Modifications concern: (a) Data packet structure (b) Route discovery, and (c) Route maintenance. For the data packet structure two flags are introduced (i) trigger partitioning bridging flag and (ii) Long hop flag. Then a new *Passive Acknowledgement table* is introduced which is available at each node and contains information about the received

RREQs that this node receives. It includes the target address, the time when the entry is inserted (the RREQ is received), list of angular ranges around the node in which a potential destination may exist, and a list of RREQ packets having different source nodes but the same destination node. The source node sends an omnidirectional RREQ to start the Route Discovery process for the route discovery process. The trigger partitioning bridging flag is cleared if the node have not sent a RREQ for this destination node before and it is set if the source node has already sent a RREQ for this destination. Then, when a node receives the RREQ, it forwards it omni-directionally and updates its Passive Acknowledgement table. Once the RREQ is received by the destination node it replies by a Route Reply. When an intermediate node receives a Route Reply creates a route reply packet for each lister RREQ and deletes this entry from it Passive Acknowledgement table. The route maintenance phase consists of returning a Route Error to the source node if the intermediate node does not receive an acknowledgment. It considers two simulation scenarios. In the first one all nodes are moving in two separated regions and in the second two nodes are stationary in the border of each region. The second scenario ensures that nodes in each side are located close to each other to bridge partition with longer transmission range. Results evaluate the PDR, latency and overhead and show that the directional version of DDSR offer better performance that the basic DSR.

In table 8.4 we summarize all the previously detailed work.

Paper	Scheme	Idea	Metric
[116]	EEDR	Wireless Sensor and Actor Network (WSAN) routing	Netwrok life time
[112]	DDSR	Directional version of DSR	PDR, latency and overhead

Table 8.4: Classification of DAs Routing algorithms.

We discussed works proposing appropriate routing algorithms for DAs networks. However, none of them provides analysis and shows the impact of the *number of links* on the network performance. Furthermore, only the energy consumption is studied and no work discussed the *energy efficiency* which is an important metric capturing the amount of energy needed for a given throughput.

8.6 Conclusion

In this chapter, we have introduced related works dealing with WMNs equipped with DAs capabilities. We classified these works depending on the considered layer and the studied performance metric. We conclude that DAs improve network performance compared to traditional OAs.

Based on these encouraging results which show the impact of DAs on network performance, we believe that DAs are an interesting feature for usage in wireless mesh networks generally, and in the LCI4D project scenario [4] specifically.

In the next chapter, we first investigate the number of links of a given route. Then, we show the impact of DAs on network performance in terms of throughput, loss ratio, energy consumption and energy efficiency using extensive simulations.

Chapter 9

Energy Efficiency Evaluation in Directional Antennas Mesh Networks

Contents

9.1 Chapter Summary

Energy Efficiency is an important feature in poor-covered areas where not only the access to a cellular network is scarce but also energy sources are limited. In this chapter, we consider a wireless mesh network to act as a local backhaul network to cover rural and remote villages. The shortage of energy in these settlements motivates the optimization of the energy consumption of the wireless backhaul network. Therefore, we propose to use Directional Antennas (DAs) to improve the throughput and the network energy consumption. DAs focus the RF signals toward the desired

destination to reduce the collisions and the number of hops between the source and the destination. We provide for both OAs and DAs networks, the number of links (hops) that a packet passes through to reach the destination. Using extensive simulation, we evaluate the network performance in terms of packet loss, mean throughput, mean energy consumption and energy efficiency for the chain and grid topologies. Simulations results show that using DAs improves the throughput and the energy efficiency, and reduces the mean loss ratio and the consumed energy.

9.2 Introduction

In the two last decades, Mutihop Wireless Mesh Networks (WMNs) [13] have attracted much attention in both academia and industry due to their wide range of applications such as sensor networks, military services and cellular networks. In the last case, a mesh network is expected to be used to offload the cellular traffic of macro base stations in urban areas [54] [21], and used as a cost-efficient solution to offer the connectivity service in rural environment by extending the coverage of a macro base station [21], as proposed in the LCI4D project [4].

Indeed, activities related to planning, deployment and maintenance of the radio access network are costly for the operator (Capex & Opex) [19,88], compared to the number of concerned customers in rural areas. An alternative approach is the use of a self-configured WMN to connect outdoor multimode femtocells to a remote base station as explained in Section 7.5.

Directional Antennas (DAs) are demonstrated to be an efficient solution to reduce the power consumption of the overall network [69,97]. Unlike an Omnidirectional Antenna (OA) which radiates in all directions, a DA focuses its transmission power in the intended direction, to set up strongest links due to the highest DAs gain. Hence, the spatial reuse is increased. The interference and collisions are reduced and more simultaneous transmissions are allowed. As a consequence, the transmission delay is reduced, the throughput is improved and less energy is consumed in the network [105]. Moreover, the narrower beamwidth provides a larger coverage range as shown in [71]. We claim that combining DA features with mesh technology will improve the mesh backhaul network operation and its energy efficiency.

In this chapter, we aim at evaluating the performance of a mesh backhaul network with DAs considering the scenario of Fig. 7.2. We consider two types of scenarios. The first one is the uplink to carry data from the mesh nodes to the gateway, denoted *NSources-1Destination*. The second one is the downlink for the opposite transmission which is from the gateway to the mesh nodes denoted as *1Source-NDestinations*.
Note that the considered scenario of Fig. 7.2 is distinctive from other related works, where the performance evaluation focuses primarily on two performance metrics, the energy consumption/efficiency and the throughput and considers one of both scenarios: either an ad hoc WiFi networks using DAs like in [41, 97, 119] or a mesh network with several gateways where the nodes

use DAs as in [26, 69, 127] or OAs as in [16, 93].
In this chapter, our aim is to highlight the gain of DAs compared to OAs in a typical mesh network of Fig. 7.2. Thus, we evaluate the performance of this system using intensive simulations in terms of throughput, loss ratio, energy consumption and energy efficiency. Our second contribution consists of providing the expressions of the number of links which compose the established paths over the mesh network depending on the type of the antenna (OA, DA) and the number of beams in case of DA.

The reminder of this chapter is organized as follows. Simulation scenarios and performance metrics are presented in Section 9.3. Then, we present and discuss performance analysis and simulation results in Section 9.4. Finally, in Section 9.5 we conclude the chapter.

9.3 Scenarios & Performance Metrics

The aim of this study is to evaluate the impact of DAs in a mesh network on throughput, energy consumption and energy efficiency and compare it with the traditional omni-directional ones. Firstly, we introduce our simulation scenarios. Then, we exhibit two kinds of results: *(i)* the number of links (hops) for both OAs and DAs schemes, and *(ii)* the performance in terms of packets loss, throughput, energy consumption and energy efficiency.

9.3.1 Simulation Scenarios

We simulate a WiFi mesh network composed of N nodes equipped with DAs, organized on two different topologies: chain and grid using ns-3.

Each node is equipped with M equal-size and non-overlapping sectors of beamwidth $\frac{2\pi}{M}$, where $M \in \{1, 2, 4\}$. Nodes are spaced by 200m x 200m in the x-axis and y-axis. The Optimized Link State Routing (OLSR) [35] protocol is used to route packets from the source to the destination. The RTS/CTS are exchanged directionally. For each flow, a Constant Bit Rate (CBR) traffic of 68 Kbps is generated by a source which matches to a voice traffic plus signaling overhead rate. The transmission power is set to 16.02dBm (40mW). The antenna gains are: 0dB, 1.5dB and 3dB for the omni, 2-beams and 4-beams DAs, respectively. The other simulation parameters are summarized in table 9.1.

As our case study is a local backhaul based on wireless mesh network to connect outdoor multimode femtocells to a remote base station, we consider two different scenarios: *(i) 1-Source/N-Destinations*, to simulate the downlink transmissions between the edge gateway to the mesh WiFi boxes, and *(ii) N-Sources/1-Destination*which is sthe uplink transmissions, i.e., from the mesh boxes to the gateway. In our simulation scenarios, the position of the gateway is either at the center or at the edge of the mesh network, since the aim is to extend the coverage of the cellular

Parameters	Values
Simulation time	1000 s
Packet size	1024 Bytes
Inter-packet interval	0.117s
Inter-node distance	200m
Y-axis distance	200m
Propagation Loss Model	Log distance ($\alpha = 3$)
Antenna gains	0dB, 1.5dB and 3dB

Table 9.1: Simulation parameters.

macro base station. The source(s) and destination(s) nodes are specified as follows:

For the grid topology:

- *1-Source/N-Destinations*: the source located at the top left corner of the grid and the remaining nodes are the (N-1) destinations (nodes {2,...,N}).
- *N-Sources/1-Destination*: the destination at the lower right corner (node N) receives data from the remaining source nodes (nodes {1,...,N-1}).

For the chain topology:

- *1-Source/N-Destinations*: the source is the first node of the chain and the remaining nodes are the (N-1) destinations (nodes {2,...,N}).
- *N-Sources/1-Destination*: the destination is last node of the chain and it receives data from the remaining source nodes (nodes {1,...,N-1}).

9.3.2 Performance Metrics

In this work, we evaluate five performance metrics: the Mean Loss Ratio (MLR), the Mean Collision Ratio (MCR), the throughput (R), the consumed energy (EC) and Energy Efficiency (EE).

Let A_i be the number of packets transmitted by node i, B_i be the number of packets received by the gateway from node i and C_i be the number of retransmitted packets by node i. Then, we define:

- *Mean Loss Ratio (MLR)*:

$$\text{MLR} = 1 - \frac{\sum_i \frac{B_i}{A_i}}{N-1} \tag{9.0}$$

  It is computed at the gateway/destination level (taking into account the flow coming *from* each source).

- *Mean Collision Ratio (MCR)*:

$$\text{MCR} = \frac{\sum_i \frac{C_i}{A_i}}{N-1} \tag{9.0}$$

It is evaluated *at* the source level. This metric helps us to see if the DAs reduce collisions. The smaller MCR is, the better it is.

- *Throughput*: It is computed at the destination node as the average of all flows. The throughput of a given flow is measured as the number of received bytes over the time period between the first and last received bytes (Δt).

We compute the throughput of each flow (each node) at the gateway level using equation (9.3.2) as following

$$R_i = 8 \times \frac{\text{Number of received Packets}}{\Delta t} \times 1024 \ (kbps) \tag{9.0}$$

Then the average rate is computed as the mean rate of all flows:

$$R = \frac{\sum_i R_i}{N-1} \ (kbps) \tag{9.0}$$

- *Consumed Energy*: It measures the mean energy consumed (EC) by all nodes in the networks. The energy consumed by a node is the transmission energy if packets are generated by this node, and the reception plus the forwarding energy otherwise (the node serves as an intermediate node). Let $E_{p,i}$ be the energy consumed when node i sends a packet $p \in \mathcal{P}_i$, where $\mathcal{P}_i$ is the number of packets sent by node i. Then the mean consumed energy is

$$EC = \frac{\sum_{i=1}^{N} \sum_{p \in \mathcal{P}_i} E_{p,i}}{N-1} \ \ (J). \tag{9.0}$$

- *Energy Efficiency*: The energy efficiency (EE) is defined as follows

$$EE = \frac{R}{EC} (Mb/s/J) \tag{9.0}$$

where R is the mean throughput and EC is the mean energy consumption defined in Equations 9.3.2 and 9.3.2, respectively. It reflects the amount of energy consumed for a give throughput. Since capturing the tradeoff between the throughput and the energy consumed is an important task, we consider nodes operating on batteries.

9.3.3 Number of Links (NL)

A route from the source to the destination is composed of one or many links (hops), defined by the routing protocol. In the following, we derive the total number of links for the OAs, 2-beams and a 4-beams networks.

From the routing tables, we compute the total number of links (number of hops) to reach each node in the network for both OAs and DAs networks. Note that, we use OLSR routing protocol which performs shortest path routes.

9.3.3.1 Chain topology

Let consider a chain topology composed of N mesh nodes. The number of links (hops) is given as follows:

- Omni antennas

$$NL_{omni} = N - 1 \tag{9.0}$$

- M-beams antennas

$$NL_{M-beams} = [\frac{N-1}{M}] + a \tag{9.0}$$

where $[x]$ is the integer part of x, and

$$a = \begin{cases} 1, & \text{if } [\frac{N-1}{M}] \notin \mathbb{N} \\ 0, & \text{otherwise} \end{cases} \tag{9.0}$$

9.3.3.2 Grid topology

Let consider a grid of N nodes, where $\sqrt{N} \in \mathbb{N}^* \backslash \{1, 2\}$. $\sqrt{N}$ is the number of nodes on the grid edge ($\sqrt{N}$=3 for the example in Fig. 9.4). The number of links is defined as following for both OAs and DAs.

- Omni antennas

$$NL_{omni}^{(\sqrt{N})} = 2\sqrt{N} \sum_{i=0}^{\sqrt{N}-1} i \tag{9.0}$$

- 2 beams antennas

$$NL_{2b}^{(\sqrt{N})} = \sqrt{N}(\sqrt{N}-1) + \sum_{k=1}^{\sqrt{N}-1} \left[(\sqrt{N}-k)(\sqrt{N}-k-1) + \sum_{j=1}^{k} (\sqrt{N}-j) \right]$$

- 4 beams antennas We derive the number of links of a 4-beams DAs network considering the three possible cases: $\sqrt{N} = 3k$, $\sqrt{N} = 3k+1$ and $\sqrt{N} = 3k+2$, where $k \in \{0, 1, 2, .., \left[\frac{\sqrt{N}}{3}\right]+1\}$. k is used to re-write values that $\sqrt{N}$ takes and help to find general expressions of NL. For $k = 0$, $\sqrt{N}$ takes values 1, 2 or 3 where it corresponds to a 1, 4 or 9 grid network sizes, respectively. For $k = 1$, $\sqrt{N}$ takes values of 4, 5 and 6 and so on. If

  - $\underline{\sqrt{N} = 3k}$

$$NL_{4b}^{(3k)} = NL_{4b}^{(3k-1)} + 2k + \left(\left[\frac{\sqrt{N}}{2}\right] \times \left[2\sqrt{N} - 1\right]\right) \tag{9.-1}$$

  - $\underline{\sqrt{N} = 3k + 1}$

$$NL_{4b}^{(3k+1)} = NL_{4b}^{(3k)} + (2k \times 5) + \left(2\left[\frac{\sqrt{N}}{2}\right] \times (\sqrt{N} - 3)\right)$$

  - $\underline{\sqrt{N} = 3k + 2}$

$$NL_{4b}^{(3k+2)} = NL_{4b}^{(3k+1)} + 3 \times (2k + 1) + \left(2\left[\frac{\sqrt{N}}{2}\right] \times (\sqrt{N} - 2)\right)$$

From the above NL equations, we can conclude that increasing the number of beams can reduce the number of links.

$$NL_{4b}^{(3k+2)} < NL_{4b}^{(3k+1)} < NL_{4b}^{(3k)} < NL_{2b}^{(\sqrt{N})} < NL_{omni}^{(\sqrt{N})} \tag{9.-3}$$

We use proof by induction (on the number of nodes on the grid edge) to prove equations (9.3.3.2-9.3.3.2).

For the grid topology, we consider a grid of size N, and $\sqrt{N} \in \mathbb{N}^* - \{1, 2\}$:

- The number of links in the omni scheme is

$$NL_{omni} = 2\sqrt{N} \sum_{i=0}^{\sqrt{N}-1} i \tag{9.-3}$$

- For the 2 beams antennas we have

$$NL_{2b}^{(\sqrt{N})} = \sqrt{N}(\sqrt{N}-1) + \sum_{k=1}^{\sqrt{N}-1}\left[(\sqrt{N}-k)(\sqrt{N}-k-1) + \sum_{j=1}^{k}(\sqrt{N}-j)\right] \quad (9.\text{-}3)$$

- For the 4 beams antennas: For $k \in \{0,1,2,..,\left[\frac{\sqrt{N}}{3}\right]+1\}$, we derive the number of links of a 4beams DAs network considering the three possible cases: $\sqrt{N} = 3k$, $\sqrt{N} = 3k+1$ and $\sqrt{N} = 3k+2$.

  if

  - $\underline{\sqrt{N} = 3k}$

$$NL_{4b}^{(3k)} = NL_{4b}^{(3k-1)} + 2k + \left(\left[\frac{\sqrt{N}}{2}\right] \times \left[2\sqrt{N}-1\right]\right) \quad (9.\text{-}3)$$

  - $\underline{\sqrt{N} = 3k+1}$

$$NL_{4b}^{(3k+1)} = NL_{4b}^{(3k)} + (2k \times 5) + \left(2\left[\frac{\sqrt{N}}{2}\right] \times (\sqrt{N}-3)\right) \quad (9.\text{-}3)$$

  - $\underline{\sqrt{N} = 3k+2}$

$$NL_{4b}^{(3k+2)} = NL_{4b}^{(3k+1)} + (2k+1) \times 3 + \left(2\left[\frac{\sqrt{N}}{2}\right] \times (\sqrt{N}-2)\right) \quad (9.\text{-}3)$$

  It can be seen that

$$NL_{4b}^{(3k+2)} < NL_{4b}^{(3k+1)} < NL_{4b}^{(3k)} < NL_{2b}^{(\sqrt{N})} < NL_{omni} \quad (9.\text{-}3)$$

That is the number of links in a OAs network are higher than the number of links in a DAs network.

Proof 4 *We use recurrence (induction) to proof equations (9.3.3.2-9.3.3.2)*

- *For the case of $\sqrt{N} = 3$ the above expressions of NLs are valid.*

- *Let suppose that the equations bellows are verified for a network of size N and proof that they are valid with a network of size $(\sqrt{N}+1)^2$.*

  <u>2-beams networks</u>

$$
\overbrace{
\begin{array}{cccccccccc}
(\sqrt{N}-1) & (\sqrt{N}-1) & & & & \cdots & \cdots & (\sqrt{N}-1) & (\sqrt{N}-1) & (\sqrt{N}-1) \\
(\sqrt{N}-2) & (\sqrt{N}-2) & & & & \cdots & \cdots & (\sqrt{N}-2) & (\sqrt{N}-2) & (\sqrt{N}-1) \\
(\sqrt{N}-3) & (\sqrt{N}-3) & & & & \cdots & \cdots & (\sqrt{N}-3) & (\sqrt{N}-2) & (\sqrt{N}-1) \\
\vdots & & & & & \vdots & & & & \vdots \\
\vdots & & & & & \vdots & & & & \vdots \\
2 & 2 & 2 & 3 & 4 & \cdots & \cdots & (\sqrt{N}-3) & (\sqrt{N}-2) & (\sqrt{N}-1) \\
1 & 1 & 2 & 3 & 4 & \cdots & \cdots & (\sqrt{N}-3) & (\sqrt{N}-2) & (\sqrt{N}-1) \\
0 & 1 & 2 & 3 & 4 & \cdots & \cdots & (\sqrt{N}-3) & (\sqrt{N}-2) & (\sqrt{N}-1)
\end{array}
}^{\sqrt{N}}
$$

(left brace labelled $\sqrt{N}$)

The bellow matrix, the link matrix, shows the number of links to each node for the 2beams network. The total number of links is the sum of all the matrix coefficients.

$$
\overbrace{
\begin{array}{ccccccccc}
\color{red}{\sqrt{N}} & \color{red}{\sqrt{N}} & & & \cdots & \color{red}{\sqrt{N}} & \color{red}{\sqrt{N}} & \color{red}{\sqrt{N}} & \color{red}{\sqrt{N}} \\
(\sqrt{N}-1) & (\sqrt{N}-1) & & & \cdots & (\sqrt{N}-1) & (\sqrt{N}-1) & (\sqrt{N}-1) & \color{red}{\sqrt{N}} \\
(\sqrt{N}-2) & (\sqrt{N}-2) & & & \cdots & (\sqrt{N}-2) & (\sqrt{N}-2) & (\sqrt{N}-1) & \color{red}{\sqrt{N}} \\
(\sqrt{N}-3) & (\sqrt{N}-3) & & & \cdots & (\sqrt{N}-3) & (\sqrt{N}-2) & (\sqrt{N}-1) & \color{red}{\sqrt{N}} \\
\vdots & & & & & \vdots & & \vdots & \\
\vdots & & & & & \vdots & & \vdots & \\
2 & 2 & 2 & 3 & \cdots & (\sqrt{N}-3) & (\sqrt{N}-2) & (\sqrt{N}-1) & \color{red}{\sqrt{N}} \\
1 & 1 & 2 & 3 & \cdots & (\sqrt{N}-3) & (\sqrt{N}-2) & (\sqrt{N}-1) & \color{red}{\sqrt{N}} \\
0 & 1 & 2 & 3 & \cdots & (\sqrt{N}-3) & (\sqrt{N}-2) & (\sqrt{N}-1) & \color{red}{\sqrt{N}}
\end{array}
}^{\sqrt{N}+1}
$$

(left brace labelled $\sqrt{N}+1$)

The red $\sqrt{N}$ ones are the new number of new links for the $\sqrt{N}+1 \times \sqrt{N}+1$ topology. The amount of new links is $\sqrt{N}(\sqrt{N}+1)+(\sqrt{N}\times\sqrt{N})$

Let suppose that equation (9.3.3.2) is valid for $m=\sqrt{N}$ and let us show that it is valid for $m+1$. That is, suppose that

$$NL_{2b}^{\sqrt{N}} = \sqrt{N}(\sqrt{N}-1) + \sum_{k=1}^{\sqrt{N}-1}\left[(\sqrt{N}-k)(\sqrt{N}-k-1) + \sum_{j=1}^{k}(\sqrt{N}-j)\right] \tag{9.-3}$$

and show that

$$NL_{2b}^{(\sqrt{N}+1)} = \sqrt{N}(\sqrt{N}+1) + \sum_{k=1}^{\sqrt{N}} \left[(\sqrt{N}-k+1)(\sqrt{N}-k) + \sum_{j=1}^{k} (\sqrt{N}-j+1) \right] \tag{9.-3}$$

For a network of size m+1, ($(\sqrt{N}+1)^2$ nodes), the link matrix is as follows:

$$\begin{aligned}
NL_{2b}^{(\sqrt{N}+1)} &= \sqrt{N}(\sqrt{N}+1) + \sum_{k=1}^{\sqrt{N}} \left[(\sqrt{N}-k+1)(\sqrt{N}-k) + \sum_{j=1}^{k} (\sqrt{N}-j+1) \right] \\
&= \sqrt{N}(\sqrt{N}+1) + \sum_{k=0}^{\sqrt{N}-1} \left[(\sqrt{N}-k)(\sqrt{N}-k-1) + \sum_{j=1}^{k+1} (\sqrt{N}-j+1) \right] \\
&= \sqrt{N}(\sqrt{N}+1) + \sum_{k=0}^{\sqrt{N}-1} \left[(\sqrt{N}-k)(\sqrt{N}-k-1) + \sum_{j=0}^{k} (\sqrt{N}-j) \right] \\
&= \sqrt{N}(\sqrt{N}+1) + \sum_{k=0}^{\sqrt{N}-1} \left[(\sqrt{N}-k)(\sqrt{N}-k-1) + \sum_{j=1}^{k} (\sqrt{N}-j) + \sqrt{N} \right] \\
&= \sqrt{N}(\sqrt{N}+1) + \sum_{k=0}^{\sqrt{N}-1} \left[(\sqrt{N}-k)(\sqrt{N}-k-1) + \sum_{j=1}^{k} (\sqrt{N}-j) \right] + \sqrt{N}\sqrt{N} \\
&= \sqrt{N}(\sqrt{N}+1) + (\sqrt{N}-1)\sqrt{N} \\
&+ \sum_{k=1}^{\sqrt{N}-1} \left[(\sqrt{N}-k)(\sqrt{N}-k-1) + \sum_{j=1}^{k} (\sqrt{N}-j) \right] + \sqrt{N}\sqrt{N} \\
&= \sqrt{N}(\sqrt{N}+1) + \sqrt{N}\sqrt{N} + NL_{2b}^{(\sqrt{N})}
\end{aligned}$$

Remark 7 *Note that we provide the number of links of node number 1, which is at the opposite corner to the gateway. Funding the number of links to other nodes will follow the same reasoning.*

4-beams networks

In the following, we consider three cases of the edge grid: $\sqrt{N} = 3k$, $\sqrt{N} = 3k+1$ and $\sqrt{N} = 3k+2$, where $k \in \{0, 1, 2, .., \left[\frac{\sqrt{N}}{3}\right] + 1\}$.

These cases are considered taking into account the number of links of each network size. In a way to find general formulas for the number of links.

The next matrix represents the number links for the 4-beams DAs network.

$2k$	$2k$			$\cdots$	$2k$	$2k$	$2k+1$	$2k+1$	$2(k+1)$
$2k$	$2k$			$\cdots$	$2k$	$2k$	$2k+1$	$2k+1$	$2k+1$
$2k$	$2k$			$\cdots$	$2k-1$	$2k-1$	$2k$	$2k+1$	$2k+1$
$2k-1$	$2k-1$			$\cdots$	$2k-1$	$2k$	$2k-1$	$2k$	$2k+1$
$2k-1$	$2k-1$			$\cdots$	$2k-1$	$2k-1$	$2k-1$	$2k$	
$\vdots$					$\vdots$		$\vdots$		
$\vdots$					$\vdots$		$\vdots$		
2	2	2	2	$\cdots$	$2k-1$	$2k-1$	$2k-1$	$2k$	$2k+1$
1	1	2	2	$\cdots$	$2k-1$	$2k-1$	$2k-1$	$2k$	$2k+1$
1	1	1	2	$\cdots$	$2k-2$	$2k-1$	$2k-1$	$2k$	$2k+1$
0	1	1	2	$\cdots$	$2k-2$	$2k-1$	$2k-1$	$2k$	$2k+1$
						k			$k+1$

We define the *link utilization* of a given scheme as:

$$LU_{scheme} = \frac{\#\text{ links of the scheme}}{\#\text{links of the OAs}} \tag{9.-4}$$

The smallest LU_{scheme} is, the lowest is the number of links for the considered scheme and hence, the better are the performance.

9.3.3.3 Example

In the following, we give an example of a 4×4 grid topology.

Antennas	NLs
Omni	42
2 beams	34
4beams	12

Figure 9.1: Number of Links for a 4×4 grid topology.

9.3.3.4 Distance between nodes

Not that we provided the number of links of each topology based on a given (fixed) distance nodes (200m). In the following, we study the maximum distance between two nodes above it no communication is possible. Table 9.2 presents these maximum distances for an OA, 2beams and 4beams DAs for a given antenna gain.

Antennas	Antenna Gain	$d_{max}(m)$
Omni	0 dB	215
2 beams	1.5dB	290
4beams	3dB	460

Figure 9.2: Maximum communication distances between nodes for different antennas beams.

9.4 Numerical Results

In this section, we first discuss the impact of DAs on routes and the number of links in the networks. Then, we present and analyze the simulation results.

9.4.1 Mesh topology

Derived from the routing table of the nodes, Fig. 9.3 and 9.4 show that the routes are used to transmit packets from the source (node 1) to a given destination for the chain and grid topologies, respectively.

For the chain topology, we observe from Fig. 9.3 that all paths in the omnidirectional case are one hop. 2-hops paths appear when we use 2-beams antennas. With 4-beams antennas, we can reach 3-hops nodes directly.

Links for a 3×3 grid topology are shown in Fig. 9.4. For the OAs, a flow from a source (node 1) to a destination (node 9) goes through three intermediate nodes (nodes 2, 3, 6) using 4 links (red arrows). When 2-beams DAs are used only two intermediate nodes are used (nodes 5, 8) considering 3 links (red arrows), whereas only one relay (node 6) is used in case of 4-beams through two links.

The LU of Eq. (9.3.3.2) for the 2-beams DAs network is $\frac{3}{4}$ and $\frac{1}{2}$ for the 4-beams DAs network. Compared to an OAs network, the number of links is reduced by 75% for the 2-beams network and 50% for the 4-beams network.

9.4.2 Performance discussion

In the following, we show the impact of both DAs, network size and network load on throughput, mean loss, energy consumption and energy efficiency.

For all the considered scenarios, the 4-beams antennas setting offers better network performance in terms of mean loss, collision, energy consumption and throughput, followed by the 2-beams antennas network, and then the OAs network. In fact, the more the antennas are directive and the narrower the beamwidth is, the performance is better as shown in Fig. 9.3 and 9.4. A packet visits a high number of intermediate nodes between the source and the destination, to reach the destination using OAs. This requires additional forwarding energy from the nodes lying between the source and destination. Furthermore, as the beamwidth size is 2π, the packets are transmitted

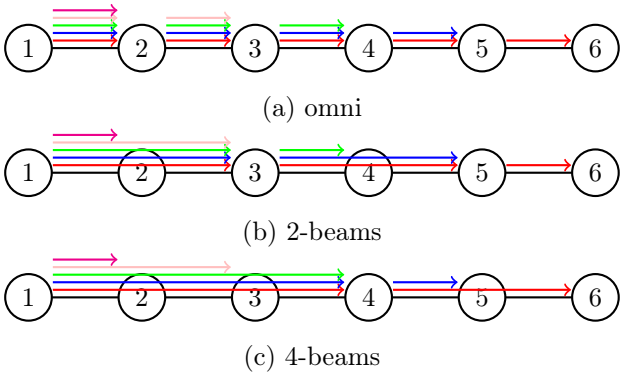

Figure 9.3: Routes from node 1 to nodes in the network - 6 nodes chain topology.

in all directions increasing the collisions probability, as shown in Fig. 9.5.

For the 2-beams and 4-beams antennas, the number of intermediate nodes is reduced due to the extended coverage range of DAs and furthest neighbors in the routing path can be reached directly. This is justified by Eq. (9.3.3.2) which shows that the number of links decreases by increasing the number of beams.

9.4.2.1 Mean Collision and Loss Ratios

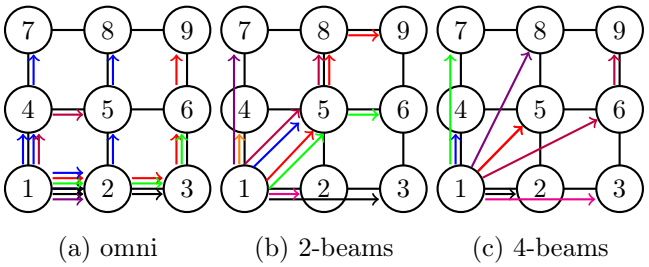

Figure 9.4: Routes from node 1 to nodes in the network - (3×3) Grid.

In Fig. 9.5 we show the histograms of the mean loss (MLR) and collision (MCR) ratios defined in Eq. (9.3.2) and (9.3.2), respectively, for different network sizes for the grid topology. Both these ratios are increasing with the number of nodes. Furthermore, the OAs have the highest MCR and MLR followed by the 2-beams and then the 4-beams. Moreover, the MCR is higher than the MLR for all network sizes because when a collision occurs the packet is retransmitted until the maximum number of retransmissions, then it will be considered as a lost packet.

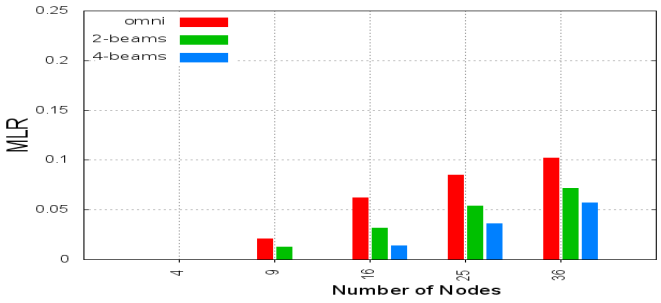

(a) MLR.

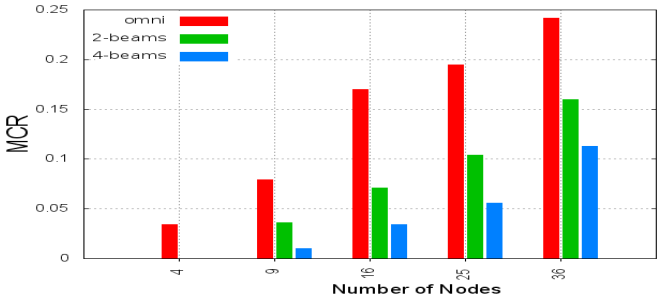

(b) MCR.

Figure 9.5: Mean loss and collision ratios for the grid topology.

9.4.2.2 Impact of the sending rate

The next presented results are the average over 20 simulation runs with 95% of confidence interval.

System load can be increased either by increasing the bit rate of individual flows or the number of flows per node. Fig. 9.6 shows the impact of the sending rate on network performance. We vary the sending rate in the range [50, 850 kbps]. The throughput shown in 9.6a is increasing until it reaches a maximum value, then it starts decreasing. This maximum value corresponds to the maximum network load for each scheme. Furthermore, increasing the number of beams increases the maximum network load. In other words, when using DAs the network saturation is reached for higher network loads. In Fig. 9.6b we show the energy consumption while varying the network load. Increasing the network load increases the mean energy consumed by the network. This is because increasing the load causes network collisions which require packets retransmission. Additionally, after reaching the network capacity, the consumed energy continue growing. This is explained by the retransmission activity of the collided packets under the saturated regime.

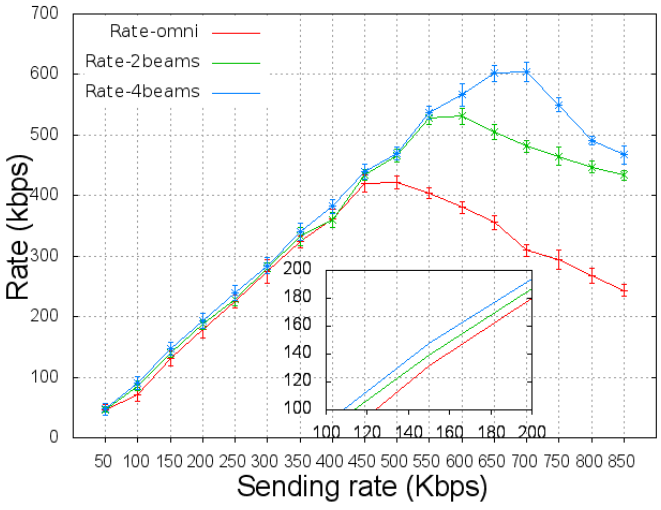

(a) Throughput

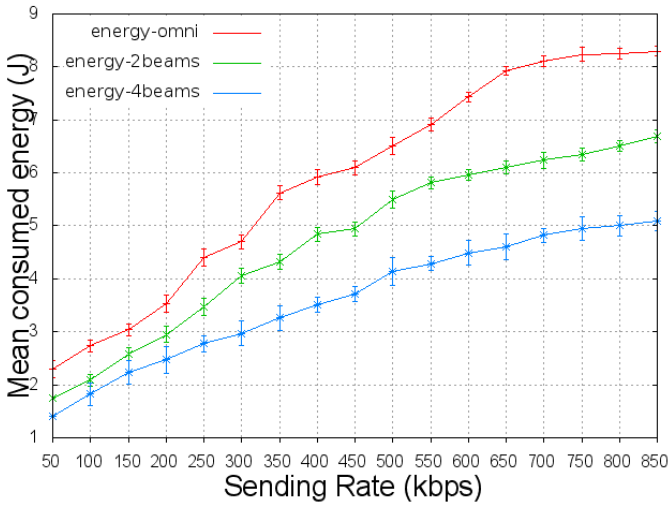

(b) Energy

Figure 9.6: Mean rate vs load for the grid topology (16 nodes).

9.4.2.3 Impact of number of nodes

The average consumed energy is shown in Figs. 9.8a-9.7a and 9.9a-9.10a, and the mean throughput in Figs. 9.8b-9.7b and 9.9b-9.10b for the grid and chain topologies, respectively, for the three considered scenarios. For the grid topology, increasing the number of nodes in the network results in an increase of the mean energy consumed by nodes, and a decrease of the receiving throughput. In fact, when the network size gets larger, the network faces congestion phenomena and the probability

of collision increases leading to packet retransmissions and increase of energy consumption. For the chain topology, the mean energy consumed increases until reaching a maximum value and then it decreases. In fact, a high amount of collisions occurs on nodes near to the source node and nodes in the vicinity of the destination node (last nodes on the chain) have less activity, therefore consume less energy.

We define the gain of energy of a given scheme as follows:

$$G_{\text{scheme}} = \frac{\text{EC}_{\text{omni}} - \text{EC}_{\text{scheme}}}{\text{EC}_{\text{omni}}} \tag{9.-4}$$

Table 9.2 summarizes the energy consumption gains which can be reached for each scenario, topology and scheme.

	Grid		Chain	
	1-N	N-1	1-N	N-1
2-beams	44%	27%	12%	20%
4-beams	46%	71%	43%	30 %

Table 9.2: Energy consumption gains of the 2-beams and 4-beams antennas for chain and grid topologies.

It can be seen from Table 9.2 that the gains of grid topology are much higher than those of chain topology, as the former one has more spatial diversity hence, more possible routes.

Note that, for the OAs network, the energy consumed by the *N-Sources/1-Destination* scenario is higher than the one consumed by the *1-Source/N-Destination* scenario. In fact, for the *N-Sources/1-Destination* scenario, unlike the *1-Source/N-Destination* scenario where intermediate nodes have only a forwarding activity, nodes have also a transmission activity.

9.4.2.4 Energy Efficiency

In the considered network setting, nodes operate on batteries, and reduce the consumed energy while ensuring a given throughput is an important task. Energy efficiency is a metric representing tradeoff between the consumed energy and the throughput.

In Figs. 9.7c-9.8c and 9.9c-9.10c, we show the energy efficiency for different network sizes for the grid and chain topologies, respectively.

The EE reaches 50 Mb/s/J for a 4-beams grid and chain topologies. It is a decreasing function of number of nodes.

In fact, as shown in Figs. 9.5a and 9.5b increasing the network size induces more collisions and hence packet retransmissions which require additional energy consumption. In other words, increasing the number of nodes reduces EE because the nodes consume more energy to retransmit

the collided packets and the useful throughput of the network is low. Furthermore, the more the antennas are directive, the better the EE is because as investigated in the two last subsections, increasing the number of beams improves the throughput and reduces the energy consumption of the network.

	Grid		Chain	
	1-N	N-1	1-N	N-1
2-beams	6×	2×	2×	5×
4-beams	8×	3×	4×	14×

Table 9.3: Energy Efficiency improvements of the 2-beams and 4-beams antennas for chain and grid topologies.

In Table 9.3 we show the influence of DAs on EE improvement. It can be seen that EE can be improved 14 times for the *N-Sources/1-Destination* chain scenario and 8 times for the *1-Source/N-Destinations* grid scenario.

9.4.2.5 Impact of Gateway placement

In the following, we change the gateway placement and study the impact of the placement on the network performance.

We consider a 5×5 grid and the *N-Sources/1-Destination* scenario where all nodes send traffic the gateway placed at the grid center (node number 13).

It can be shown that placing the gateway in a strategic position, the center, improves the network performance. This is because, in the corner-case gateway, all the traffic is aggregated to the node which causes high collisions in nodes around the gateway and leads to low throughput and high energy consumption. However traffic comes from nodes around the gateway and produces less collisions, in the center-case gateway.

9.5 Conclusion

In this chapter, we consider a wireless mesh network to act as a local backhaul network to cover rural and remote villages. The shortage of energy in these settlements motivates the optimization of the energy consumption of the wireless backhaul network. Therefore, we propose to use Directional Antennas (DAs) to improve the throughput and the network energy consumption. We study the impact of DAs on the topology of the WMN and on several performance criteria: mean loss ratio, throughput, energy consumption and energy efficiency. We consider two main scenarios to model the downlink and uplink communications to a cellular gateway. Concerning the topology of the wireless mesh network, we show that using directional antennas reduces the number of hops to

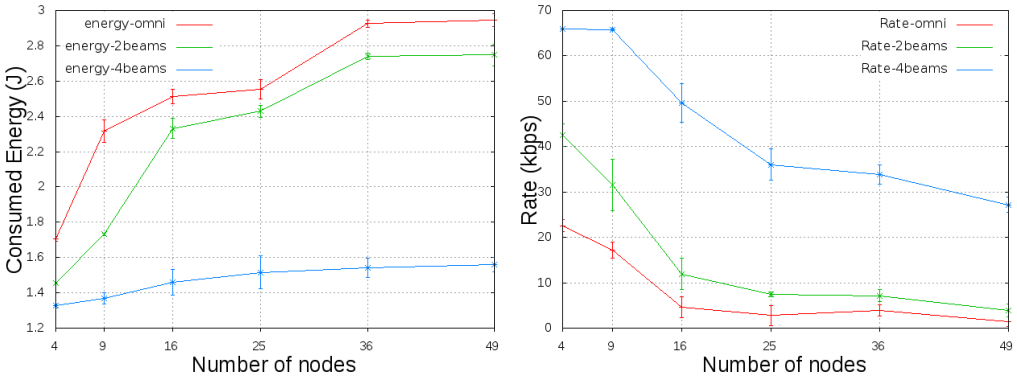

(a) Consumed Energy

(b) Throughput

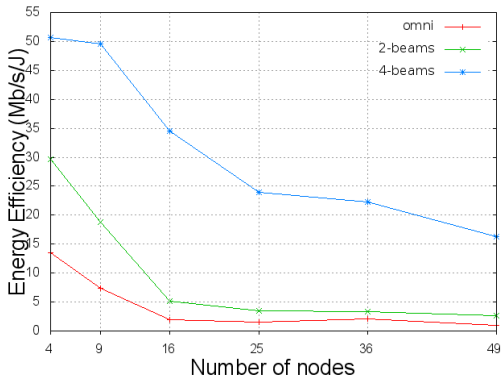

(c) Energy Efficiency

Figure 9.7: *N-Sources/1-Destination* - Grid topology (vs Number of nodes).

reach the desired destination. Concerning the loss ratio and the network throughput, they are improved with the use of DAs, especially for 4-beams, in all scenarios. Concerning the energy efficiency, DAs improve the energy efficiency and throughput for all considered scenarios. Indeed, for the grid topology the energy consumption is improved by 71% for the a 4-beams network and by 43% for a 2-beams network. For the chain topology, it reaches 43% and 20% for the 4-beams and 2-beams, respectively. Additionally, energy efficiency is improved up to 14 times by using 4-beams DAs and up to 6 times using 2-beams DAs. Furthermore, increasing the number of beams improves the maximum network load because DAs enhances the spatial diversity by adding new links and reducing collisions.

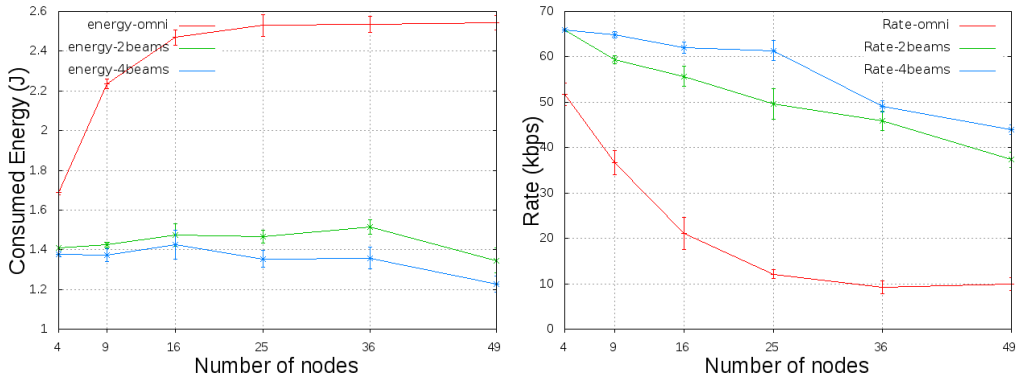

(a) Consumed Energy

(b) Throughput

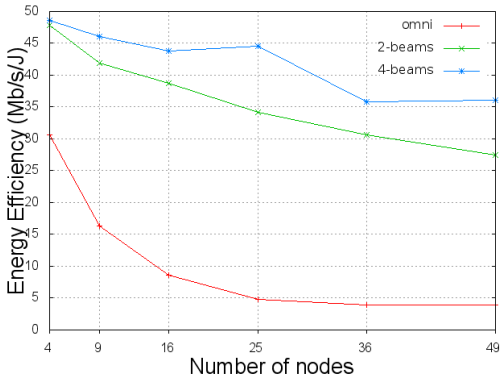

(c) Energy Efficiency

Figure 9.8: *1-Source/N-Destinations* - Grid topology (vs Number of nodes).

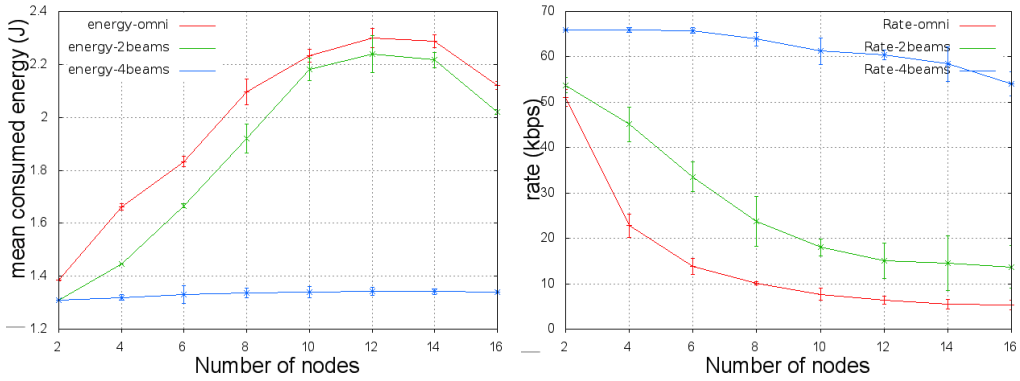

(a) Consumed Energy

(b) Throughput

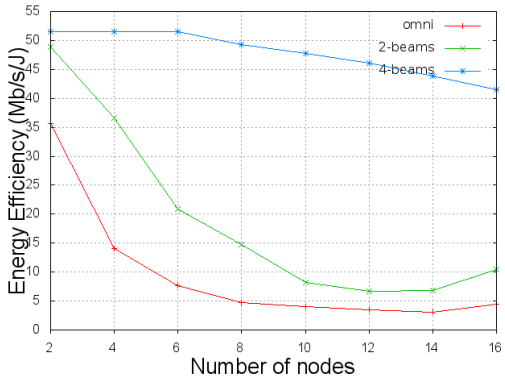

(c) Energy Efficiency

Figure 9.9: *N-Sources/1-Destination* - Chain topology (vs Number of nodes).

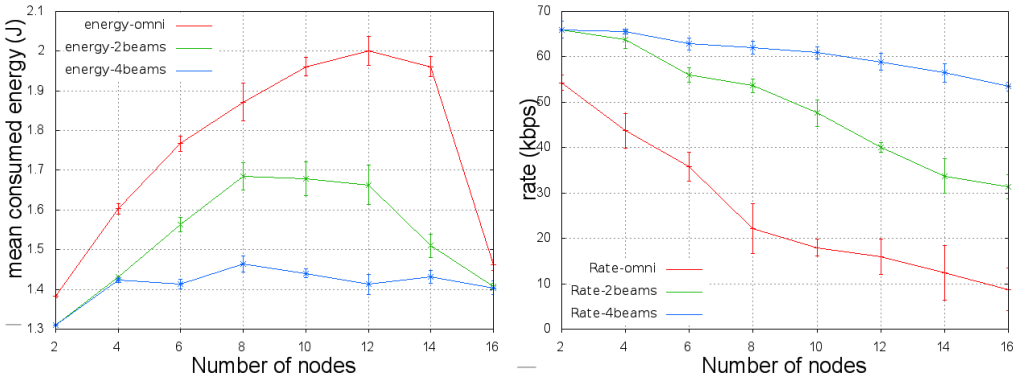

(a) Consumed Energy

(b) Throughput

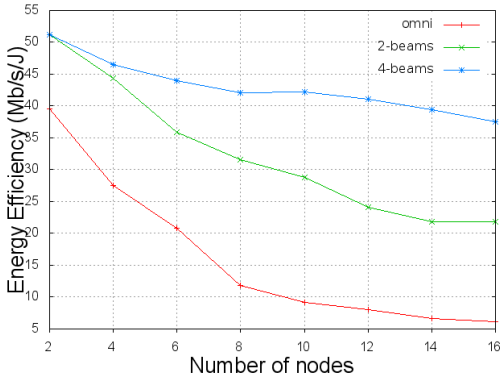

(c) Energy Efficiency

Figure 9.10: *1-Source/N-Destinations* - Chain topology (vs Number of nodes).

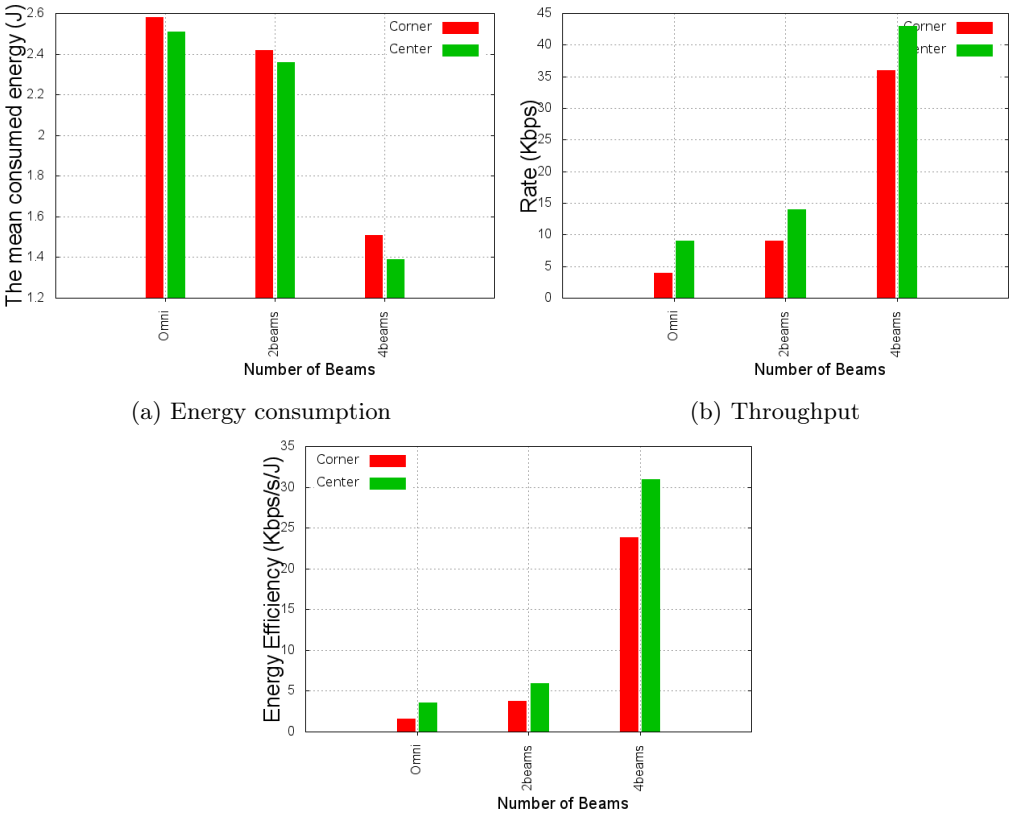

(a) Energy consumption

(b) Throughput

(c) Energy Efficiency

Figure 9.11: *N-Sources/1-Destination* - center vs corner located gateway.

Chapter 10

Joint Optimization of Energy Consumption and Throughput of Directional WMNs

Contents

10.1 Chapter Summary

In this chapter, we propose a new joint optimization framework considering the energy consumption and throughput in directional antennas (DAs) WMNs. In this work we formulate the joint optimization problem as a Mixed Integer Linear Problem (MILP) with a weighted objective function of both the consumed energy and the throughput. We use ILOG Cplex [8], a software based on branch and cut method, to find the optimal solution of the optimization problem.

This chapter is organized as follows. The model is presented in Section 10.3. In Section 10.4, we formulate the joint energy consumption and throughput optimization problem. We outline the objective function and the constraints, then we proceed to linearization of non linear variables. Simulation results are presented in Section 10.5. Finally, we conclude the chapter in Section 10.6.

10.2 Introduction

As investigated in Chapter 7 Wireless Mesh Networks (WMNs) have many benefits and advantages as backhaul networks [13]. WMNs are low cost and easy to deploy, and do not require existing infrastructure. Recently, it has been shown that the mesh backhaul topology is an efficient solution to connect cellular small cell networks [21]. Following the same idea, in this thesis we proposed to use WMNs to connect femtocells to each other and to the remote Macro cell (gateway) connected to the internet [4] as shown in Figure 7.2.

However, in such scenario and especially in rural areas lacking from reliable electricity ressources, reducing the energy consumed by nodes while ensuring a given throughput is an important task.

In this direction, Directional Antennas (DAs) proved their efficiency in terms of improving the network throughput and reducing the consumed energy. As stated in Chapter 8 DAs have the ability to focus the transmission toward the desired receiver, without radiating in all direction as omni Directional Antennas (OAs). DAs technology has many advantages for WMNs such as improving the transmission range. Indeed farthest nodes can be reach thanks to the high antenna gain of DAs. Furthermore, spatial reuse is improved and concurrent transmissions can occur without collisions. Additionally, as demonstrated in the last chapter, the more antennas are directive, the less number of links is. Hence, packets transit through few intermediate hops to arrive to the destination.

In this chapter, we aim at finding a balance between the consumed energy and the throughput using tools from optimization theory. To the best of our knowledge no previous work models DAs networks using optimization tools in order to optimize jointly the energy consumption and the throughput. Previous work were limited to OAs networks [16, 93, 106] and throughput optimization in DAs networks [94].

10.3 System Model

10.3.1 Interference Model

Various interference models have been used in OAs considering either the locations of nodes or the received power as a metric to characterize the interference. However, these models are not valid in DAs networks, since (i) some directions are free of interference because DAs radiate only toward a given direction and (ii) DAs can reach farther nodes since the directional range is extended.

In this work we consider a new interference model by combining the ones used in [65] to compute the overlap count representing the number of overlaps between beams, and in [57, 108] to insure a minimum distance between nodes. It takes into account the position and distance between nodes.

Let (i, j) and (p, q) two pairs of transmitting-receiving nodes, at positions (X_i, X_j) and (X_p, X_q), respectively. Communications between pairs (i, j) and (p, q) can occur simultaneously, without generating interference, if and only if

$$\mid X_p - X_j \mid \geq (1 + \nu) \mid X_i - X_j \mid \tag{10.0}$$

$$(X_i\widehat{X_j, X_i}X_p) \geq \gamma \quad \text{and} \quad (X_p\widehat{X_q, X_p}X_i) \geq \gamma \tag{10.0}$$

where $\mid . \mid$ is the euclidean distance, γ is a threshold angle and ν models a guard zone to prevent a neighbouring node from transmitting at the same time.

Hence, the set of interferers to the communication between nodes i and j is defined as follows:

$$\mathbb{I}_{(i,j)}^{(p,q)} = \{(p, q) \in \mathcal{I}^2 \text{ s.t. Eq. (10.3.1) and Eq. (10.3.1) are not verified}\} \tag{10.0}$$

10.3.2 Energy Model

In this work, we consider that each node have three state, either (i) transmitting, (ii) receiving, or (iii) idle. A node is in an active state, transmitting or receiving if it has some packets to forward or receive, receptively. Otherwise, it goes to the idle state.

10.3.3 Power Control scheme

We consider that each node has many transmission levels $\mathcal{L} = \{1, ..., \mid \mathcal{L} \mid\}$ available to use depending on the location of the next hop. In this way, energy can be saved.

Lets consider that a node have three power level, either transmitting at full power (P_{max}), at $\frac{P_{max}}{2}$, or not transmitting 0, and suppose that the next hop is close and can be reached using $\frac{P_{max}}{2}$, therefore $\frac{P_{max}}{2}$ of power is saved.

10.4 Problem formulation

In this section we define the optimization problem. Firstly, we start by presenting variables and parameters, then we introduce the objective function followed by the problem constraints. We conclude the section by linearizing the non linear variables.

10.4.1 Variables and Parameters

In the following, we presents the sets and parameters used in the optimization problem.

Sets:

- $\mathcal{I} = \{1, ..., \mid \mathcal{I} \mid\}$: the set of nodes.
- $\mathcal{G} = \{g_1, ..., g_n\}$ the set of mesh getaways in the network.
- $\mathcal{U} = \{1, ..., \mid \mathcal{U} \mid\}$ the set users generating the traffic.
- $\mathcal{L} = \{1, ..., \mid \mathcal{L} \mid\}$ set of possible power level that can be used by a node.

Parameters & Input:

- Let c_{ij} be the capacity of the link between node i and j.
- Each user have a amount of traffic to send at time t, $d_{i,t}$.
- Each user is connected to its nearest AP (MR).

Binary variables:

- $x^{l,L}_{u,ij,t}$ is used to express the linking between two nodes and the beams used in communication at time t:

$$x^{l,L}_{u,ij,t} = \begin{cases} 1 & \text{if } \begin{array}{c}\text{node } i \text{ and node } j \text{ are connected with beam } l \text{ at transmission} \\ \text{power level } L \text{ at time } t \text{ to forward traffic of user } u\end{array} \\ 0 & \text{otherwise} \end{cases} \tag{10.0}$$

- The binary variable $a^{l,L}_{i,t}$ describes if node i is transmitting at time t using beam l at power level L.

$$a^{l,L}_{i,t} = \begin{cases} 0 & \text{if } \sum_{j=1}^{|\mathcal{I}|} \sum_{u=1}^{|\mathcal{U}|} \sum_{l=1}^{|\mathcal{B}_i|} x^{l,L}_{u,ij,t} = 0 \\ 1 & \text{otherwise} \end{cases} \qquad \forall i \in \mathcal{I}, \quad t \in [0, T], \quad l \in \mathcal{B}_i, \quad L \in \mathcal{L} \tag{10.0}$$

- $b_{i,t}$ is to indicate if node i is receiving at time t.

$$b_{i,t} = \begin{cases} 0 & \text{if} \quad \sum_{u=1}^{|\mathcal{U}|} \sum_{k=1}^{|\mathcal{I}|} \sum_{l=1}^{|\mathcal{B}_i|} \sum_{L=1}^{|\mathcal{L}|} x_{u,ki,t}^{l,L} = 0 \\ 1 & \text{otherwise} \end{cases} \qquad \forall i \in \mathcal{I}, \quad t \in [0,T] \tag{10.0}$$

- $c_{i,t}$ is to indicate that node i is on the idle state at time t.

$$c_{i,t} = \begin{cases} 1 & \text{if} \quad \text{If node } i \text{ is at } idle \text{ state at time t} \\ 0 & \text{otherwise} \end{cases} \tag{10.0}$$

- $u_{li,t}$ is for user association.

$$u_{li,t} = \begin{cases} 1 & \text{if} \quad \text{If user } l \text{ is attached to node } i \text{ at time slot t} \\ 0 & \text{otherwise} \end{cases} \tag{10.0}$$

Note that, to reduce the complexity of the neighbor discovery process and the optimization problem, we consider that reception is omnidirectional.

10.4.2 Objective function

Parametrized objective function is a weighted function which captures the impact of the consumed energy and the throughput.

A node can be in three possible states: either (i) transmitting, or (ii) receiving or, (iii) idle. Therefore, the total energy consumed by this node depends on the state of the node on the considered time interval ([1,T]).

The energy consumed by node i can be written as:

$$\mathcal{P}_{i,t} = \underbrace{\sum_{l=1}^{|\mathcal{B}_i|} \sum_{L=1}^{|\mathcal{L}|} a_{i,t}^{l,L} \mathcal{P}_{\mathrm{TX},L}}_{\substack{\text{Energy consumed when node } i \\ \text{is transmitting at powre level L}}} + \underbrace{b_{i,t} \mathcal{P}_{\mathrm{RX}}}_{\substack{\text{Energy consumed} \\ \text{if node } i \text{ is receiving}}} + \underbrace{\left(1 - \sum_{l=1}^{|\mathcal{B}_i|} \sum_{L=1}^{|\mathcal{L}|} a_{i,t}^{l,L}\right) .(1 - b_{i,t}).c_{i,t} \mathcal{P}_{\mathrm{idle}}}_{\substack{\text{Energy consumed} \\ \text{if node } i \text{ is idle}}}$$

where $\mathcal{P}_{\mathrm{TX},L}$ is the energy consumed by an AP when it is transmitting in the directional mode (use one beam) at level L, $\mathcal{P}_{\mathrm{RX}}$ when it is receiving and $\mathcal{P}_{\mathrm{idle}}$ when it is idle.

The total energy consumed in the network is

$$\mathcal{P} = \sum_{t=1}^{T} \sum_{i=1}^{|\mathcal{I}|} \mathcal{P}_{i,t} \tag{10.-1}$$

The throughput can be modelled as:

$$\mathcal{IR} = \frac{\sum_{t=1}^{T} \sum_{i=1}^{|\mathcal{I}|} \sum_{L=1}^{|\mathcal{L}|} \sum_{l=1}^{|\mathcal{B}_i|} a_{i,t}^{l,L}}{T} \tag{10.-1}$$

where $\mathcal{IR}$ stands for Inverse Rate.

Minimizing the time when APs are transmitting and teceiving is equivalent to maximizing the rate.

Eq. (10.4.2) represents the objective function to minimize. It consists on minimizing the energy consumed by the network during the considered period and the network throughput.

$$min\ \alpha\mathcal{P} + (1-\alpha)\mathcal{IR} \tag{10.-1}$$

where $\alpha \in \{0, 1\}$ is a weighted coefficient used to balance the energy consumed and the rate. If $\alpha = 0$ Then we principally maximize the achievable rate and if $\alpha = 1$ we minimize the energy.

Next, we outline constraints of the joint energy consumption and throughput optimization problem.

10.4.3 Constraints

- Link capacity constraint:

$$\sum_{u=1}^{|\mathcal{U}|} x_{u,ij,t}^{m,L} \times d_u \leq c_{i,j}, \qquad \forall (i,j) \in \mathcal{I} \times \mathcal{I},\ \forall u \in \mathcal{U},\ L \in \mathcal{L},\ t \in [0,T], m \in \mathcal{B}_i \tag{10.-1}$$

  Constraint (10.4.3) is to ensure that the traffic on links between nodes i and j do not exceed the total link capacity.

- Flow conservation (at node i):

$$\sum_{u=1}^{|\mathcal{U}|}\sum_{t=1}^{T}\sum_{l=1}^{|\mathcal{L}|}\sum_{j=1}^{|\mathcal{I}|}\sum_{h=1}^{|\mathcal{B}_i|} x_{u,ij,t}^{h,L} = \sum_{u=1}^{|\mathcal{U}|}\sum_{t=1}^{T}\sum_{l=1}^{|\mathcal{L}|}\sum_{j=1}^{|\mathcal{I}|}\sum_{m=1}^{|\mathcal{B}_j|} x_{u,ji,t}^{m,L}$$
$$+\sum_{u=1}^{|\mathcal{U}|} w_{ui}\sum_{t=1}^{T}\sum_{l=1}^{|\mathcal{L}|}\sum_{j=1}^{|\mathcal{I}|}\sum_{m=1}^{|\mathcal{B}_i|} x_{u,ij,t}^{m,L} \qquad \forall i \in \mathcal{I}\backslash\{G\}$$

Constraint (10.4.3) ensures that all the flows entering an intermediate node are forwarded. The left hand side corresponds to the number of flows going from node i, while the right hand side is the number of both flows coming from neighbors of node i and flows generated by the attached users.

- Flow conservation at the gateway:

$$\sum_{t=1}^{T}\sum_{l=1}^{|\mathcal{L}|}\sum_{i=1}^{|\mathcal{I}|}\sum_{m=1}^{|\mathcal{B}_i|} x_{u,ij,t}^{m,L} = 1 \qquad \forall u \in \mathcal{U} \text{ and } \; j =\mid \mathcal{I} \mid +1 \tag{10.-2}$$

Constraint (10.4.3) ensures that all the flows must arrive to the gateway ($\mid \mathcal{I} \mid +1$).

- Interference constraint:

$$x_{u,ij,t}^{m,L} + x_{u',pq,t}^{l,L'}\mathbb{I}_{(i,j)}^{(p,q)} \leq 1$$
$$\forall (i,j),(p,q) \in \mathcal{I}^2,\ (L,L') \in \mathcal{L}^2,\ t \in [0,T]; (u,u') \in \mathcal{U}^2, (m,l) \in \mathcal{B}_i \times \mathcal{B}_p$$

where $\mathbb{I}_{(i,j)}^{(p,q)}$ is the set of interferers defined in Eq.(10.3.1).

- One direction constraint:

$$\sum_{l=1}^{|\mathcal{B}_i|} x_{u,ij,t}^{l,L} \leq 1 \qquad \forall (i,j) \in \mathcal{I}^2, \forall u \in \mathcal{U}, L \in \mathcal{L}, t \in [1,T] \tag{10.-3}$$

- One power level constraint:

$$\sum_{L=1}^{|\mathcal{L}|} x_{u,ij,t}^{l,L} \leq 1 \qquad \forall (i,j) \in \mathcal{I}^2, \forall u \in \mathcal{U}, l \in \mathcal{B}_i, t \in [1,T] \tag{10.-3}$$

Constraints (10.4.3) and (10.4.3) are stated to ensure that an AP can transmit only at one power level, and in one direction in a given time.

- Simultaneous transmissions and receptions constraints:

$$\sum_{u=1}^{|\mathcal{U}|}\sum_{l=1}^{|\mathcal{L}|}\sum_{j=1}^{|\mathcal{I}|}\sum_{m=1}^{|\mathcal{B}_i|} x_{u,ij,t}^{m,L} + \sum_{u=1}^{|\mathcal{U}|}\sum_{l=1}^{|\mathcal{L}|}\sum_{j=1}^{|\mathcal{I}|}\sum_{m=1}^{|\mathcal{B}_i|} x_{u,ji,t}^{m,L} \leq 1 \qquad \forall i \in \mathcal{I} \text{ and } \; t \in [0,T] \qquad \text{(10.-3)}$$

  Constraint (10.4.3) prevents that a node transmits and receives at the same time slot.

- Loops avoidance

$$\sum_{t=1}^{T}\sum_{l=1}^{|\mathcal{L}|}\sum_{j=1}^{|\mathcal{I}|}\sum_{m=1}^{|\mathcal{B}_i|} x_{u,ij,t}^{m,L} \leq 1, \text{ and} \qquad \sum_{t=1}^{T}\sum_{l=1}^{|\mathcal{L}|}\sum_{j=1}^{|\mathcal{I}|}\sum_{m=1}^{|\mathcal{B}_j|}\sum_{n=1}^{|\mathcal{B}_i|} x_{u,ji,t}^{m,L} \leq 1, \qquad \forall i \in \mathcal{I}, \; \forall u \in \mathcal{U} \qquad \text{(10.-3)}$$

  Constraint (10.4.3) ensures that the traffic of a given user passes through a node only one time in order to prevent loops.

- $$x_{u,ij,t}^{m,L} = 0 \qquad \forall j \in \mathcal{I} \text{ and } \; t \in [0,T], \; i =\mid \mathcal{I} \mid +1, \; \forall L \in \mathcal{L}, \; \forall m \in \mathcal{B}_{N+1} \qquad \text{(10.-3)}$$

  Constraint (10.4.3) ensures that the traffic is not forwarded back to nodes after reaching the gateway.

- Binary varibales constraints:

$$x_{u,ij,t}^{m,L}, \quad a_{i,t}^{m,L}, \quad b_{i,t}, \quad c_{i,t}, \quad u_{li,t} \in \{0,1\}, \quad \forall (i,j) \in \mathcal{I}^2, \quad m \in \mathcal{B}_i, \quad L \in \mathcal{L}, \quad u \in \mathcal{U} \qquad \text{(10.-3)}$$

Equations (10.4.3) is to insure that variables take binary values. Equations (10.4.3 - 10.4.3) represent the optimization problem constraints.

10.4.4 Variables/Constraints Linearisation

In order to reduce the complexity of our problem and to use linear solvers to solve the optimization problem in (10.4.2), we proceed to variables linearisation.

Note that, the complexity of the MILP depends on the number of its number of binary variables.

The energy consumption function in (10.4.2)

$$\begin{aligned}\mathcal{P}_{i,t} = &\sum_{l=1}^{|\mathcal{B}_i|}\sum_{L=1}^{|\mathcal{L}|} a_{i,t}^{l,L}\mathcal{P}_{\text{TX},L} + b_{i,t}\mathcal{P}_{\text{RX}} + c_{i,t}\mathcal{P}_{\text{idle}} - b_{i,t}\cdot c_{i,t}\mathcal{P}_{\text{idle}} \\ &- \sum_{l=1}^{|\mathcal{B}_i|}\sum_{L=1}^{|\mathcal{L}|} a_{i,t}^{m,L}\cdot c_{i,t}\mathcal{P}_{\text{idle}} + \sum_{l=1}^{|\mathcal{B}_i|}\sum_{L=1}^{|\mathcal{L}|} a_{i,t}^{m,L}\cdot c_{i,t}\cdot b_{i,t}\mathcal{P}_{\text{idle}} + \sum_{l=1}^{|\mathcal{B}_i|} a_{i,t}^{l,0}\mathcal{P}_{\text{idle}}\end{aligned}$$

Terms in blue represent non linear variables. In the following we proceed to variables linearization.

For the term $b_{i,t} \times c_{i,t}$ can be linearized as follows:

$$m_{i,t} = b_{i,t} \times c_{i,t} \qquad \forall i \in \mathcal{I}, \quad \forall m \in \mathcal{B}_i \tag{10.-4}$$

where the binary variable (m) must satisfy the following constraints:

$$m_{i,t} - b_{i,t} \leq 0 \qquad \forall i \in \mathcal{I}, \quad \forall m \in \mathcal{B}_i \tag{10.-4}$$

$$m_{i,t} - c_{i,t} \leq 0 \qquad \forall i \in \mathcal{I}, \quad \forall m \in \mathcal{B}_i \tag{10.-4}$$

$$b_{i,t} + c_{i,t} - m_{i,t} \leq 1 \qquad \forall i \in \mathcal{I}, \quad \forall m \in \mathcal{B}_i \tag{10.-4}$$

We follow the same process for $a_{i,t}^{m,L} \times c_{i,t}$ linearization.

For the term $a_{i,t}^{m,L} \times c_{i,t} \times b_{i,t}$

$$o_{i,t}^{m,L} = a_{i,t}^{m,L} \times c_{i,t} \times b_{i,t} \qquad \forall i \in \mathcal{I}, \quad \forall m \in \mathcal{B}_i \tag{10.-4}$$

where the binary variable (o) must satisfy the following constraints:

$$o_{i,t}^{m,L} - a_{i,t}^{m,L} \leq 0 \qquad \forall i \in \mathcal{I}, \quad \forall m \in \mathcal{B}_i \tag{10.-4}$$

$$o_{i,t}^{m,L} - c_{i,t} \leq 0 \qquad \forall i \in \mathcal{I}, \quad \forall m \in \mathcal{B}_i \tag{10.-4}$$

$$o_{i,t}^{m,L} - b_{i,t} \leq 0 \qquad \forall i \in \mathcal{I}, \quad \forall m \in \mathcal{B}_i \tag{10.-4}$$

$$a_{i,t}^{m,L} + c_{i,t} + b_{i,t} - o_{i,t}^{m,L} \leq 2 \qquad \forall i \in \mathcal{I}, \quad \forall m \in \mathcal{B}_i \tag{10.-4}$$

Therefore, replacing the non linear terms by the new introduced variables, the new linear objective function can be written as follows:

$$\begin{aligned}\mathcal{P}_{i,t} = &\sum_{l=1}^{|\mathcal{B}_i|}\sum_{L=1}^{|\mathcal{L}|} a_{i,t}^{l,L}\mathcal{P}_{\mathrm{TX},L} + b_{i,t}\mathcal{P}_{\mathrm{RX}} + c_{i,t}\mathcal{P}_{\mathrm{idle}} - m_{i,t}\mathcal{P}_{\mathrm{idle}} \\ &- \sum_{l=1}^{|\mathcal{B}_i|}\sum_{L=1}^{|\mathcal{L}|} n_{i,t}^{l,L}\mathcal{P}_{\mathrm{idle}} + \sum_{l=1}^{|\mathcal{B}_i|}\sum_{L=1}^{|\mathcal{L}|} o_{i,t}^{l,L}\mathcal{P}_{\mathrm{idle}} + \sum_{l=1}^{|\mathcal{B}_i|} a_{i,t}^{l,0}\mathcal{P}_{\mathrm{idle}}\end{aligned}$$

Hence, the new MILP can be written as:

$$\begin{cases} \text{minimize Eq.} \quad 10.4.4 \\ \text{s.t. Eq. (10.4.3) - Eq. (10.4.3)} \end{cases} \tag{10.-4}$$

In the next section, we present the evaluation methodology followed by the simulation results.

10.5 Performance Evaluation

10.5.1 Evaluation methodology

We use ILOG Cplex solver [8] [1] to find the optimal solution of the joint optimization problem of Eq. (10.4.2). Many software solutions to solve the linear optimization problems were compared in [90]. Cplex is the most efficient one in term of resolution time and handled number of variables. It is based on the brand-and-cut algorithm [37].

- *Inputs*: The inputs are the simulations parameters summarized in Table 10.1.
- *Variables*: Since the number of variables increases exponentially with the network size, we consider relatively small size networks equipped with few number of beams for our simulations.
- *Outputs*: The output of the optimization problem are the set of variables ($x_{u,ij,t}^{l,L}$) indicating which beam l, and power level L are active in a given time slot t for node i to communicate with node j.

10.5.2 Simulation Parameters

For simulations, we consider a WMN with a regular topology. The distribution of nodes follows a grid topology of 25 nodes and equipped with DAs capabilities. We consider that nodes are deployed within an area of 1km×1km and spaced between each other by 200m in the x- and y- axises. We consider a network composed of one gateway placed at the top-right corner of the grid. We fix the transmission rate to 300Kbps for each node. Note that each node is equipped with *one* beam.

The input values of the joint optimization problem are summarized in table 10.1.

10.5.3 Simulation Results

In this subsection, we present simulation results. We show the impact of the number of beams (beamwidth), the number of power level on the consumed energy and on the throughput.

10.5.3.1 Performance vs beamwidth

We consider different cases where we vary the value of the weight factor α. We consider the two extreme cases: (i) α=1, where we focus only on optimizing the energy consumption, (ii) α= 0, where we maximize only the throughput and (iii) two intermediate cases, α=0.5 and α=0.7.

Figure 10.1 illustrates the consumed energy versus the beamwidth for different values of the weight factor α. We vary the beamwidth from $\frac{\pi}{6}$ to $2{\cdot}\pi$. Note that the case of a beamwidth of 2π is equivalent to a network of OAs. The consumed energy increase when the beamwidth gets larger.

[1] Java is used to implement the optimization model into Cplex solver

Parameters	Values
$\mathcal{P}_{\text{Tx}}$	1 (J)
$\mathcal{P}_{\text{RX}}$	0.5 (J)
$\mathcal{P}_{\text{idle}}$	0.1 (J)
L	1,2, and 3
α	[0,1]
$\mid \mathcal{U} \mid$	50
$\mid \mathcal{G} \mid$	1 (Top-right)
Topology	Grid
$\mid \mathcal{I} \mid$	25 (5×5)
$\mid \mathcal{B} \mid$	[1,12]
ν	0.1
γ	$\frac{\pi}{3}$

Table 10.1: Simulations parameters

The maximum energy consumed is when the beamwidth is $2{\cdot}\pi$ (OA). For a given beamwidth, the more α close the one is, the less energy consumed is.

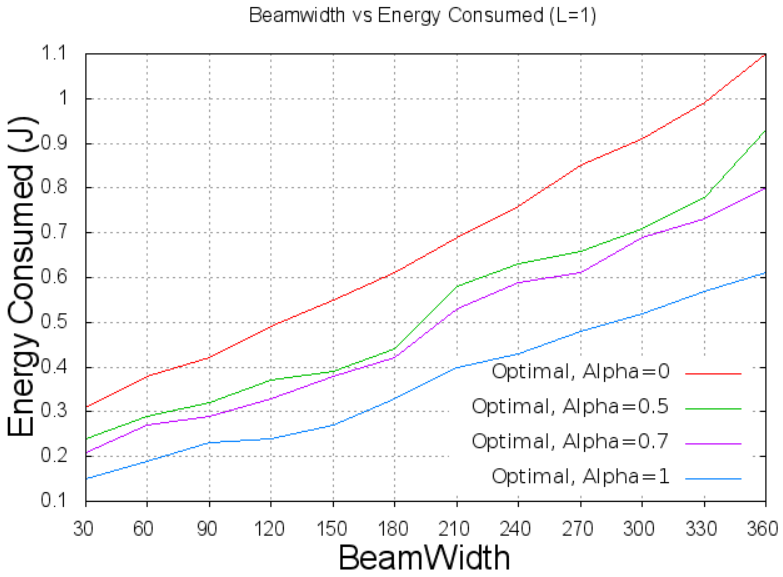

Figure 10.1: Consumed Energy vs BeamWidth for different values of α and for L=1

Figure 10.2 shows the throughout versus the beamwidth for the optimal solution. As expected, the throughput is decreasing in function of the beamwidth. As for the energy consumption, for a given beamwidth, when α gets closer to 1 the throughput gets worse and when it goes closer to 0 it goes better.

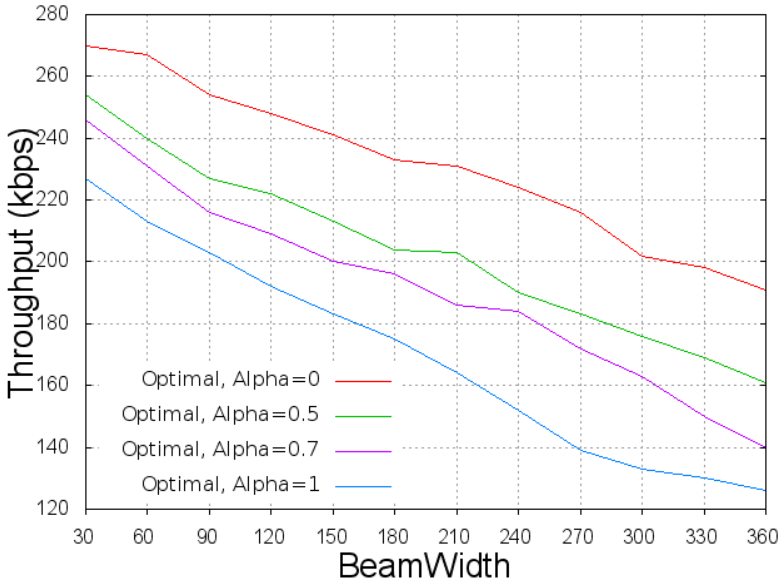

Figure 10.2: Throughput vs BeamWidth for different values of α and for L=1

10.5.3.2 Performance vs Power Levels

For simulations, we take the case of L=3, that is, each node selects its transmit power form the set $\{0, \frac{P_{max}}{2}, P_{max}\}$. The impact of power control is considered in figure 10.3, where we show the energy consumed vs the beamwidth for different values of L, the number of power levels. The more power level are, the less is the consumed energy. In fact, having more power levels, allow to save more power. If the next hop can be reached with less power than the full power only. The node uses less power to reach the destination

10.5.3.3 Throughput vs Consumed Energy

In figure 10.4, we show the energy consumption-throughput tradeoff for different values of L, the number of power levels. For each value of α, we show the corresponding energy consumed and throughput. The two extremal points $P_0(E_{min}, \mathcal{R}_{min})$ and $P_1(E_{max}, \mathcal{R}_{max})$ correspond to values of α=1 and α=0, respectively. For P_0 the consumed energy is minimized but the throughput is worse. On the other hand, for P_1 the throughput is maximized but the energy consumed is high. The curve between these two points represents the *front-pareto*, where each point of the front is derived for a given value of α as shown in the figure. Furthermore, it can be seen that power control improves the performance.

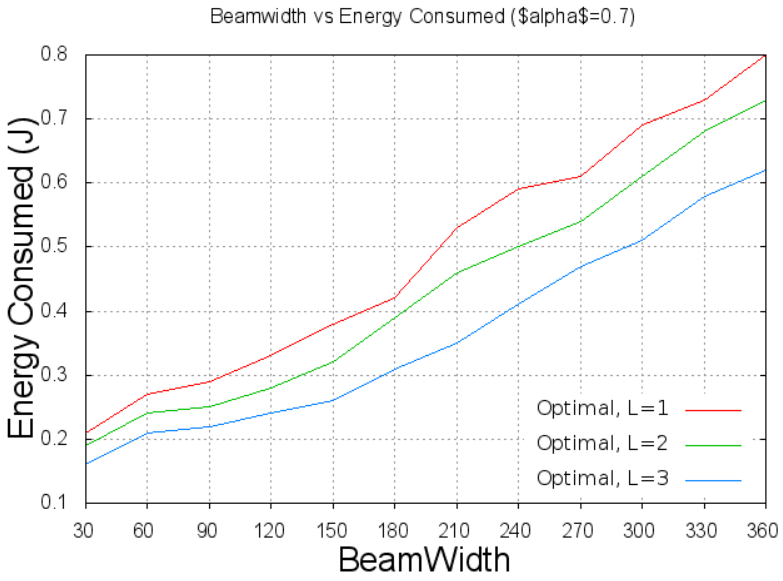

Figure 10.3: Consumed Energy vs BeamWidth for different values of L and for α=0.7

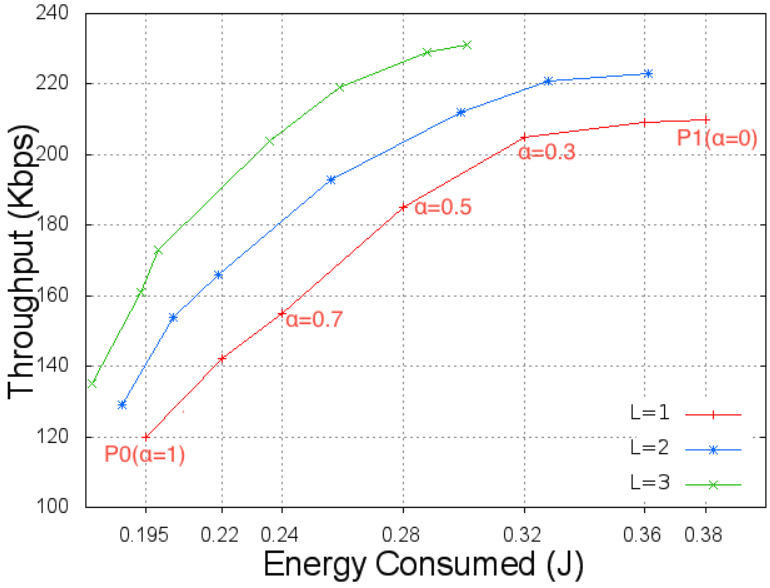

Figure 10.4: Throughput vs Consumed Energy for different values of L

10.6 Conclusion

In this chapter we proposed a new joint energy consumption and throughput optimization model for directional antennas networks in order to improve network performance. We used ILOG Cplex solver to solve numerically the optimization problem. We showed that the energy consumption is an increasing function of the beamwidth, that is, the more the antenna is directive the lower the consumed energy is. Furthermore, we showed that the more power levels we have, the more flexibility on choosing the transmission power level and the less we consume energy. Additionally, we showed the the throughput-energy consumption tradeoff, for different values of α, follows a Pareto front.

Chapter 11

General Conclusion & Perspective Work

Contents

11.1 Conclusion

Next generation networks are expected to be dense, complex and heterogeneous. Therefore, the need of new tools such as point processes to model the nodes distribution in the networks. Stochastic geometry provides a natural way of defining and computing performance metrics of the wireless networks, such as the interference distribution, outage probability and throughout. Furthermore, network densification leads to high interference. The interference arises when adjacent base stations (BSs) use the same resources. Hence, managing the interference is a primary task in wireless networks.

On the other hand, low cost infrastructure mainly composed of WMNs [4] is used to connect isolated rural and sub-urban areas to the Internet. Therefore, finding technologies to connect mesh nodes in a WMN with less energy is attracting for network operators.

The objective of this thesis is to provide tools to manage interference in wireless networks while considering stochastic geometry models and to reduce energy consumption in WMNs. With these objectives our contributions follow several axis.

On the axis of modeling tools, we used stochastic geometry to model the node locations in wireless networks. Specifically, we use the Poisson p.p. and the r-l Square p.p.. These choices are motivated by the fact that these p.p. can either accurately model the actual network, the r-l Square p.p. case, or are tractable for analyzing the system performance, the Poisson p.p. case.

On the axis of interference mitigation, we studied the performance of Coordination MultiPoint-Joint (CoMP-JT) in two different scenarios

- The first contribution of this work concerned the analysis of CoMP-JT model for next generation cellular networks using r-l Square p.p.. We provided formula of the coverage probability and throughput. Using simulations, we showed that CoMP-JT improves considerably the performance metrics and it can be considered as a promising scheme for both wireless cellular and local area networks.

- We extended this work to a Dense Very High WLANs scenario and take into consideration constraints of WLANs such as carrier sensing. Results show that CoMP-JT is a promising technology for Dense Very High WLANs.

Furthermore, we proposed a model based on Poisson p.p. to assess downlink interference in LTE networks. It consists of resource blocks (RBs) assignment strategies and realistic traffic patterns included in the model. We derived tractable formula for the mean and variance of interference. Simulations showed the accuracy of our proposals. Numerical evaluations highlight the behavior of the LTE network for different traffic patterns/load, eNodeB density, amount of resource blocks, and offer insights about possible parameterization of the LTE network with regard to the spatial reuse.

On the axis of energy efficiency, we investigated WMNs by focusing on the impact of Directional Antennas (DAs) on the energy consumption, throughput and energy efficiency. In one hand by using extensive simulations we showed that DAs improve the network performance in terms of throughput, energy consumption and energy efficiency. On the other hand, we derived analytical expressions of the number of links (NLs) for each network setting and showed that increasing the number of antenna beams reduces the NLs.

Furthermore, we proposed a joint optimization framework in order to minimize the consumed energy and maximize the network throughput. We used ILOG Cplex to solve numerically the optimization problem. Numerical results show that DAs reduce the consumed energy in the network and improves the throughput. Specifically, more the antenna are directive the more energy is saved. Furthermore, we showed that the power control improve the network performance in terms of energy consumption. The more power levels we have, the less is the consumed energy.

11.2 Perspective Work

In the following we outline the short and long terms perspective of this work.

11.2.1 Short-term Perspective Work

Several improvements can be made on both parts.

- Since the number of variables increases exponentially with the network size, we are actually studying an heuristic based on Ant-Q algorithm to reduce the complexity of the proposed optimization model in Chapter 10 (work in progress).
- Multi-channels networks [80] use multiple channels in order to increase the effective bandwidth available to wireless mesh network nodes. It is interesting to analyze the impact of using DAs in a multi-channels WMN on the network performance in terms of throughput and energy consumption/efficiency.
- As explained before, CoMP-JT consists of sending multiple copies of the same data to cell edge users experiencing high interference level. Previous to data transmission, data is exchanged among BSs in the coordinated set via the backhaul. This produce a high amount of data to be carried out through X2 interfaces. Analyzing the impact of CoMP-JT on backhaul can be considered as a further of this thesis.
- Studying the impact of other point processes (p.p.) on network performance is an interesting direction. Recently, many point processes [43, 56, 96, 117] are used such as Clustered p.p. (Gauss-Poisson p.p.) and Determinantal p.p (Ginibre p.p.).
- Furthermore, in our DA-WMN scenarios we considered chain and grid topologies. Extension of this work could be considering a random distribution of points modeled and use stochastic geometry tools and derive tractable formula of network performance.

11.2.2 Long-term Perspective Work

Among others, my research interest topics lie on Device to Device (D2D) communications, Millimeter-Waves (mmWaves), Caching and Cloud processing, which aim to meet requirements of 5G networks. In fact, the spatial distribution of BSs and users is important in future wireless networks. Using stochastic geometry tools are primary to analyze and derive performance of next generation technologies:

- In *D2D communications*, users can communicate directly or act as relay to forward the traffic of other users to the nearest base stations. This can improve spectrum utilization, overall

throughput, and energy efficiency while enabling new peer-to-peer and location-based applications and services. In this direction, I am interested in studying issues including: Energy efficiency, Resource allocation and Spectrum sharing between cellular and D2D users.

- Due to potential of availability of wider bandwidths, the *mmWaves* bands above 30 GHz hold promise for providing high peak data rates in specific areas where traffic demands are very high. Many interesting aspects can be tackled such as evaluation of the coverage and the rate of mmWaves systems and developing new channel models.

- In *Wireless Caching*, popular contents are cached at intermediate servers. This eliminates redundant traffic by removing duplicate transmissions form remote servers and allows low-latency delivery of the cached files. An interesting research direction is the development of new algorithms and machine learning tools to predict and estimate content popularity.

Appendices

Appendix A

Publications

- Journals:
  1. I. Lahsen Cherif, A. Busson, "Impact of Resource Blocks Allocation strategies on Downlink Interference distribution in LTE Networks," to be submitted for a journal publication.
  2. I. Lahsen Cherif, L. Zitoune, V. Veque, "Joint Optimization of Energy Consumption and Throughput of Directional WMNs," to be submitted for a journal publication.
- Conferences:
  1. I. Lahsen Cherif, L. Zitoune, V. Veque, "Throughput and Energy Consumption Evaluation in Directional Antennas Mesh Networks," IEEE WiMob 2016, New York, USA.
  2. I. Lahsen Cherif, L. Zitoune, V. Veque, "Performance Evaluation of Joint Transmission Coordinated-MultiPoint in Dense Very High Throughput WLANs Scenario," IEEE LCN 2015, ClearWater Beach, Florida, USA.
  3. I. Lahsen Cherif, L. Zitoune, V. Veque, "The r-l square point process: The effect of Coordinated-MultiPoint Joint Transmission," IEEE IWCMC 2015, Dubrovnik, Croatia.
- Deliverable:
  1. D2.4, "Inter-home Routing using Directional Antennas and White Space", LCI4D project.
  2. D1.4, "Cooperative interference management in femto cells networks", LCI4D project.

Bibliography

[1] http://hubpages.com/technology/Wireless-Communication-Systems-OFDM-OFDMA.

[2] http://www.telxperts.com/lte/.

[3] http://www.hitachi-america.us/rd/about_us/nsl/past-projects/.

[4] Low-cost infrastructure for development of emerging countries. Technical report.

[5] Requirements for further advancements for e-utra (lte-advanced). 3gpp technical specification ts 36.913, release 13, 2015, http://www.3gpp.org.

[6] Technical specification group radio access network; base station (bs) radio transmission and reception, 2012. Release 11.2; 3gpp ts 36.104 v11.2.

[7] GLPK (GNU linear programming kit), 2006.

[8] IBM ILOG CPLEX Optimizer. urlhttp://www-01.ibm.com/software/integration/optimization/cplex-optimizer/, Last 2010.

[9] IEEE standard for information technology–telecommunications and information exchange between systems local and metropolitan area networks–specific requirements part 11: Wireless lan medium access control (MAC) and physical layer (PHY) specifications. *IEEE Std 802.11-2012 (Revision of IEEE Std 802.11-2007)*, pages 1–2793, March 2012.

[10] Global mobile data traffic forecast update 2014–2019 white paper, feb 2015. 2015.

[11] A. Akella, G. Judd, S. Seshan, and P. Steenkiste. Self-management in chaotic wireless deployments. *Wireless Networks*, 13(6):737–755, December 2007.

[12] S. Akoum and R. W. Heath. Interference coordination: Random clustering and adaptive limited feedback. *IEEE Transactions on Signal Processing*, 61(7):1822–1834, 2013.

[13] I. Akyildiz and X. Wang. A survey on wireless mesh networks. *Communications Magazine, IEEE*, 43(9):S23–S30, Sept 2005.

[14] B. Alawieh and C. Assi. Modeling and analysis of power-aware ad hoc networks with directional antennas. In *Computers and Communications, 2007. ISCC 2007. 12th IEEE Symposium on*, pages 33–38, July 2007.

[15] B. Alawieh, C. Assi, and H. Mouftah. Power-aware ad hoc networks with directional antennas: Models and analysis. *Ad Hoc Networks*, 7(3):486 – 499, 2009.

[16] A. Amokrane, R. Langar, R. Boutaba, and G. Pujolle. Energy efficient management framework for multihop tdma-based wireless networks. *Computer Networks*, 62:29 – 42, 2014.

[17] J. Andrews, F. Baccelli, and R. Ganti. A tractable approach to coverage and rate in cellular networks. *Communications, IEEE Transactions on*, 59(11):3122–3134, November 2011.

[18] J. G. Andrews, S. Buzzi, W. Choi, S. V. Hanly, A. Lozano, A. C. Soong, and J. C. Zhang. What will 5g be? *IEEE Journal on Selected Areas in Communications*, 32(6):1065–1082, 2014.

[19] G. Auer, V. Giannini, C. Desset, I. Godor, P. Skillermark, M. Olsson, M. Imran, D. Sabella, M. Gonzalez, O. Blume, and A. Fehske. How much energy is needed to run a wireless network? *Wireless Communications, IEEE*, 18(5):40–49, October 2011.

[20] F. Baccelli, B. Blaszczyszyn, and P. Muhlethaler. Stochastic analysis of spatial and opportunistic aloha. *IEEE Journal on Selected Areas in Communications*, 27(7):1105–1119, September 2009.

[21] M. Bennis, M. Simsek, A. Czylwik, W. Saad, S. Valentin, and M. Debbah. When cellular meets WiFi in wireless small cell networks. *IEEE Communications Magazine*, 51(6), 2013.

[22] S. Berger, Z. Lu, R. Irmer, and G. Fettweis. Modelling the impact of downlink comp in a realistic scenario. In *Wireless Communications and Networking Conference (WCNC), 2013 IEEE*, pages 3932–3936, April 2013.

[23] M. Blanco, R. Kokku, K. Ramachandran, S. Rangarajan, and K. Sundaresan. On the effectiveness of switched beam antennas in indoor environments. In *International Conference on Passive and Active Network Measurement*, pages 122–131. Springer, 2008.

[24] B. Blaszczyszyn, M. Jovanovicy, and M. K. Karray. How user throughput depends on the traffic demand in large cellular networks. In *Modeling and Optimization in Mobile, Ad Hoc, and Wireless Networks (WiOpt), 2014 12th International Symposium on*, pages 611–619, May 2014.

[25] B. Błaszczyszyn and H. P. Keeler. Studying the SINR process of the typical user in poisson networks using its factorial moment measures. *IEEE Transactions on Information Theory*, 61(12):6774–6794, 2015.

[26] S. Boiardi, A. Capone, and B. Sansó. Joint design and management of energy-aware mesh networks. *Ad Hoc Networks*, 10(7):1482–1496, 2012.

[27] R. Bruno, M. Conti, and E. Gregori. Mesh networks: commodity multihop ad hoc networks. *IEEE Communications Magazine*, 43(3):123–131, 2005.

[28] A. Busson, L. Zitoune, V. Veque, and B. Jabbari. Outage analysis of integrated mesh lte femtocell networks. In *2014 IEEE Global Communications Conference*, pages 187–192, Dec 2014.

[29] A. Capone, F. Malandra, and B. Sansò. Energy savings in wireless mesh networks in a time-variable context. *Mobile Networks and Applications*, 17(2):298–311, 2012.

[30] C. S. Chen, V. M. Nguyen, and L. Thomas. On small cell network deployment: A comparative study of random and grid topologies. In *Vehicular Technology Conference (VTC Fall), 2012 IEEE*, pages 1–5, Sept 2012.

[31] S. Chilukuri, R. Sharma, D. R. Borade, and G. R. Kadambi. Simulation studies on an energy efficient multipath routing protocol using directional antennas for manets. *International Journal of Wireless & Mobile Networks*, 4(4):123, 2012.

[32] R. R. Choudhury and N. H. Vaidya. Deafness: A mac problem in ad hoc networks when using directional antennas. In *Network Protocols, 2004. ICNP 2004. Proceedings of the 12th IEEE International Conference on*, pages 283–292. IEEE, 2004.

[33] R. R. Choudhury, X. Yang, R. Ramanathan, and N. H. Vaidya. On designing mac protocols for wireless networks using directional antennas. *IEEE Transactions on Mobile Computing*, 5(5):477–491, May 2006.

[34] Cisco. *802.11ac: The Fifth Generation of Wi-Fi*, August 2012. Technical White Paper.

[35] T. Clausen and P. Jacquet. Optimized link state routing protocol (OLSR). *RFC 3626*, Oct. 2003.

[36] M. Cooper. Antennas Get Smart. *Scientific American*, July 2003.

[37] I. I. CPLEX. V12. 1: Users manual for cplex. *International Business Machines Corporation*, 46(53):157, 2009.

[38] E. Dahlman, S. Parkvall, and J. Skold. *4G: LTE/LTE-advanced for mobile broadband*. Academic press, 2013.

[39] H.-N. Dai. Throughput and delay in wireless sensor networks using directional antennas. In *5th International Conference on Intelligent Sensors, Sensor Networks and Information Processing (ISSNIP)*, pages 421–426, Dec 2009.

[40] H.-N. Dai, K.-W. Ng, R.-W. Wong, and M.-Y. Wu. On the capacity of multi-channel wireless networks using directional antennas. In *27th IEEE Conference on Computer Communications*, pages –, April 2008.

[41] D. N. M. Dang, H. T. Le, H. S. Kang, C. S. Hong, and J. Choe. Multi-channel MAC protocol with directional antennas in wireless ad hoc networks. In *the International Conference on Information Networking (ICOIN)*, pages 81–86, Jan 2015.

[42] S. M. Das, H. Pucha, D. Koutsonikolas, Y. C. Hu, and D. Peroulis. Dmesh: Incorporating practical directional antennas in multichannel wireless mesh networks. *IEEE Journal on Selected Areas in Communications*, 24(11):2028–2039, Nov 2006.

[43] N. Deng, W. Zhou, and M. Haenggi. The ginibre point process as a model for wireless networks with repulsion. *IEEE Transactions on Wireless Communications*, 14(1):107–121, 2015.

[44] H. Dhillon, R. Ganti, F. Baccelli, and J. Andrews. Modeling and analysis of K-tier downlink heterogeneous cellular networks. *IEEE Journal on Selected Areas in Communications*, 30(3):550–560, April 2012.

[45] M. Di Renzo, A. Guidotti, and G. Corazza. Average rate of downlink heterogeneous cellular networks over generalized fading channels: A stochastic geometry approach. *IEEE Transactions on Communications*, 61(7):3050–3071, July 2013.

[46] N. Dinur and D. Wulich. Peak-to-average power ratio in high-order ofdm. *IEEE Transactions on Communications*, 49(6):1063–1072, 2001.

[47] R. Draves, J. Padhye, and B. Zill. Routing in multi-radio, multi-hop wireless mesh networks. In *Proceedings of the 10th annual international conference on Mobile computing and networking*, pages 114–128. ACM, 2004.

[48] M. A. Ergin, K. Ramachandran, and M. Gruteser. Understanding the effect of access point density on wireless lan performance. In *Proceedings of the 13th Annual ACM International Conference on Mobile Computing and Networking*, MobiCom '07, pages 350–353, New York, NY, USA, 2007. ACM.

[49] S. M. Faccin, C. Wijting, J. Kenckt, and A. Damle. Mesh wlan networks: concept and system design. *IEEE Wireless Communications*, 13(2):10–17, 2006.

[50] P. Frossard, J. C. De Martin, and M. R. Civanlar. Media streaming with network diversity. *Proceedings of the IEEE*, 96(1):39–53, 2008.

[51] R. K. Ganti. A stochastic geometry approach to the interference and outage characterization of large wireless networks. *Ph.D. Thesis, Notre Dame*, 2009.

[52] D. Gesbert, M. Shafi, D.-s. Shiu, P. J. Smith, and A. Naguib. From theory to practice: an overview of mimo space-time coded wireless systems. *IEEE Journal on selected areas in Communications*, 21(3):281–302, 2003.

[53] A. Ghosh, N. Mangalvedhe, R. Ratasuk, B. Mondal, M. Cudak, E. Visotsky, T. A. Thomas, J. G. Andrews, P. Xia, H. S. Jo, et al. Heterogeneous cellular networks: From theory to practice. *IEEE Communications Magazine*, 50(6):54–64, 2012.

[54] A. Gkelias and K. K. Leung. *Multiple Antenna Techniques for Wireless Mesh Networks*, chapter Wireless Mesh Networks, pages 277–307. Springer, 2008.

[55] A. Guo and M. Haenggi. Asymptotic deployment gain: A simple approach to characterize the sinr distribution in general cellular networks. *IEEE Transactions on Communications*, 63(3):962–976, 2015.

[56] A. Guo, Y. Zhong, W. Zhang, and M. Haenggi. The Gauss-Poisson process for wireless networks and the benefits of cooperation. *IEEE Transactions on Communications*, 64(5):1916–1929, May 2016.

[57] P. Gupta and P. Kumar. The capacity of wireless networks. *IEEE Transactions on Information Theory*, 46(2):388–404, Mar 2000.

[58] M. Haenggi. *Stochastic geometry for wireless networks*. Cambridge University Press, 2012.

[59] M. Haenggi, J. G. Andrews, F. Baccelli, O. Dousse, and M. Franceschetti. Stochastic geometry and random graphs for the analysis and design of wireless networks. *IEEE Journal on Selected Areas in Communications*, 27(7):1029–1046, 2009.

[60] A. S. Hamza, S. S. Khalifa, H. S. Hamza, and K. Elsayed. A survey on inter-cell interference coordination techniques in ofdma-based cellular networks. *IEEE Communications Surveys Tutorials*, 15(4):1642–1670, Fourth 2013.

[61] R. Heath and M. Kountouris. Modeling heterogeneous network interference. In *Information Theory and Applications Workshop (ITA), 2012*, pages 17–22, Feb 2012.

[62] R. W. Heath, M. Kountouris, and T. Bai. Modeling heterogeneous network interference using poisson point processes. *IEEE Transactions on Signal Processing*, 61(16):4114–4126, Aug 2013.

[63] J. Hofmann, V. Rexhepi-van der Pol, G. Sébire, and S. Parolari. 3gpp release 8. *GSM/EDGE: Evolution and Performance*, pages 63–99, 2011.

[64] A. Hourani, R. J. Evans, and S. Kandeepan. Nearest neighbour distance distribution in hard-core point processes. *IEEE Communications Letters*, PP(99):1–1, 2016.

[65] B. Hu and H. Gharavi. Directional routing protocols for ad-hoc networks. *Communications, IET*, 2(5):650–657, 2008.

[66] A. Hunter, J. Andrews, and S. Weber. Transmission capacity of ad hoc networks with spatial diversity. *IEEE Transactions on Wireless Communications*, 7(12):5058–5071, December 2008.

[67] A. M. Ibrahim, T. ElBatt, and A. El-Keyi. Coverage probability analysis for wireless networks using repulsive point processes. In *Personal Indoor and Mobile Radio Communications (PIMRC), 2013 IEEE 24th International Symposium on*, pages 1002–1007, Sept 2013.

[68] M. Imran, E. Katranaras, G. Auer, O. Blume, V. Giannini, I. Godor, Y. Jading, M. Olsson, D. Sabella, P. Skillermark, et al. Energy efficiency analysis of the reference systems, areas of improvements and target breakdown. Technical report, Tech. Rep. ICT-EARTH deliverable, 2011.

[69] S. Kandasamy, R. Campos, R. Morla, and M. Ricardo. Using directional antennas on stub wireless mesh networks: Impact on throughput, delay, and fairness. In *Computer Communications and Networks (ICCCN), 2010 Proceedings of 19th International Conference on*, pages 1–6, Aug 2010.

[70] D. H. Kang, K. W. Sung, and J. Zander. Cost efficient high capacity indoor wireless access: Denser Wi-Fi or coordinated pico-cellular? *CoRR*, abs/1211.4392, 2012.

[71] I. Kang, R. Poovendran, and R. Ladner. Power-efficient broadcast routing in adhoc networks using directional antennas: technology dependence and convergence issues. *University of Washington, Washington, USA, Tech. Rep. UWEETR-2003-0015*, 2003.

[72] V. V. Kapadia, S. N. Patel, and R. H. Jhaveri. Comparative study of hidden node problem and solution using different techniques and protocols. *arXiv preprint arXiv:1003.4070*, 2010.

[73] E. Karapistoli, I. Gragopoulos, I. Tsetsinas, and F.-N. Pavlidou. A MAC protocol for low-rate UWB wireless sensor networks using directional antennas. *Computer Networks*, 53(7):961–972, 2009.

[74] A. Karnik, A. Iyer, and C. Rosenberg. Throughput-optimal configuration of fixed wireless networks. *IEEE/ACM Transactions on Networking*, 16(5):1161–1174, Oct 2008.

[75] S. Katikala. Google project loon. *InSight: Rivier Academic Journal*, 10(2), 2014.

[76] T.-H. Kim and T.-J. Lee. Throughput enhancement of macro and femto networks by frequency reuse and pilot sensing. In *2008 IEEE International Performance, Computing and Communications Conference*, pages 390–394. IEEE, 2008.

[77] Y.-B. Ko, V. Shankarkumar, and N. H. Vaidya. Medium access control protocols using directional antennas in ad hoc networks. In *In 9th Annual Joint Conference of the IEEE Computer and Communications Societies*, volume 1, pages 13–21 vol.1, 2000.

[78] K. Krickeberg. Moments of point processes. In *Probability and Information Theory II*, pages 70–101. Springer, 1973.

[79] Y. Kwon, O. Lee, J. Lee, M. Chung, Y. Kwon, O. Lee, J. Lee, and M. Chung. Power control for soft fractional frequency reuse in ofdma system. *Computational Science and Its Applications ICCSA 2010*, 6018:63–71, 2010.

[80] P. Kyasanur, J. So, C. Chereddi, and N. H. Vaidya. Multichannel mesh networks: challenges and protocols. *IEEE Wireless Communications*, 13(2):30–36, 2006.

[81] I. Lahsen Cherif, L. Zitoune, and V. Veque. Performance evaluation of joint transmission coordinated multipoint approach in dense very high throughput wlans scenario,. In *Local Computer Networks (LCN), 2015 IEEE 40th Conference on*, Octobre 2015.

[82] I. Lahsen Cherif, L. Zitoune, and V. Veque. The r-l square point process: The effect of coordinated multipoint joint transmission,. In *International Wireless Communications & Mobile Computing Conference (IWCMC), 2015 IEEE*, August 2015.

[83] Y. Leo, A. Busson, C. Sarraute, and E. Fleury. Call detail records to characterize usages and mobility events of phone users. *Computer Communications, To Appear*, pages –, 2016.

[84] Y. Li, Z. Luo, M. Yang, and B. Sun. Feasibility of coordinated transmission for HEW. doc.: IEEE 802.11-13/1157r3, September 2013.

[85] D. Lopez-Perez, I. Guvenc, G. De la Roche, M. Kountouris, T. Q. Quek, and J. Zhang. Enhanced intercell interference coordination challenges in heterogeneous networks. *IEEE Wireless Communications*, 18(3):22–30, 2011.

[86] D. López-Pérez, A. Ladányi, A. Jüttner, H. Rivano, and J. Zhang. Optimization method for the joint allocation of modulation schemes, coding rates, resource blocks and power in

self-organizing lte networks. In *INFOCOM, 2011 Proceedings IEEE*, pages 111–115, April 2011.

[87] D. B. J. D. A. Maltz and J. Broch. DSR: The dynamic source routing protocol for multi-hop wireless ad hoc networks. *Computer Science Department Carnegie Mellon University Pittsburgh, PA*, pages 15213–3891, 2001.

[88] J. Markendahl and O. Makitalo. A comparative study of deployment options, capacity and cost structure for macrocellular and femtocell networks. In *IEEE PIMRC 2010*, pages 145–150, Sept 2010.

[89] B. Matern. Spatial variation. *Meddelanden fran Statens Skogsforskningsinstitut*, 49, No. 5, 1960.

[90] B. Meindl and M. Templ. Analysis of commercial and free and open source solvers for linear optimization problems. 2012.

[91] C. Metz. Facebook will build drones and satellites to beam internet around the world, 2014.

[92] N. Miyoshi, T. Shirai, et al. A cellular network model with ginibre configured base stations. *Advances in Applied Probability*, 46(3):832–845, 2014.

[93] F. Moety, S. Lahoud, K. Khawam, and B. Cousin. Joint power-delay minimization in green wireless access networks. In *IEEE PIMRC*, pages 2819–2824, Sept 2013.

[94] A. H. Mohsenian-rad and V. W. S. Wong. Joint logical topology design, interface assignment, channel allocation, and routing for multi-channel wireless mesh networks. *IEEE Transactions on Wireless Communications*, 6(12):4432–4440, December 2007.

[95] S. Muthaiah, A. Iyer, A. Karnik, and C. Rosenberg. Design of high throughput scheduled mesh networks: A case for directional antennas. In *Global Telecommunications Conference, 2007. GLOBECOM '07. IEEE*, pages 5080–5085, Nov 2007.

[96] I. Nakata and N. Miyoshi. Spatial stochastic models for analysis of heterogeneous cellular networks with repulsively deployed base stations. *Performance Evaluation*, 78(0):7 – 17, 2014.

[97] A. Nasipuri, K. Li, and U. Sappidi. Power consumption and throughput in mobile ad hoc networks using directional antennas. In *Computer Communications and Networks*, pages 620–626, Oct 2002.

[98] V. Navda, A. P. Subramanian, K. Dhanasekaran, A. Timm-Giel, and S. Das. Mobisteer: using steerable beam directional antenna for vehicular network access. In *Proceedings of the 5th international conference on Mobile systems, applications and services*, pages 192–205. ACM, 2007.

[99] R. v. Nee and R. Prasad. *OFDM for wireless multimedia communications*. Artech House, Inc., 2000.

[100] H. Nguyen, F. Baccelli, and D. Kofman. A stochastic geometry analysis of dense IEEE 802.11 networks. In *In proccedings of the 26th IEEE International Conference on Computer Communications*, pages 1199–1207, May 2007.

[101] G. Nigam, P. Minero, and M. Haenggi. Coordinated multipoint in heterogeneous networks: A stochastic geometry approach. In *IEEE GLOBECOM Workshop on Emerging Technologies for LTE-Advanced and Beyond 4G (GLOBECOM-B4G'13)*, Atlanta, GA, December 2013.

[102] T. Novlan, R. Ganti, A. Ghosh, and J. Andrews. Analytical evaluation of fractional frequency reuse for ofdma cellular networks. *Wireless Communications, IEEE Transactions on*, 10(12):4294–4305, December 2011.

[103] T. Novlan, R. Ganti, A. Ghosh, and J. Andrews. Analytical evaluation of fractional frequency reuse for heterogeneous cellular networks. *Communications, IEEE Transactions on*, 60(7):2029–2039, July 2012.

[104] J. Núñez-Martínez, J. Baranda, and J. Mangues-Bafalluy. Experimental evaluation of self-organized backpressure routing in a wireless mesh backhaul of small cells. *Ad Hoc Networks*, 24:103–114, 2015.

[105] E. A. Omar and K. M. F. Elsayed. Directional antenna with busy tone for capacity boosting and energy savings in wireless ad-hoc networks. In *High-Capacity Optical Networks and Enabling Technologies (HONET), 2010*, pages 91–95, Dec 2010.

[106] A. Ouni, H. Rivano, F. Valois, and C. Rosenberg. Energy and throughput optimization of wireless mesh networks with continuous power control. *IEEE Transactions on Wireless Communications*, 14(2):1131–1142, Feb 2015.

[107] T. Pollet, M. Van Bladel, and M. Moeneclaey. Ber sensitivity of ofdm systems to carrier frequency offset and wiener phase noise. *IEEE transactions on communications*, 43(2/3/4):191–193, 1995.

[108] V. Ramamurthi, A. Reaz, S. Dixit, and B. Mukherjee. Link scheduling and power control in wireless mesh networks with directional antennas. In *Communications, 2008. ICC '08. IEEE International Conference on*, pages 4835–4839, May 2008.

[109] A. Raniwala and T.-c. Chiueh. Architecture and algorithms for an ieee 802.11-based multi-channel wireless mesh network. In *Proceedings IEEE 24th Annual Joint Conference of the IEEE Computer and Communications Societies.*, volume 3, pages 2223–2234. IEEE, 2005.

[110] Ruckus Wireless, Inc. *Deploying Very High Density WiFi, Design and Configuration Guide for Stadiums*, 2012. best practice design guide.

[111] N. Sadeghianpour, T. C. Chuah, and S. W. Tan. Joint channel assignment and routing in multiradio multichannel wireless mesh networks with directional antennas. *International Journal of Communication Systems*, 28(9):1521–1536, 2015.

[112] A. K. Saha and D. B. Johnson. Routing improvement using directional antennas in mobile ad hoc networks. In *In proccedings of IEEE GLOBECOM*, volume 5, pages 2902–2908 Vol.5, Nov 2004.

[113] A. H. Sakr and E. Hossain. Location-aware cross-tier coordinated multipoint transmission in two-tier cellular networks. *IEEE Transactions on Wireless Communications*, 13(11):6311–6325, 2014.

[114] A. H. Sakr and E. Hossain. Location-aware cross-tier coordinated multipoint transmission in two-tier cellular networks. *IEEE Transactions on Wireless Communications*, 13(11):6311–6325, 2014.

[115] N. Saquib, E. Hossain, and D. I. Kim. Fractional frequency reuse for interference management in LTE-advanced hetnets. *Wireless Communications, IEEE*, 20(2):113–122, April 2013.

[116] K. Selvaradjou, N. Handigol, A. A. Franklin, and C. S. R. Murthy. Energy-efficient directional routing between partitioned actors in wireless sensor and actor networks. *IET Communications*, 4(1):102–115, January 2010.

[117] T. Shirai and N. Miyoshi. A cellular network model with ginibre configurated base stations. *Advances in Applied Probability*, 2013.

[118] A. Spyropoulos and C. Raghavendra. Asympotic capacity bounds for ad-hoc networks revisited: the directional and smart antenna cases. In *In IEEE GLOBECOM*, volume 3, pages 1216–1220 vol.3, Dec 2003.

[119] A. Spyropoulos and C. S. Raghavendra. Energy efficient communications in ad hoc networks using directional antennas. In *IEEE INFOCOM*, pages 220–228 vol.1, 2002.

[120] D. Stoyan, S. Kendall, and J. Mecke. *Stochastic geometry and its applications, second edition.* John Wiley & Sons, 1995.

[121] M. Takai, J. Martin, R. Bagrodia, and A. Ren. Directional virtual carrier sensing for directional antennas in mobile ad hoc networks. In *Proceedings of the 3rd ACM international symposium on Mobile ad hoc networking & computing*, pages 183–193. ACM, 2002.

[122] M. Takata, M. Bandai, and T. Watanabe. A MAC protocol with directional antennas for deafness avoidance in ad hoc networks. In *IEEE GLOBECOM*, pages 620–625. IEEE, 2007.

[123] R. Tanbourgi, S. Singh, J. Andrews, and F. Jondral. A tractable model for noncoherent joint-transmission base station cooperation. *IEEE Transactions on Wireless Communications*, 13(9):4959–4973, Sept 2014.

[124] International Telecommunication Union. Measuring the information society 2013, 2013.

[125] R. Ullah, N. Fisal, H. Safdar, Z. Khalid, W. Maqbool, and H. Ullah. Stochastic geometry based dynamic fractional frequency reuse for OFDMA systems. *jurnal teknologi*, 67(1):61–67, March 2014.

[126] D. M. West. Digital divide: Improving internet access in the developing world through affordable services and diverse content. *Center for Technology Innovation at Brookings*, 2015.

[127] W. Wong, X. Chen, F. Long, and S. H. G. Chan. Joint topology control and routing assignment for wireless mesh with directional antennas. In *Global Communications Conference (GLOBECOM), 2012 IEEE*, pages 5699–5704, Dec 2012.

[128] P. Xia, C.-H. Liu, and J. G. Andrews. Downlink coordinated multi-point with overhead modeling in heterogeneous cellular networks. *IEEE Transactions on Wireless Communications*, 12(8):4025–4037, 2013.

[129] X. F.-m. T. Xiao-feng and X. Xiao-dong. Soft fractional frequency reuse. *ZTE Communications*, 2:008, 2007.

[130] Y. Yifan, R. Yun, L. MingQi, S. Bin, and S. RongFang. Achievable rates of coordinated multi-point transmission schemes under imperfect CSI. *In Proc. IEEE ICC*, pages 1–6, 2011.

[131] S. M. Yu and S. L. Kim. Downlink capacity and base station density in cellular networks. In *Modeling Optimization in Mobile, Ad Hoc Wireless Networks (WiOpt), 2013 11th International Symposium on*, pages 119–124, May 2013.

[132] Z. Yu, J. Teng, X. Bai, D. Xuan, and W. Jia. Connected coverage in wireless networks with directional antennas. In *Proceedings IEEE INFOCOM, 2011*, pages 2264–2272, April 2011.

[133] X. Zhang and M. Haenggi. A stochastic geometry analysis of inter-cell interference coordination and intra-cell diversity. *Wireless Communications, IEEE Transactions on*, 13(12):6655–6669, Dec 2014.

[134] J. Zhao, T. Q. Quek, and Z. Lei. Heterogeneous cellular networks using wireless backhaul: Fast admission control and large system analysis. *IEEE Journal on Selected Areas in Communications*, 33(10):2128–2143, 2015.

[135] H. Zhuang and T. Ohtsuki. A model based on poisson point process for downlink tiers fractional frequency reuse heterogeneous networks. *Physical Communication*, 2014.

[136] M. Żotkiewicz and M. Pióro. Exact approach to reliability of wireless mesh networks with directional antennas. *Telecommunication Systems*, 56(1):201–211, 2013.

Titre : Efficacité spectrale et énergétique dans les réseaux 5G.

Mots clés : Réseaux cellulaire, Réseaux mesh, Allocation de ressources, Géométrie stochastique, Optimisation, Antennes directives, Gestion des interférences, CoMP

La pénurie d'énergie et le manque d'infrastructures dans les régions rurales représentent une barrière pour le déploiement et l'extension des réseaux cellulaires. Les approches et techniques pour relier les stations de base (BSs) entre elles à faible coût et d'une manière fiable et efficace énergiquement sont l'une des priorités des opérateurs. Ces réseaux peu denses actuellement, peuvent évoluer rapidement et affronter une croissance exponentielle due principalement à l'utilisation des téléphones mobiles, tablettes et applications gourmandes en bande passante. La densification des réseaux est l'une des solutions efficaces pour répondre à ce besoin en débit élevé. Certes, l'introduction de petites BSs apporte de nombreux avantages tels que l'amélioration du débit et de la qualité du signal, mais entraîne des contraintes opérationnelles telles que le choix de l'emplacement des noeuds dans ces réseaux de plus en plus denses ainsi que leur alimentation. Les problèmes où la contrainte spatiale est prépondérante sont bien appropriés à la modélisation par la géométrie stochastique qui permet une modélisation réaliste de distribution des BSs. Ainsi, l'enjeu est de trouver de nouvelles approches de gestions d'interférence et de réductions de consommation énergétique dans les réseaux sans fil.

Le premier axe de cette thèse s'intéresse aux méthodes de gestion d'interférence dans les réseaux cellulaires se basant sur la coordination entre les BSs, plus précisément, la technique Coordinated MultiPoint Joint Transmission (CoMP-JT). En CoMP-JT, les utilisateurs en bordure de cellules qui subissent un niveau très élevé d'interférences reçoivent plusieurs copies du signal utile de la part des BSs qui forment l'ensemble de coordination. Ainsi, nous utilisons le modèle r-l Square Point Process (PP) à fin de modéliser la distribution des BSs dans le plan. Le processus r-l Square PP est le plus adapté pour modéliser le déploiement réel des BSs d'un réseau sans fil, en assurant une distance minimale, (r - l), entre les points du processus. Nous discutons l'impact de la taille de l'ensemble de coordination sur les performances évaluées. Ce travail est étendu pour les réseaux denses WiFi IEEE 802.11, où les contraintes de portées de transmission et de détection de porteuse ont été prises en compte.

Dans le deuxième axe du travail, nous nous intéressons à l'efficacité énergétique des réseaux mesh. Nous proposons l'utilisation des antennes directionnelles (DAs) pour réduire la consommation énergétique et améliorer le débit de ces réseaux mesh. Les DAs ont la capacité de focaliser la transmission dans la direction du récepteur, assurant une portée plus importante et moins d'énergie dissipée dans toutes les directions. Pour différentes topologies, nous dérivons le nombre de liens et montrons que ce nombre dépend du nombre de secteurs de l'antenne. Ainsi, en utilisant les simulations, nous montrons que le gain, en énergie et en débit, apporté par les DAs peut atteindre 70\% dans certains cas. De plus, on propose un modèle d'optimisation conjointe d'énergie et du débit adapté aux réseaux WMNs équipés de DAs. La résolution numérique de ce modèle conforte les résultats de simulation obtenus dans la première partie de cette étude sur l'impact des DAs sur les performances du réseau en termes de débit et d'énergie consommée.

Ces travaux de thèse s'inscrivent dans le cadre du projet collaboratif (FUI16 LCI4D), qui consiste à concevoir et à valider une architecture radio ouverte pour renforcer l'accès aux services broadband dans des lieux ne disposant que d'une couverture minimale assurée par un réseau macro-cellulaire traditionnel. Le projet s'intéresse à accélérer l'extension de couverture cellulaire dans les pays émergents en concevant une architecture de réseau à faible coût qui s'appuie sur de nouvelles technologies backhaul apportant de la capacité et réduisant la consommation énergétique dans des zones non couvertes, ainsi sur la baisse des coûts de déploiement de l'architecture.

Université Paris-Saclay
Espace Technologique / Immeuble Discovery
Route de l'Orme aux Merisiers RD 128 / 91190 Saint-Aubin, France

Title : Spectral and Energy Efficiency in 5G Wireless Networks.

Keyworks : Cellular networks, mesh networks, resource allocation, stochastic geometry, optimization, directional antennas, interference mangement, CoMP

Today's networks continue to evolve and grow resulting more dense, complex and heterogeneous networks. This leads to new challenges such as finding new models to characterize the nodes distribution in the wireless network and approaches to mitigate interference. On the other hand, the energy consumption of WMNs is a challenging issue mainly in rural areas lacking of default electrical grids. Finding alternative technologies and approaches to reduce the consumed energy of these networks is a interesting task.

This thesis focus on proposing and evaluating interference management models for next generation wireless networks (5G and Very Dense High WLANs), and providing tools and technologies to reduce energy consumption of Wireless Mesh Networks (WMNs). Two different problems are thus studied, naturally the thesis is divided into two parts along the following chapters.

The contribution of the first part of the thesis is threefold. Firstly, we develop our interference management coordination (CoMP-JT) model. The main idea of CoMP-JT is to turn signals generating harmful interference into useful signals. We develop a new model where BSs inside the coordinated set send a copy of data to border's users experiencing high interference. We consider the r-l Square point process to model the BSs distribution in the network. We derive network performance in terms of coverage probability and throughput. Additionally, we study the impact of the size of coordination set on the network performance. Secondly, we extend these results and provide a new model adopted for Dense Very high throughput WLANs. We take into consideration constraints of WLANs in our model such as carrier sensing range. Thirdly, we tackle resource allocation strategies to limit the interference in LTE networks. We study three cyclic allocation strategies: (i) the independent allocation, (ii) the static allocation and (iii) the load-dependent strategy. We derive tractable analytical expression of the first and second mean of interference. We validate the model using extensive simulations.

Reducing the energy consumption and improving the energy efficiency of WMNs is our concern in the second part of the thesis. Indeed, we aim at studying the impact of directional antennas technology on the performance of WMNs, using both analysis and simulations. Fisrt, We derive the Number of Links (NLs) for the chain and grid topologies for different antennas beams. These results are based on the routing tables of nodes in the network. We consider different scenarios such as 1Source-NDestinations to model the downlink communications, NSources-1Destination to model the uplink communications and the 1Source-1Destination as a baseline scenario. Using ns-3 simulator, we simulate network performance in terms of Mean Loss Ratio, throughput, energy consumption and energy efficiency. Then, we study the impact of number of beams, network topology and size, the placement of the gateway on the network performance. Next, we go beyond simulations and propose an optimization framework minimizing the consumed energy while maximizing the network throughput for DAs WMNs. We consider a weighted objective function combining the energy consumption and the throughput. We use discrete power control to adapt transmission power depending on the location of the next hop. This model is a first step to aprove the obtained simulation results. We use ILOG Cplex solver to find the optimal solution. Results show that DAs improves the network throughput while reduce the energy consumption and that power control allows to save more energy.

In this direction, the LCI4D Project aims at providing low cost infrastructure to connect isolated rural and sub-urban areas to the Internet. In order to reduce the installation and maintenance costs, LCI4D proposes the usage of self-configured Wireless Mesh Networks (WMNs) to connect outdoor femtocells to the remote Marco cell (gateway). These femtocells are multimode embedding both cellular and mesh WiFi technologies. The mesh WiFi part is used to form a mesh backhaul to relay cellular data of cellular devices to the gateway.